# THE ACTIVITY OF pH MEMBRANE DISRUPTIVE PSEUDOPEPTIDES AND THEIR SUBCELLULAR FATE IN MAMMALIAN CELLS CULTURED *IN-VITRO*

by

FIONA MARY GILCHRIST

A thesis submitted to

The University of Aston in Birmingham

for the degree of

DOCTOR OF PHILOSOPHY

Aston University, Birmingham

September, 2002

# THESIS SUMMARY

This thesis describes investigations upon pseudopeptides which were conducted to improve our understanding of the fate of synthetic macromolecules in cells and to develop approaches to influence that fate. The low uptake of molecules across the external cellular membrane is the principal barrier against effective delivery of therapeutic products to within the cell structure. In nature, disruption of this membrane by amphiphilic peptides plays a central role in the pathogenesis by bacterial and toxin infections. These amphiphilic peptides contain both hydrophobic and weakly charged hydrophilic amino acid residues and upon activation they become integrated into the lipid bilayers of the extracellular or endosomal membranes. The architectures of the pseudopeptides described here were designed to display similar pH dependent membrane rupturing activity to that of peptides derived from the influenza virus hemagglutinin HA-2. This HA protein promotes fusion of the influenza virus envelope with the cell endosome membrane due to a change in conformation in response to the acidic pH of the endosome lumen (pH 5.0-6.0). The pseudopeptides were obtained by the copolymerisation of L-lysine and L-lysine ethyl-ester with various dicarboxylic acid moieties. In this way a linear polyamide comprising of alternating pendant carboxylic acids and pendant hydrophobic moieties was made. At physiological pH (pH 7.4), electrostatic repulsion of pendant anionic carboxyl groups along the polymer backbone is sufficient to overcome the intramolecular association of the hydrophobic groups resulting in an extended conformation. At low pH (typically pH 4.8) loss of charge results in increased intramolecular hydrophobic association and the polymer chain collapses to a compact conformation, leading to precipitation of the polymer. Consequently, a conformation dependent functional property could be made to respond to small changes in the environmental pH.

Pseudopepides were invesigated for their cytoxicity towards a well known cell line, namely C26 (colorectal adenocarcinoma) and were shown through the use of a cell viability assay, MTT (3-(4,5-dimethylthiazol-2-yl)-2,5 diphenyltetrazolium bromide) to be well tolerated by C26 cells over a range of concentrations (2-500$\mu$g/ml) at physiological pH (pH 7.4). A modified version of a shorter 30-minute coupled enzymatic assay, the LDH (lactate dehydrogenase) assay was used to evaluate the ability of the pseudopeptides to disrupt the membrane of two different cell lines (COS-1; African green monkey, kidney and A2780; human ovarian carcinoma) at low pH (pH 5.5). The cell membrane disruption property of the pseudopeptides was successfully demonstrated for COS-1 and A2780 cell lines at this pH (pH 5.5). A variety of cell lines were chosen owing to limited availability and to compare the cytotoxic action of these pH responsive psudopeptides towards normal and tumorogenic cell lines.

To investigate the intracellular delivery of one of the pseudopeptides, poly (L-lysine *iso*-phthalamide) and its subcellular location, a Cy3 bisamine fluorophore was conjugated into its backbone, at ratios of dye:lysine of 1:20, 1:30, 1:40, 1:60 and 1:80. Native polyacrylacrylamide gel electrophoresis (PAGE) and high voltage paper electrophoresis (HVPE) studies of the polydyes were conducted and provided evidence that that the Cy3 bisamine fluorophore was conjugated into the backbone of the polymer, poly (L-lysine *iso*-phthalamide). The subcellular fate of the fluorescently labelled "polydye" (hereafter PD20) was monitored by laser scanning confocal microscopy (LSCM) in CHO (Chinese hamster ovary) cells cultured *in-vitro* at various pH values (pH 7.4 and 5.0). LSCM images depicting time-dependent internalisation of PD20 indicated that PD20 traversed the extracellular membrane of CHO cells cultured *in-vitro* within ten minutes and migrated towards the endosomal regions where the pH is in the region of 5.0 to 6.0. Nuclear localisation of PD20 was demonstrated in a

subpopulation of CHO cells. A further study was completed in CHO and HepG2 (hepatocellular carcinoma) cells cultured *in-vitro* using a lower molecular weight polymer to demonstrate that the molecular weight of "polydye" could be tailored to attain nuclear trafficking in cells. Prospective use of this technology encompasses a method of delivering a payload into a living cell based upon the hypercoiling nature of the pseudopeptides studied in this thesis and has led to a patent application (**GB0228525.2;** 2002).

# ACKNOWLEDGEMENTS

Firstly, I would like to thank my supervisor Professor Nigel Slater and Dr. Andy Sutherland for their supervision and guidance.

This studentship was funded by the Engineering and Physical Sciences Research Council (EPSRC) and Amersham Biosciences. I gratefully acknowledge researchers at Amersham Biosciences in Cardiff for their technical assistance.

I also acknowledge Dr. Mark Eccleston, Dr. Sharon Williams, Graham Page and my family for their support and guidance.

# LIST OF ABBREVIATIONS AND DEFINITIONS

| | |
|---|---|
| A2780: | human ovarian cancer cell line designation |
| ADR: | Adriamycin |
| Affi-Gel 701: | aminoethyl polyacrylamide beads |
| ATP: | adenosine triphosphate |
| CCD: | charged-couple device |
| CHO: | chinese hamster ovary cell line designation |
| COS-1: | monkey, African green, kidney cell line designation |
| Cy3: | Cy bisamine and Cy bissulphonic acid fluorophore designation |
| D: | Daltons |
| DMEM: | Dulbecco's modified eagle medium |
| DMSO: | dimethyl sulfoxide |
| DNA: | deoxyribonucleic acid |
| DOX: | doxorubicin |
| D-PBS: | Dulbecco's phosphate buffered saline |
| DT: | Diptheria Toxin |
| EDTA: | ethylenediaminetetraacetic acid |
| EGF: | epidermal growth factor |
| EPR: | enhanced permeability and retention effect |
| EBV: | Epstein-Barr virus cell line designation |
| FACT III: | fast attachment collagen-treated microcarrier beads |
| FBS: | foetal bovine serum |
| FITC: | fluorescein isothiocyanate |
| FRET: | fluorescence resonance energy transfer |

| | |
|---|---|
| GALA: | amphipathic peptide, (WEAALAEALAEALAEHLAEALAEALEALAA) |
| GFC: | gel filtration chromatography |
| $H_5$WYG: | synthetic pore-forming peptide |
| HA: | hemagglutinin virus |
| HeLa: | human cervix epitheloid carcinoma cell line designation |
| HCl: | hydrochloric acid |
| HepG2: | human hepatocellular carcinoma cell line designation |
| HPMA: | N-(2-hydroxypropyl)methacrylamide) |
| HVPE: | high voltage paper electrophoresis |
| INF: | influenza hemagglutinin, (GLFEAIAGFIENGWEGMIDGGGC [amino acid single letter code]) |
| INT: | 2-(p-iodophenyl)-3-(p-nitrophenyl)-5-phenyltetrazolium chloride |
| JTS1: | pore-forming peptide synthetic peptide, (GLFEALLELLESLWLLEA) |
| KDa: | kilo daltons |
| LDH: | lactate dehydrogenase |
| LoVo: | colorectal adenocarcinoma cell line designation |
| LSCM: | laser scanning confocal microscopy |
| MTT: | {3-(4,5-dimethylthiazol-2-yl)-2,5 diphenyltetrazolium bromide) |
| NaCl: | sodium chloride |
| PAA: | poly(acrylic acid) |
| PAGE: | polyacrylamide gel electrophoresis |
| PD: | polydye designation |
| PE: | *Pseudomonas exotoxin* |
| PEAAc: | poly(ethylacrylic acid) |
| PPAAc: | poly(propylacrylic acid) |

| | |
|---|---|
| KALA: | cationic oligopeptide (WEAK-LAKA-LAKH-LAKA-LAKA-LKAC-EA) |
| NRET: | non-radiative energy transfer |
| PEG: | polyethylene glycol |
| RBC: | red blood cell |
| RCCS: | rotary cell culture system |
| RPMI: | Roswell Park Memorial Institute |
| RNA: | ribonucleic acid |
| $S_1$': | excited singlet state |
| $S_1$: | relaxed singlet state |
| $S_o$: | ground state |
| SDS: | sodium dodecyl sulfate |
| SMANCS: | poly(styrene-co-maleic acid)-conjugated neocarzinostatin |
| SMA: | poly(styrene-co-maleic acid-half-butylate} |
| SPA: | scintillation proximity assay |
| TGN: | trans golgi network |

# TABLE OF CONTENTS

# LIST OF FIGURES

# LIST OF TABLES

# CHAPTER 1

# INTRODUCTION

## 1.1 General

The increased understanding of normal and diseases states has prompted a search for a more rational approach towards the design of drugs. Compounds may be synthesised and tailored so that they reach a precise location within the target disease. Usually, this involves the action of a drug at a specific organ in the body, or more specifically, at a defined cellular location, such as that of the nucleus. Such specificity has placed a great demand to deliver the drug to a specific site, whilst simultaneously, minimising its accumulation in non-targeted sites. The delivery of the drug to its target site is of paramount importance, as even the most potent drug will be ineffective if it is unable to interact with its target.

The advances in molecular biology and chemical synthesis, and the increased knowledge of disease states, has enabled the design and production of drugs with high molecular weights. Polymeric drug delivery systems are often employed to circumvent problems associated with the use of low molecular weight drugs. Some of the issues which polymeric drug delivery systems have been designed to overcome are listed in Table 1-1 and the key features include: increased solubility, pharmacokinetics, a decrease in side effects, increase in biocompatibility, stability, a reduction in immunogenecity, an increase in controlled drug release, and greater cellular distribution (Putnam and Kopecek, 1995; Langer, 1998; Veronese and Morpurgo, 1999; Kost and Langer, 2001).

The simplest path by which drugs enter cells is by diffusion. It is well known that diffusion through a plasma or organelle membrane is restricted to small molecules

(Foster and Lloyd, 1988) which is one of the main reasons why most therapeutics are small molecules. The large size and potential charge of high molecular weight

| The advantages of bioconjugation of polymers |
|---|
| Protection of labile drugs from chemical degradation |
| Reduction in proteolytic degradation |
| Reduction of problems associated with immunogenecity |
| A decrease in antibody recognition |
| A greater increase in body residence time |
| Increased targeting of specific organs |
| Drug penetration via endocytosis |
| New advances in drug targeting |

**Table 1-1 A list of the advantages of a polymer intended for conjugation to chemical and biological entities (modified from Veronese and Morpurgo, 1999).**

compounds prevents them from entering as many compartments as small molecules. The biodistribution of small molecules is principally governed by their permeability and affinity for biological components with diffusion being the typical method of entry into biological compartments. If the desired balance in solubility and permeability of small drug molecules can be obtained by chemical modification, the drug should be able to reach most compartments and interact with its target. In contrast to small molecules, large molecular weight material is internalised via endocytosis (refer to Section 1.2.5.2). Adding ligands to macromolecules can target the compound to specific cells and thereby result in increased uptake; however, once the material becomes endocytosed, it

still remains separated from the cell's interior by a biological membrane (refer to Section 1.2.5.1; Duncan *et al*, 1983; Blakey, 1992; Hoes *et al*, 1996; Brocchini and Duncan, 1999).

Once material has become endocytosed it is commonly delivered to the lysosomal compartment where high levels of lysosomal enzymes are present. Drugs which are sensitive to these enzymes are degraded quickly if preventive measures are not employed to protect them or to facilitate their escape into the cytosol. Their probability of success is limited by the inaccessibility of compartments to certain macromolecules in addition to a decrease in pH and the presence of degradative enzymes. The successful delivery of these and other large molecular weight compounds to their target site is currently one of the greatest obstacles limiting their success. Currently, many drugs are designed to act at specific sites within cells. As such, there is an increasing demand for knowledge of the internalisation and subcellular fate of macromolecules so that a viable therapy can be designed. Once the subcellular fate has been determined, ensuing steps can be employed to improve their delivery to the desired cellular compartment.

## 1.2 Polymeric drug delivery rationale

### 1.2.1 Rationale

Increasing numbers of new pharmaceuticals are macromolecules, however, the vast majority of current therapeutics consist of small molecular weight compounds. Small molecules are frequently chosen over macromolecules for new therapeutics owing to several advantages. Combinatorial chemistry can be employed to produce a large number of derivatives of small molecules, hence reducing the time and cost in finding an active agent (Brocchini *et al.*, 1997). Once an active compound has been found, there is often a compromise between finding activity, solubility and permeability. Highly

active agents can be abandoned as simple chemical or formulation modifications fail to produce a compound with adequate solubility and permeability whilst maintaining high activity. These and other potential problems are often overcome by conjugating drugs to water-soluble polymers (see Table 1-1).

### 1.2.2 Polymeric controlled release systems

Two types of polymer drug delivery systems exist: polymeric controlled release systems and polymer-drug conjugates. Since the focus of this research is polymer conjugates, polymeric controlled release systems will be only briefly reviewed.

Polymers can be employed to release drugs in a controlled manner. Generally, a controlled release system delivers the drug at a predetermined rate. This is usually controlled by a physical or physio-chemical response to a particular action (Kost and Langer, 1992; Roman *et al.,* 1995). Consequently, the site of drug release and that of drug action are not the same. The ideal controlled release system would maintain drug levels in a therapeutically desirable range- whether that be at a constant level, rhythmic circadian levels, or responsive to specific conditions. This could greatly reduce side effects, effectively deliver drugs with short half-lives, potentially decrease the amount of drug and dosage required and increase patient compliance. Side effects could also be decreased due to the localised release of the drug. Several types of drug delivery strategies have been conceived to achieve controlled release of drugs such as thermo, chemical, and pH sensitive hydrogels, biodegradable polymers, drug coatings, pro-drugs, liposomes and osmotic pumps.

### 1.2.3 Polymer-drug conjugates

Drugs can be covalently bound to polymers yielding polymer-drug conjugates. Drugs conjugated to macromolecules behave differently from the parent drug. A polymer should be chosen with the correct properties to avoid interactions that may decrease efficacy as well as introducing other incompatibilities. For example, the conjugation of too many hydrophobic drugs can result in intermolecular or intramolecular aggregation. This can often lead to altered solubility, biorecognition and biodistribution (Shiah *et al.*, 1998) potentially resulting in a decrease in therapeutic efficacy. A polymer should be chosen that avoids intrinsic effects whilst maximising delivery to the active site. A suitable polymer for polymer-drug conjugation should be biocompatible, non-toxic, demonstrate immunogenicity, solubility, and biodegradability of the polymer, and the drug should be capable of release from the polymer (Veronese and Morpugo, 1999; Kost and Langer, 2001).

One of the most significant changes for a drug conjugated to a polymer is the biodistribution. For low molecular weight compounds, biodistribution is mainly controlled by diffusion, surface charge and hydrophobicity. Typically, polymers are much larger than the compounds they are attached to and mask out the properties of the small drug. Even when the drug is a macromolecule, such as a large protein, polymers conjugated to the drug will coat the surface and mask the drug's properties provided the density is sufficiently high. Thus, the properties of the polymer will most often dominate the polymer conjugate's properties resulting in changes in the biodistribution, pharmacokinetics and pharmacodynamics (Putnam and Kopecek, 1995; Duncan *et al.*, 1996; Duncan, 2000; Kopecek *et al.*, 2000). The diffusion of macromolecules through biological membranes is severely limited and these compounds typically enter cells only by endocytosis (refer to Section 1.2.5.2). If the polymers are larger than the renal

threshold then elimination via glomerular filtration is reduced or halted resulting in an increased blood half-life. Changes in size can also alter the tissue distribution, which is exploited in the enhanced filtration and retention (EPR) effect. This phenomenon can be attributed to two factors, first, that leaky tumour vessels allow macromolecular extravasation not seen in normal tissues and second, that the lack of effective tumour lymphatic drainage prevents clearance of the penetrant macromolecules thus promoting their accumulation. An example of such a water-soluble injectable drug in targeting cancer includes the use of SMANCS (poly(styrene-co-maleic acid)-conjugated neocarzinostatin) or SMA [poly-stryene-co-maleic acid-half-butylate] copolymer which has been conjugated with neocarzinostatin. First developed in 1979, SMANCS has a molecular mass of 16kDa, displays albumin binding and lipophilic characteristics (Maeda *et al.,* 1979). Since 1979 it has been employed experimentally in numerous patients. It was approved for the use in hepatoma treatment in Japan in 1994 (Maeda *et al.,* 2001). SMANCS is naturally active and its SMA portion is gradually liberated under mildly acidic conditions, such as the intracellular lysosomal pH. The maleylamide bonds between SMA (maleyl residue of styrene-co-maleic acid) and the amino group on the protein which has two free amino groups (neocarzinostatin) are cleaved and the two original amino groups of neocarzinostatin are regenerated (Maeda *et al.,* 2001).

The knowledge that macromolecular conjugates accumulate in the extracellular fluid within a solid tumour mass and are subsequently internalised by pinocytosis, poses opportunities to harness a number of biochemical mechanisms so as to control the rate of drug release (Duncan, 1992). The acidic pH of some solid tumours and the low pH within the endosomal and lysosomal compartments suggest that an acid-sensitive linker could provide both rate control of drug delivery and some tumour selectivity. Ryser and Shen (1978) describe the synthesis of polymer (poly-D-lysine) conjugates which

contain the pH-sensitive spacers, *N-cis*-aconityl and *N*-maleyl derivatives of daunomycin. When linked to Affi-Gel 701 (aminoethyl polyacrylamide beads) the *cis*-aconityl derivative had a half-life for hydrolysis of less than 3 h at pH 4, but display greater stability at pH 6, demonstrating a half-life of 96 h.

The surface charge and degree of hydrophobicity can greatly affect the distribution of the polymer-drug conjugate, more so than that of molecular weight (Matthews *et al.*, 1996). As many drugs have low water solubility, conjugation to water soluble polymers can increase their solubility and this is often a reason for employing polymeric delivery. Polymer conjugation can also impact upon the amount of protein binding and other affinities. This can lead to changes in blood half-life and tissue distribution. Hence, there could be a change in the severity, number, and types of side effects in addition to changes in the therapeutic efficacy (Putnam and Kopecek, 1995; Kopecek *et al.*, 2000).

### 1.2.4 Drug targeting

Many of the therapeutic drugs currently in use have a wide distribution throughout the body. In order to achieve a therapeutic concentration at the target compartment, large doses must be administered while the majority of the drug resides in normal tissue. The drug molecules may interact with many organs and cells which can trigger unwanted side effects. Targeted drug delivery involves the selective accumulation of a compound in a pathological organ, tissue or cell where it will have the greatest effect. Such a concept of a guided missile or a "magic bullet" in drug delivery was first described by Ehrlich (Ehrlich, 1906). Ringsdorf first described a comprehensive rationale for the use of polymers as targetable drug carriers (Ringsdorf, 1975).

By targeting a drug or a drug delivery system a large change in biodistribution can be obtained regardless of whether the targeting is active or passive. When toxic drugs are used a great advantage of targeted delivery can often be the reduction in toxic side effects. Such a reduction is brought about by the targeted drug interacting only with the targeted tissue and a reduction in the interaction with non-targeted organs or compartments. Since a larger fraction of the administered dose reaches its target, lower doses can be given thus, further reducing the possibility of side effects in addition to expensive therapies (Putnam and Kopecek, 1995; Langer, 1998; Kopecek *et al.*, 2000).

Various methods exist for targeting polymers some of which include the recognition of the target molecule by different organs, specific types of cells, cellular compartments, cellular components, and specific molecules (refer to Table 1-2 for examples of each). The various targeting methods can be grouped into four main schemes. First, the direct application of the drug to the affected site (Williams *et al.*, 1996) where polymer conjugation can reduce diffusion away from the site and or act as a pro-drug controlled release depot. Second, physical targeting based on properties such as abnormal pH or temperature (Torchilin *et al.*, 1993; Torchilin, 2002) or magnetic targeting (Torchilin *et al.*, 1988; Orekhova *et al.*, 1990) via paramagnetic drug carriers. Third, passive accumulation and fourth active targeting using ligands or other vectors. These approaches to drug targeting can have a great effect in some cases, however, they cannot be applied in many situations. Direct administration of the drug or drug conjugate into a diseased organ or tissue can be technically difficult. The affected area may not be significantly different in terms of pH, temperature or vascular permeability from that of normal tissue. Magnetic drug delivery is limited owing to low blood flow rates and hence inaccessibility to the target area.

| Level of targeting | Examples |
|---|---|
| Organ/Compartment | Liver, heart, blood |
| Cellular components | DNA, cationic proteins |
| Specific molecules | A single mRNA, reverse transcriptase |
| Cellular compartments | Mitochondria, nuclei, lysosomes |
| Cell types | Macrophages, hepatocytes |

**Table 1-2 Examples of the five levels of drug targeting.**

Passive targeting involves changing the distribution of a compound without the use of a specific targeting moiety. The altered distribution may be due to a change in size, charge or hydrophobicity from that of the parent compound. The enhanced permeability and retention (EPR) effect is an example of passive targeting (Jain, 1989; Maeda *et al.*, 2001). For polymers with a molecular weight greater than 100,000 D, the extravasation of the polymer into normal tissue is limited. In contrast, tumours possess blood vessels with increased permeability (Maeda, 2001 a;b; Maeda *et al.*, 2001) as well as a defective vasculature (Skinner *et al.*, 1990) that allow macromolecules to permeate into tumours. For example, particles such as micelles and liposomes as big as 500 nm can extravasate and accumulate within the interstitial space (Torchilin, 2000). The size of material which can penetrate this leaky vasculature may vary and can depend on various other properties such as charge and hydrophobicity or hydrophilicity (Steyger *et al.*, 1996). Extensive angiogenesis can also lead to increased tumour vasculature density (Folkman and Shing, 1992). All of these factors combined can result in the enhanced permeability of macromolecules within a tumour.

Inflamed tissue is also known to have increased permeability, and macromolecules and lipids in the interstitial space are rapidly cleared via the lymphatic system (Maeda, 2001;a). Tumours are known to have a defective lymphatic drainage resulting in very slow clearance of macromolecules and lipids from the tumour interstitium (Maeda, 2001;a,b; Maeda *et al.,* 2001). The slow clearance of macromolecules is termed as "enhanced retention" and when this is combined with enhanced permeability an increased distribution of macromolecules is obtained in tumours compared to other tissue. Hence, passive targeting can be achieved by increasing the molecular weight of anticancer drugs via polymer conjugation.

Recently, polymer-anticancer conjugates based on *N*-(2-hydroxypropyl)methacrylamide) (HPMA) copolymers have been most extensively studied (Duncan, 1999; Gianasi *et al,* 1999; Vasey *et al.*, 1999). One of the main pre-requisites of the macromolecular carrier is biocompatibility. Polymer related toxicity is generally disadvantageous, but may be useful if the effects could be targeted. Encouraging *in-vitro* and *in-vivo* results have been obtained using dextrans, *N*-(2-hydroxypropyl)methacrylamide and polyamino acids such as polyaspartic acid as inert carriers for chemotherapeutic agents such as doxorubicin and mitomicin (Jensen *et al.*, 2001). The synthetic vinyl polymers such as *N*-(2-hydroxypropyl)methacrylamide are non biodegradable and so are limited to molecular weights below the renal threshold. Since maximum retention and specific uptake of the macromolecule by a solid tumour occurs for molecular weights above the renal threshold, this requirement is an obvious disadvantage. Natural degradable polymers of higher molecular weights can be used, although covalent conjugation of pendant groups may reduce susceptibility to enzymatic attack with a consequent reduction in the biodegradability. Immunogenic

response to degradation products may also limit the applicability of degradable polymers.

Most medications are micromolecular in size (< 1000 D) and are relatively free to diffuse throughout the biological system. Consequently most drugs are inherently difficult to administer in a localised, concentrated mode within the primary target tissues or organs. Polymers however, diffuse slowly and are often absorbed at interfaces. The attachment of pharmaceutical moieties can produce a biopolymer with distinct pharmacological behaviour. These polymeric drug carriers have desirable properties such as sustained therapy, slow release, prolonged activity, and drug latency.

The terms "polymer drugs" or "polymeric drugs" have been widely used for pharmaceutically active macromolecules. The term "polymer drug" means that the polymer demonstrates its own pharmaceutical activity although the corresponding monomeric species are biologically inactive. On the other hand, for a polymeric drug carrier, the polymer acts as the drug carrier. Such polymers are defined as "polymeric drugs". They can also be denoted as "macromolecular prodrugs" or "polymeric prodrugs".

Macromolecular prodrugs are designed to protect against rapid elimination or metabolisation by adding a protective polymer to the therapeutic material, Therapeutic activity is usually lost with this attachment and regained once the protective group has been removed. Usually the protective group is removed by hydrolysis. Temporary attachment of the pharmacon (drug) is necessary if the drug is active only in its free form. A drug which is active only after being cleaved from the polymer chain is termed a prodrug. Temporary attachment usually involves a hydrolyzable bond such as an anhydride, ester, acetal, or orthoester. Permanent attachment of the drug moiety is generally used when the drug exhibits its activity in the attached form. Usually, the

pharmacon is attached away from the main polymer chain and other pendant groups by means of a spacer moiety that allows for more efficient hydrolysis. The original model for pharmacologically active macromolecular prodrug was elucidated by Ringsdorf (Ringsdorf, 1975).

### 1.2.5 Entry of macromolecular prodrugs

The main consequence of drug conjugation to a macromolecular carrier (via a covalent linkage that is not rapidly hydrolysed) is the limitation of the cellular uptake of the drug to the mechanism of pinocytosis (Duncan, 1992). At the cellular level this contrasts with the ability of most low molecular weight anti-tumour agents to enter the cell by traversing (either actively or passively) the cell membrane before exerting their pharmacological effect.

The cytosolic delivery of drugs from endosomes is critical for compounds that are susceptible to attack by lysosomal enzymes. Examples of these include DNA, RNA, oligonucleotides, proteins and peptides. It is known that cellular membranes pose a major barrier to virus infection (Luo and Saltzman, 2000). It is critical that viruses deliver their genome to the cytoplasm or nucleus of a potential host without damaging the integrity of the plasma membrane or disrupting the viability of the target cell. The trafficking routes available for therapeutics are outlined in Section 1.2.5.2 and Fig. 1-2 depicts how they can act in various intracellular compartments. Viruses have developed numerous mechanisms to penetrate their targets. The enveloped viruses utilize membrane fusion, whilst the mechanisms of non-enveloped viruses are still poorly understood (Marsh, 2001). These reactions can occur either at the cell surface or following endocytosis.

Viruses have developed sophisticated and specific mechanisms for cell attachment, penetration, and genome recognition. The process by which viruses destabilise endosomal membranes in an acidification-dependent manner has been mimicked with synthetic peptides capable of disrupting liposomes, erythrocytes, or endosomes of cultured cells (Plank *et al.*, 1994). In nature, membrane disruption by amphiphilic peptides plays a key role in the pathogenesis of certain viral and bacterial toxin infections (Carrasco, 1994; Aspendon and Groisman., 1996; Ostolaza *et al.*, 1997). Such peptides contain both hydrophobic and weakly charged hydrophilic amino acid residues. Upon activation they become integrated into the extracellular or endosomal lipid bilayer membranes. For example, viruses are activated as a result of receptor-mediated binding to the surface of the extracellular membrane and pH changes within the endosome during endocytosis. The reduction in pH within the endosome (pH 5.0-6.0) results in such peptides undergoing a conformational change by which the hydrophobic groups begin to aggregate and become integrated into the lipid bilayer of the endosomal membrane. Thereafter, transient pores begin to appear within the lipid bilayer thus permitting escape of the viral capsid into the cytoplasm. The pH-dependent membrane lysis characteristics of certain peptides have been used in the disruption and fusion of liposomes (Hahn and Kim, 1991; Dacosta and Chaimovich, 1997). They have also been employed for DNA delivery vehicles and conjugates which display amphiphilic sequences from the influenza virus hemagglutinin. The HA2 peptide has been used to enhance the efficiency of gene transfection (Wagner *et al.*, 1992; Plank *et al.*, 1994).

The delivery of pH-dependent viruses to acidic organelles is the best characterised mechanism through which endocytosis facilitates virus entry. For the influenza virus, exposure of the viral fusion protein (hemagglutinin; HA) to pH values

within the range found in endosomes (pH 5.0-6.0) triggers the release of energy held in the metastable neutral pH form of the envelope protein to drive membrane fusion. These conformational changes lead to exposure of a hydrophobic region of the protein, the so-called fusion peptide. In the latent form of Influenza A envelope glycoproteins, the fusion peptide is sequestered within a pocket at the bottom of a trimeric coiled-coil formed by the hemagglutinin HA-2 subunit (Wilson *et al.,* 1981). Through a spring-loaded mechanism, the HA2 structure undergoes a global re-arrangement, which leads to propulsion of the *N*-terminal fusion peptide to the opposite end, allowing it to interact with membranes (Bullough *et al.,* 1994). Under physiological conditions low pH is the only trigger for the fusion reaction, and as low pH is normally only encountered within intracellular organelles, endocytosis is essential for entry and infection by these viruses (refer to Section 1.2.5.2). Similarly, for pH-dependent non-enveloped viruses, low pH also triggers conformational changes in the surface proteins that are required for penetration. With adenoviruses, for example, acidification generates a form of the virus that can lyse the membrane of endosomes. The viral particle is then uncoated in the cytoplasm of the new host cell by a succession of proteolytic and reductive changes.

### 1.2.5.1 Biological cell membranes

Cell membranes are crucial to the life of the cell (Alberts *et al.,* 1994). The plasma membrane encloses the cell, defines its boundaries, and maintains the essential differences between the cytosol and the extracellular environment. Inside the cell the membranes of the endoplasmic reticulum, golgi apparatus, mitochondria, and other membrane-bound organelles in eukaryotic cells maintain the characteristic differences between the contents of each organelle and the cytosol. Ion gradients across membranes, established by the activities of specialised membrane proteins, can be used

to synthesise adenosine triphosphate (ATP) or to drive the transmembrane movement of selected solutes or in nerve and muscle cells to transmit and produce electrical signals. In all cells the plasma membrane also contains proteins that act as sensors of internal signals, allowing the cell to change its behaviour in response to environmental cues; these protein sensors, or receptors, transfer information rather than ions or molecules across the plasma membrane (Alberts *et al.*, 1994).

Despite their differing functions all biological membranes have a common general structure which consists of a very thin film of lipid and protein molecules, held together mainly by non-covalent interactions. Cell membranes are dynamic, fluid structures, and most of their molecules are able to move about in the plane of the membrane. The lipid molecules are arranged as a continuous double layer about 5 nm thick. This lipid bilayer provides the basic structure of the membrane and serves as a relatively impermeable barrier to the passage of most water-soluble molecules (Simkis, 1998). The lipid bilayer has been firmly established as the universal basis for cell-membrane structure and its structure is shown in Fig. 1-1.

Lipid molecules are insoluble in water but dissolve readily in organic solvents. They make up around 50% of most animal cell membranes, with the remainder constituting protein. There are around $5x10^6$ lipid molecules per 1 $\mu$m x 1 $\mu$m area of lipid bilayer, or about $10^9$ lipid molecules in the plasma membrane of a small animal cell. Each lipid molecule in cell membranes are amphipathic (or amphiphilic). This means that they have a hydrophilic (polar) end and a hydrophobic (nonpolar) end. The most abundant are the phospholipids. These possess a polar head group and two hydrophobic hydrocarbon tails. The tails are normally fatty acids, and may differ in

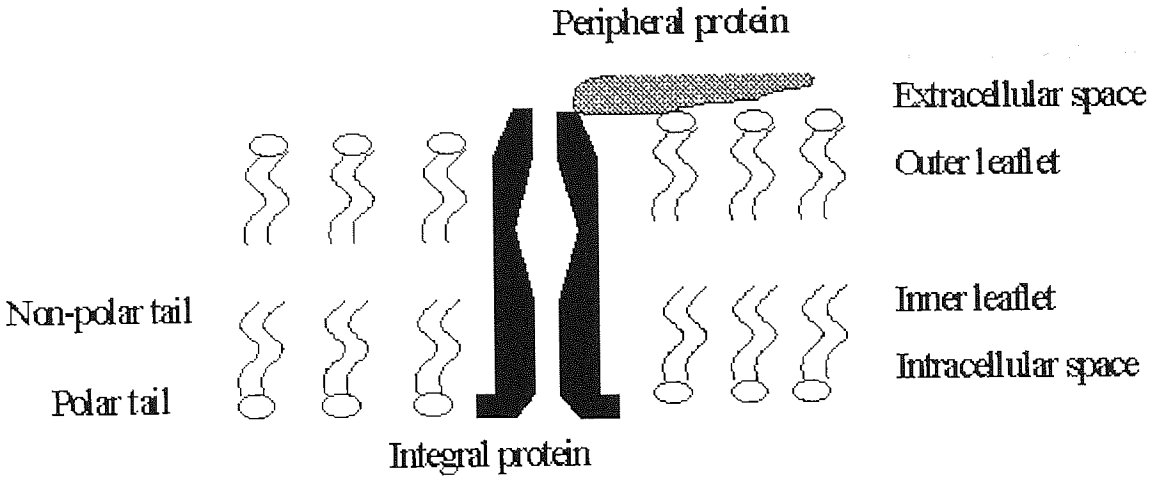


**Fig. 1-1 Cell membrane structure depicting the lipid bilayer of amphipathic molecules which consist of a polar, hydrophilic head and non-polar, hydrophobic tail. Membrane proteins make up ~50% of the total mass of membrane and consist of integral and peripheral proteins. Integral proteins are incorporated within the membrane and are associated with the hydrophobic portion of the lipid bilayer. Peripheral proteins are held at the inner or outer surface of the membrane by non-covalent electrostatic forces.**

length, usually containing between 14 and 24 carbon atoms. One tail usually has one or more *cis*-double bonds (unsaturated) while the other tail does not (saturated). Each double bond serves to create a kink in the tail. The differences in the length and saturation of the fatty acid tails are crucial as they influence the ability of phospholipid molecules to pack against one another, and thereby affect the fluidity of the membrane.

Both the shape and the amphipathic nature of the lipid molecules results in them forming bilayers spontaneously in aqueous solution. When lipid molecules are completely surrounded on all sides by water, they tend to aggregate so that their hydrophobic tails are buried in their interior and their hydrophilic heads are exposed to

water. This can be achieved in one of two ways depending on their shape: they can either form spherical micelles so that the tails are inward or they can form bimolecular sheets or bilayers with the hydrophobic tails sandwiched between the hydrophilic head groups.

Due to their cylindrical shape, membrane phospholipid molecules spontaneously form bilayers in aqueous environments. Furthermore, these lipid bilayers tend to close on themselves to form sealed compartments, thereby eliminating any free edges where the hydrophobic tails would be in contact with water. Similarly, compartments which are formed by lipid bilayers tend to reseal when they are torn.

With macromolecular prodrugs, a drug agent can enter a cell via two discrete pathways. Firstly, via a diffusion route whereby the free drug is released into the cell or secondly, via an endocytosis route which involves the entire polymer-drug conjugate. The endocytotic route is the ideal route of entry for a macromolecular prodrug. To understand the reasons for using a macromolecular drug-carrier, it is useful to consider the routes of entry for compounds into cells. Many pharmacological agents, especially low molecular weight derivatives, pass readily into cells across the plasma membrane using either passive processes or carrier-mediated transport mechanisms. As such, unless they have an inherent specificity of action, they are likely to produce unwanted side effects in cells remote from the intended site of action. For example, anticancer agents demonstrate a lack of specificity which leads to a poor therapeutic index. In contrast macromolecules do not readily pass across the plasma membrane and their capture by cells is restricted to a mechanism termed endocytosis (refer to Section 1.2.5.2).

### 1.2.5.2 Endocytosis

Endocytosis is defined as the internalisation of a portion of the plasma membrane with the concomitant engulfment of extracellular materials and extracellular fluid and this pathway is shown in Fig. 1-2. It is involved in the uptake of nutrients, the regulation of cell-surface receptor expression, cholesterol, and potentially many types of homeostasis, cell polarity and antigen presentation. Endocytosis can be divided into two types: phagocytosis and pinocytosis. Phagocytosis involves the internalisation of particulate matter by specialised cells (macrophages and monocytes). The uptake of

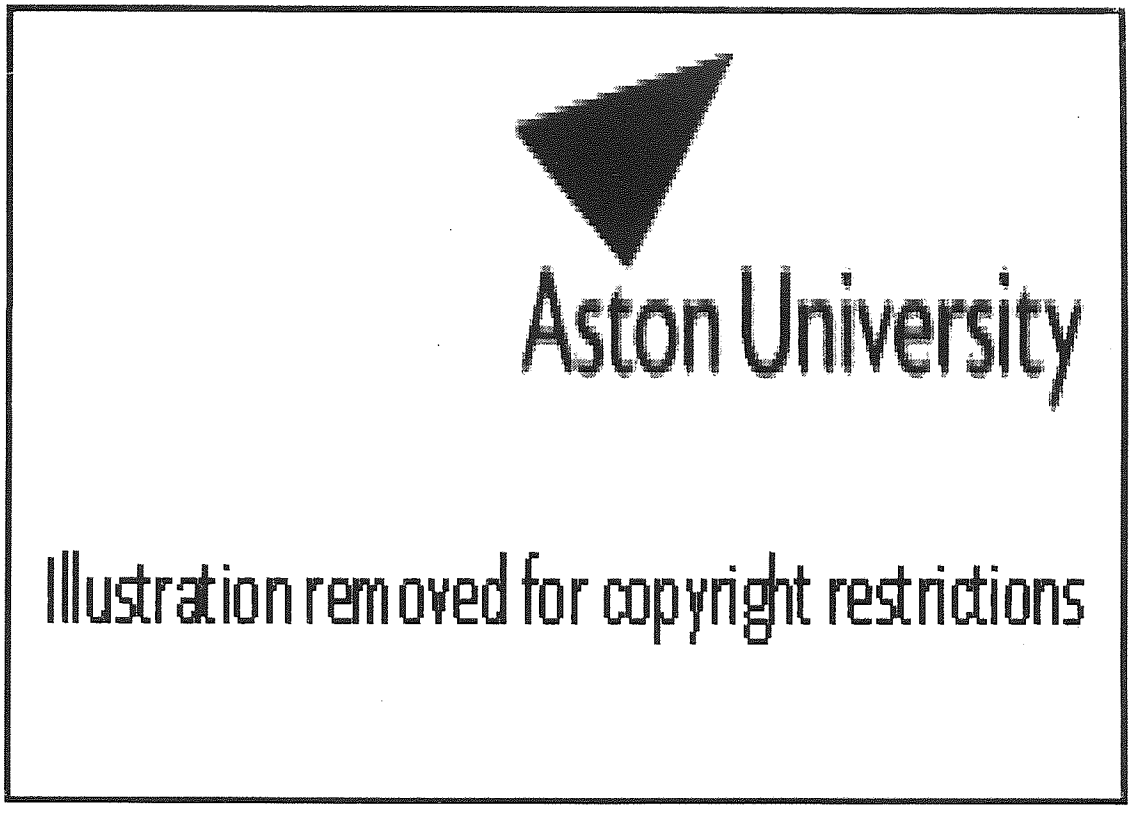


**Fig. 1-2 Methods which can facilitate the transport of DNA across cellular barriers. Ligands which interact with cell surface receptors facilitate target-cell specific uptake of DNA complexes via receptor-mediated endocytosis (reproduced from Uherek and Wels, 2000).**

particulate matter is initiated by the attachment of the particle to a cell surface with subsequent movement of the plasma membrane over the particle surface, eventually leading to the formation of a phagocytic vacuole which is then internalised. In contrast, pinocytosis is a ubiquitous process common to most, if not, all cell types (Mellman, 1996; Mukherjee *et al.*, 1997). It involves the continuous internalisation of small droplets of extracellular fluid. Unlike phagocytosis which is substrate-triggered, pinocytic membrane infolding appears to be a continual process. The newly formed pinocytic vesicles which pinch off from the cell surface are usually smaller (0.1-0.2 $\mu$m in diameter) than larger phagocytic vaculoles whose size is governed by the dimensions of the engulfed particle (generally in the order of 1 $\mu$m in diameter). During pinocytic uptake, macromolecules are captured as solutes in the extracellular fluid, a process termed fluid-phase pinocytosis. Their rate of capture is relatively slow, being directly proportional to the concentration of macromolecules in the extracellular fluid.

Pinocytosis can be divided into three classes: fluid-phase pinocytosis, adsorptive pinocytosis and receptor-mediated pinocytosis (Mellman, 1996; Mukherjee *et al.*, 1997). The terms pinocytosis and endocytosis are synonymous and no further distinction will be made in this thesis. The three classes of pinocytosis are different in terms of their interactions with cells and their rate of internalisation thereafter. In fluid-phase pinocytosis the molecule does not interact with the cell membrane. The rate of uptake here is dependent upon the concentration of the molecule in the extracellular space and the rate of endocytosis which the cell is undergoing at that particular time. Molecules with hydrophobic or charged groups display a non-specific affinity for the plasma membrane of cells. The rate of uptake here is between that of fluid-phase pinocytosis and that of receptor mediated pinocytosis (at concentrations below receptor saturation). The incorporation of macromolecular structures which are complementary

to receptors or antigens present on the cell surface leads to specific interactions and subsequent internalisation by receptor mediated endocytosis. The rate of internalisation for receptor mediated endocytosis is the highest of the three classes, with typically 10 to 50% of the material bound to receptors internalised per minute (Mukherjee *et al.,* 1997).

Pinocytosis is initiated when clathrin coated pits on the plasma membrane of the cell bud off from the cell membrane. These pits tend to be approximately 150 nm invaginations on the plasma membrane and can typically occupy about 2% of the cell surface (values vary from 0.4% in adipocytes to 3.8% for human fibroblasts; Mukherjee *et al.,* 1997). The precise role of clathrin upon internalisation is not yet known however its ubiquitous presence in endocytosis suggests that it is highly important. The formation of coated vesicles starts with the binding of coat proteins at nucleation sites in the cell membrane (Kirchhausen, 2000). The heavy and light chains of clathrin form basketlike structures around invaginations on the cytoplasmic side of the cell membrane, which possibly helps them to invaginate. Formation of clathrin coats is ATP independent which suggests spontaneous formation. It is thought that the coat assists in the physical deformation of the cell membrane to invaginate as well as localising receptors to the pits. Researchers have evidence of receptors moving to coated pits and coats forming at receptor aggregation sites (Mukherjee *et al.,* 1997). The concentration of some receptors have been found to be up to 100-fold higher in coated pits (Mellman and Warren, 2000). The mechanism by which the coated pit fuses and pinches off remains unclear however it is believed to be ATP dependent. Dynamin plays an important role as it wraps around the neck of forming vesicles and appears to help them pinch off although there is some debate about its precise role (Roos and Kelly, 1997). Clathrin coated pits are rapidly uncoated by a 70 kD ATP-dependent enzyme, and typically delivered to early endosomes (Rothman and Schmid, 1986). The amount of

endocytosis varies according to cell type; macrophages and fibroblasts may internalise 200% of their surface every hour (Mellman, 1996; Mukherjee *et al.,* 1997; Mellman and Warren, 2000).

The intermediate steps that take place between the clathrin-coated pit and the early endosomes are not well understood. It is known that 25% of internalised membrane (Presley *et al.,* 1993) and 50% of internalised sucrose (Besterman *et al.,* 1981) return to the cell surface in 2 to 3 minutes in CHO cells and 6 to 8 minutes in fibroblasts, respectively. This could either be due to the return of internalised vesicles which fuse with the membrane instead of early endosomes or rapid recycling from the early endosomes.

Once internalised, endocytosed material will become located in one of four classes of endocytic organelles, namely early endosomes, recycling vesicles, late endosomes and lysosomes (see Fig. 1-2). Early endosomes are a dynamic network of tubules and vesicles distributed throughout the cytoplasm. They have a vesicular portion of 250-400 nm in diameter with 50-60 nm outside diameter tubules up to 4 $\mu$m long. ATP-dependent pumps lower the pH to 5.9 to 6.8. The transit time is short typically lasting only 2 to 3 minutes (Mellman, 1996; Mukherjee *et al.,* 1997; Mellman and Warren, 2000).

Sorting is one of the main functions of early endosomes (Mellman, 1996; Mukherjee *et al.,* 1997; Mellman and Warren, 2000). The pH is low enough for many ligands to dissociate from their receptors. Once separated, ligands and receptors are sorted by physical and specific methods. Physical sorting is dependent upon pH, partitioning, size and solubility. Recycling is the accepted default pathway of receptors. The main recyclying pathway is geometrically driven. Various small vesicles fuse with early endosomes, resulting in a greater increase in surface area rather than an increase in

volume. Usually 60-70% of the volume is in the vesicular portion but 50-80% of the surface area is in tubules (Marsh *et al.,* 1986). Owing to their greater fractional surface area, receptors and other membrane proteins reside in the early endosomes tubular extensions which are likely sites for budding off or trafficking or recycling vesicles. These vesicles are either directed to the trans-golgi network (TGN), endosomal lumen for receptor down regulation or back to the plasma membrane.

Recycling vesicles are the main method by which receptors and other components are recycled back to the cell surface. These are thought to arise from tubular extensions of early endosomes although it is unknown whether they are created by pinching off of entire tubules or by a budding process similar to clathrin coated vesicles (Mellman, 1996; Mukherjee *et al.,* 1997). They are rich in recycled receptors with a pH slightly higher (6.4 to 6.5) than that of early endosomes. The endocytic recycling compartment mainly consists of tubules with diameters of ~50 to 70 nm which are extensively interconnected with varicosities and coats associated with them (Mukherjee *et al.,* 1997). Some recycling vesicles can fuse directly with the plasma membrane, although most perinuclear recycling vesicles stop at the microtubule organising centre before returning to the cell membrane which may serve as an intracellular pool of recycling receptors. The return of material to early endosomes has also been observed.

Endocytosed material that is not recycled back to the cell membrane ends up in late endosomes and eventually lysosomes (Mellman, 1996; Mukherjee *et al.,* 1997). Late endosomes and lysosomes are similar to each other but important differences exist. Late endosomes have similar dimensions as early lysosomes but they have a complex structure with internal membranes which are inward invaginations of the membrane

(Van Deurs *et al.,* 1993). Their pH, 5.0 to 6.0, is significantly lower than that of early endosomes.

The lysosomes have a heterogenous single membrane and consist of differently shaped organelles. They possess the lowest pH of internal organelles, 5.0 to 5.5, and are of a higher density than late endosomes. The number and appearance of lysosomes can be altered if poorly digestible solutes are endocytosed which suggests that their presence is regulated by the amount and nature of the internalised material (Mellman, 1996; Mukherjee *et al.,* 1997). A large amount of evidence suggests that the relationship between late endosomes and lysosomes is not distinct but resembles a cycle (Mellman, 1996). Soluble material is delivered from the early endosome to the late endosome. Fresh enzymes are delivered from the TGN and the pH continues to decrease. The density increases as the digestible material becomes degraded. Lower molecular weight material diffuses into the cytosol and the remaining nondigestible material is concentrated. The cycle restarts once new material is introduced. Thus, the majority of catabolism of internalised material occurs in the late endosome.

### 1.2.5.3 The nucleus of the cell

In all eukaroytes, from yeast to humans, the nuclear envelope is perforated by nuclear pores. Each pore is formed by a large, elaborate structure known as the nuclear pore complex, which has an estimated molecular mass of about 125 million and is believed to consist of more than 100 different proteins, arranged with a striking octaganol symmetry (Alberts *et al.,* 1994).

Each pore complex consists of one or more open aqueous channels whereby water-soluble molecules of specific sizes can diffuse. The size of these channels has been investigated by injecting labelled molecules that are not nuclear components into

the cytosol and then measuring the rate of diffusion into the nucleus. It was found that small molecules (5,000 D) diffuse freely into the nucleus resulting in a permeable nuclear envelope. A protein of 17,000 D takes two minutes to equilibrate between the cytosol and nucleus, while a protein of 44,000 D takes 30 minutes. A globular protein that is larger than 60,000 D does not pass easily into the nucleus (Alberts *et al.,* 1994). A quantitative analysis of such data has shown that the nuclear pore complex contains a pathway for free diffusion equivalent to a water-filled cylindrical channel about 9 nm in diameter and 15 nm long (Alberts *et al.,* 1994).

Many cellular proteins are too large to pass by diffusion through the nuclear pores. As such, the nuclear envelope allows the nuclear compartment and the cytosol to maintain different complements of proteins (Alberts *et al.,*1994). Mature cytosolic ribosomes are about 30 nm in diameter and cannot diffuse into the nucleus through the 9 nm channels. Their exclusion from the nucleus ensures that protein synthesis is confined to the cytosol. However, the nucleus has to export newly made ribosomal units and needs to import large molecules, such as DNA and RNA polymerases, which have subunit molecular weights of 100,000 to 200,000 D. These and many other protein and RNA molecules bind to specific receptor proteins located in the pore complexes and then are actively transported across the nuclear envelope through the complexes.

Generally, the more active the nucleus is in transcription, the greater the number of pore complexes its envelope contains. The nuclear envelope of a typical mammalian cell contains 3,000 to 4,000 pore complexes. If the cell is synthesising DNA, it needs to import around $10^6$ histone molecules from the cytosol every three minutes in order to package newly made DNA into chromatin, which means that, on average, each pore complex, needs to transport around 100 histone molecules per minute. If a cell is growing rapidly, a feature which is characteristic of a tumour cell, then each pore

complex needs to transport around six newly assembled large and small ribosomal subunits per minute from the nucleus to the cytosol where they are used (Alberts *et al.*, 1994).

When proteins are experimentally extracted from the nucleus and microinjected back into the cytosol, even the very large ones efficiently re-accumulate in the nucleus. The selectivity of this nuclear protein import resides in nuclear localisation signals, which are present only in nuclear proteins.

The active transport of nuclear proteins through the nuclear pore complexes have been directly visualised by coating gold particles with a nuclear protein, injecting the particles into the cytosol, and then following their fate by electron microscopy. The initial interaction of a nuclear protein with the nuclear pore complex requires one or more cytosolic proteins that bind to the nuclear localisation signals and aid in directing the nuclear protein to the pore complex, where it has been shown to bind to the fibrils that project from the rim of the complex. The nuclear protein then moves to the centre of the pore complex, where it is actively transported across the nuclear envelope by a process that requires ATP hydrolysis. The mechanism of macromolecular transport across nuclear pores is fundamentally different from the transport mechanisms involved in the transport of proteins across the membranes of other organelles, in that it occurs through a large, regulated aqueous pore, rather than through a protein transporter that spans one or more lipid bilayers. It is thought that nuclear proteins are transported through the pores while in a fully folded conformation, by contrast proteins have to be unfolded during their transport into other organelles (Alberts *et al.*, 1994).

## 1.3 Thesis Outline

The aim of the studies presented in Chapter 3 was to characterise the unlabelled pseudopeptides (refer to Chapter 3; Fig. 3-1). Polymer toxicity towards a C26 (colorectal adenocarcinoma) was investigated at physiological pH (pH 7.4) following dosing of the polymer, poly (L-lysine *iso*-phthalamide) and the copolymer, poly (L-lysine ethyl ester co L-lysine *iso*-phthalamide). An MTT-tetrazolium based assay was used to evaluate cell viability following dosing of each of the polymers at physiological pH (pH 7.4). Polymer toxicity was further examined by dosing and acidifing cell culture supernatants (pH 5.5) and measuring the pH dependent lactate dehydrogenase (LDH) release upon dosing of the polymers, poly (L-Lysine dodecanamide), and poly (L-lysine *iso*-phthalamide) and the copolymer, poly (L-lysine ethyl ester co L-lysine *iso*-phthalamide) to COS-1 and A2780 cells. These subsequent experiments were designed to investigate the cell membrane rupturing activities of these pseudopeptides at low pH (pH 5.5). A panel of different cell lines, both tumourogenic and non-tumourogenic, were chosen for the cell based cytoxicity studies. It was envisaged that owing to the pH responsive nature of the amphiphilic psudopeptides investigated in this study that their cytotoxic effects would be greater in tumour cell lines. Tumour cells proliferate at a much faster rate than normal cells. They display an increased metabolism resulting in a requirement for more glucose leading to greater lactate production and thus display a lower pH than that of normal tissue (McSheehy *et al.*, 2000).

In Chapter 4, physical characterisation of the Cy3 bisamine conjugated poly (L-lysine iso-phthalamide) polymers was completed. A Cy3 bisamine fluorophore was conjugated into the backbone of the polymer, poly (L-lysine *iso*-phthalamide) at a dye:lysine molar ratio of 1:20, 1:40, 1:60 and 1:80. Fluorophore labelling of the polymer was employed as a tool to investigate its internalisation and subcellular

localisation in cells cultured *in-vitro* (refer to Chapter 5). Native polyacrylamide gel electrophoresis (PAGE) and high voltage paper electrophoresis (HVPE) techniques were used to verify that the Cy3 bisamine fluorophore was conjugated into the backbone of the polymer, poly (L-lysine *iso*-phthalamide).

Chapter 5 summarises the use of laser scanning confocal microscopy (LSCM) to provide a realistic picture of the subcellular fate of PD20 in CHO (Chinese hamster ovary) cells cultured *in-vitro*. Fluorescence conjugation of the polymer, poly (L-lysine *iso*-phthalamide) with a fluorophore (Cy3 bisamine) was thought to be useful in examining the interaction of the polymer with cell membranes at various pH values (pH 7.4 and 5.0) and its subcellular fate following internalisation by cells cultured *in-vitro*. Fluorescence microscopy was employed to determine if PD20 interacted with the extracellular membrane of CHO cells cultured *in-vitro* and to show that this binding was enhanced at low pH (pH 5.5). Subsequent experiments precluded the use of LSCM to determine if one of the polydyes (PD20) became internalised by CHO cells cultured *in-vitro* and to determine its subcellular fate once it became internalised. Subsequently, the subcellular fate of PD30, tailored to be of a lower molecular weight than PD20 was investigated in both CHO and HepG2 cells cultured *in-vitro* using LSCM to determine if nuclear uptake could be enhanced.

Some of the data presented in this thesis was published in the *Journal of Controlled Release* (Eccleston *et al.*, 2000). In addition, a patent entitled 'Polymers and their uses' has been filed with the UK Patent Office by Cambridge University Technical Services [Application number: **GB0228525.2** (2002)]. The principal claims of the patent are as follows: (i) A method of delivering a payload into a living cell, comprising contacting the cell with a hypercoiling polymer which incorporates, or is otherwise associated, said

payload and (ii) A method of delivering a payload into the nucleus of a living cell, comprising contacting the cell with a hypercoiling carrier polymer which incorporates, or is otherwise associated with, said payload.

### 1.4 Aim of the Study

The aim of the study presented here was to investigate the subcellular fate of amphiphilic polymers comprised of amino acids containing both α- and ω-amine groups (i.e. L-Lysine and L-ornithine) that have been co-polymerised with a range of dicarboxylic acids possessing pendant hydrophobic groups (refer to Chapter 3; Fig. 3-1). It was thought that these pseudopeptides could be employed as potential polymer-drug conjugates owing to their targeting and pH-dependent conformational self-regulating properties. As such, linear polyamides with alternating, pendant hydrophilic and hydrophobic moieties were investigated.

The ability of certain polymers to hypercoil or to associate hydrophobically to form compact molecules offers one mechanism by which macromolecules can be made to change their conformation, and therefore, their function, in response to local stimuli. Polymers with weakly charged pendant groups, that is, either weak acids or bases form an extended structure as a result of intramolecular repulsion between the charged groups. The polymers which have been investigated in this study, poly (L-lysine dodecanamide) and poly (L-lysine *iso*-phthalamide), and the copolymer poly (L-lysine ethyl ester co-lysine *iso*-phthalamide), are capable of hypercoiling. Hypercoiling polymers are weak polyanions or polycations which also contain asymmetrically positioned hydrophobic moieties within, or as pendant groups on a flexible backbone. These polymers adopt an extended chain conformation at high pH (typically pH >6.0). As the pH is reduced progressive association of the pendant carboxyl groups with

protons leads to folding of the polymer molecule upon the formation of intra-molecular hydrophobic sub-domains. At pH <5.2 the carboxyl groups are completely associated and the polymers precipitate from aqueous solution (refer to Chapter 3; Fig. 1-3). This effect arises from intramolecular hydrophobic association and is referred to as hypercoiling, a process that ultimately results in the formation of a compact, insoluble, globular molecule, which precipitates from aqueous solution.

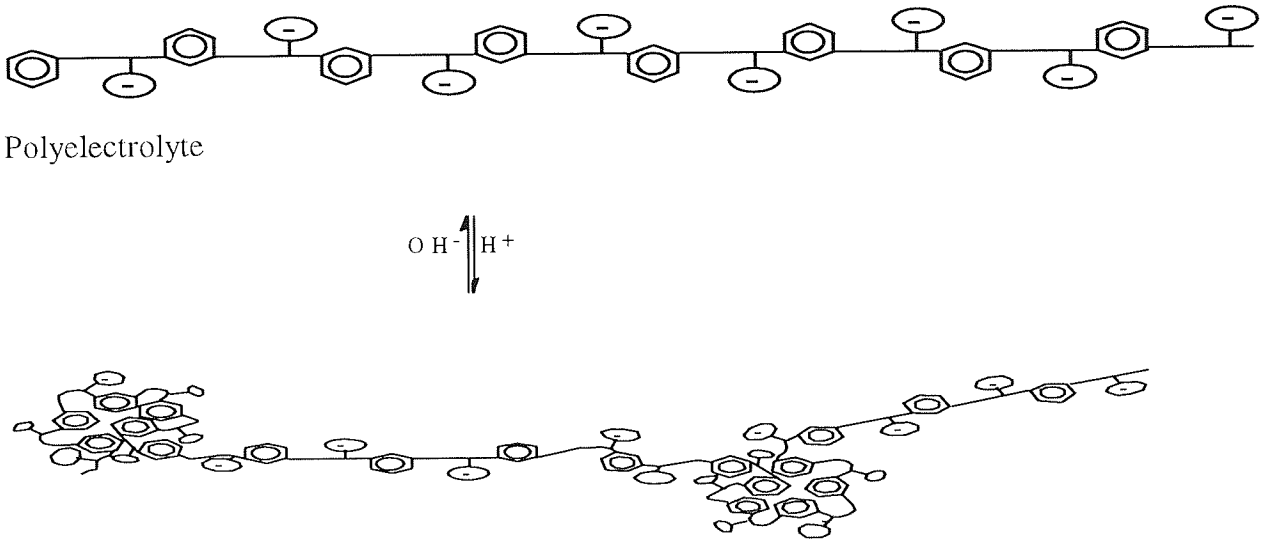


**Fig. 1-3 The proposed conformational change of poly (L-lysine *iso*-phthalamide) with a decrease in pH (reproduced with permission from Dr. Eccleston).**

Manipulation of the hydrophobic and hydrophilic balance within the polymer gives control over the pH range of conformational transition. The switch in conformation occurs over a narrow enough pH range to make such a mechanism feasible.

It was thought that these pseudopeptides could be used as novel delivery vehicles as they are capable of responding to local pH stimuli. Thus, hypercoiling polymers in their amphiphilic state could be used to encapsulate hydrophobic drugs within the core of the amphiphile. Selective delivery could be achieved by expansion of the polymer to the extended confirmation in response to localised pH change. The relatively acidic microenvironment of some solid tumours and the low pH in endosomes (pH 5.0-6.0) presents an ideal opportunity for targeting by such a mechanism.

In this study, a novel arrangement was provided so that a Cy3 bisamine fluorophore was conjugated into the polymer backbone rather than pendant to the backbone at dye-lysine ratios of 1:20, 1:30, 1:40, 1:60 and 1:80. This novel arrangement was provided so that the subcellular fate of polydye could be investigated in cells cultured *in-vitro*. The fluorescent labelling of the polymer poly (L-lysine *iso*-phthalamide; refer to Fig. 1-4) also provided a useful tool to study the polymer conformation at various pH values.

### 1.4.1 Synthetic DNA delivery systems

DNA delivery systems have traditionally been ordered into either viral-vector mediated systems and non-viral vector-mediated systems (the majority of which are synthetic). Owing to their highly evolved and specialised components, viral systems are currently the most effective means of DNA delivery. They achieve high efficiencies, usually greater than 90% for both delivery and expression. However, no evidence has

been presented for the clinical effectiveness of any gene therapy protocol. Such lack of effectiveness can be attributed to some of the limitations of viral-mediated delivery, including toxicity, restricted targeting of specific cell types, limited DNA carrying capacity, production and packaging problems, recombination and high cost. Furthermore, the inherent toxicity and viral problems associated with viral systems hinder their routine use in basic research laboratories. As such, nonviral systems, such

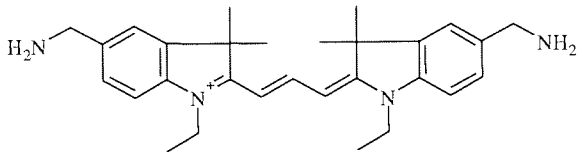


Bis-amino Cy 3

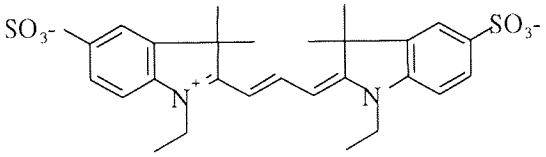


Bis-sulphonic acid Cy 3

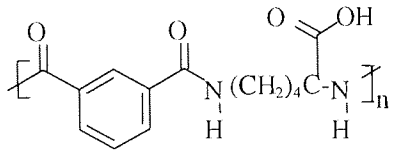


Poly (lysine *iso*-phthalamide)

General Polydye

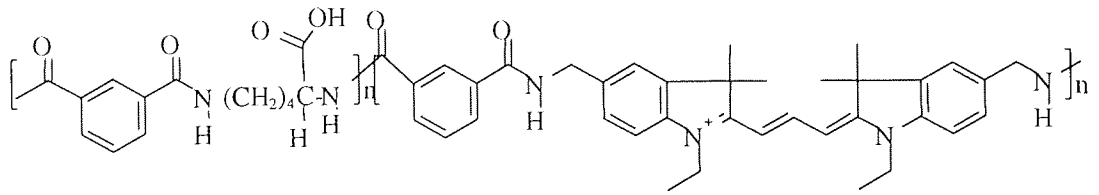


**Fig. 1-4 represents the structures of the fluorophores, Cy3 bisamine and Cy3 bissulphonic acid, the structure of the polymer, poly (L-lysine *iso*-phthalamide) and the conjugated polydye (reproduced with permission from Dr. Eccleston).**

as that of synthetic DNA delivery systems have become increasingly appealing in both basic research laboratories and clinical settings.

Most DNA delivery systems operate at one of three general levels: DNA condensation and complexation, endocytosis and nuclear targeting or entry. Negatively charged DNA molecules are usually condensed and or complexed with cationic transfection reagents before delivery. These complexes are taken up by cells, usually by an endocytic route whereby the route of uptake determines subsequent DNA release, trafficking and lifetime within the cell. Endocytosis is a multistep process which involves binding, internalisation, formation of endosomes, fusion with lysosomes and lysis (see Section 1.2.5.2). The extremely low pH and enzymes within endosomes and lysosomes usually leads to the degradation of entrapped DNA and associated complexes. Finally, DNA which has survived both endocytosis and cytoplasmic nucleases must then dissociate from the condensed complexes either before or after entry into the nucleus. Entry is believed to occur through nuclear pores which are roughly 10 mm in diameter or during cell division. Once DNA is delivered into the nucleus its transfection efficiency is dependent on the composition of the gene expression system.

The low efficiency of DNA delivery from outside the cell to inside the nucleus is a natural consequence of this multistep process. The number of DNA molecules decrease at each step in this process owing to the number of steps which are required for efficient delivery of DNA to the nucleus. As such, it is necessary to identify and overcome potential barriers so as to improve DNA delivery. Three major barriers exist in DNA delivery: low uptake across the plasma membrane (Luo and Saltzman, 2000), inadequate release of DNA molecules with limited stability, and lack of nuclear targeting.

Improvements have been made in the efficiency of DNA uptake by cells. These include mechanical, electrical and chemical methods. However, it is also essential that the DNA delivered to the nucleus is protected from both extracellular and intracellular degradation. Extracellularly, DNA can be protected from degradation by complex formation with various polymers and lipids. If the DNA is delivered systemically, it can become susceptible to blood clearance. A process known as 'opsinisation' removes 80-90% of hydrophobic particles in blood, and is thus a major limiting factor for DNA delivery when using artificial lipids.

Intracellularly, DNA must escape from normal endosomal pathways, which lead to degradation. On comparing three different cationic lipid compounds (El Ouahabi *et al.,* 1997) have observed that the efficiency of DNA delivery is correlated not only with uptake but with destabilisation and escape from endosomes. Methods to enhance DNA early release from endosomal pathways are thus being actively explored. Chloroquine, which raises endosomal pH has been used to decrease DNA degradation by inhibiting lysis (Wagner *et al.,* 1992). Synthetic peptides that include a carrier domain and an amphipathic domain for pH-dependent endosome lysis have also been investigated (Duguid *et al.,* 1998). Some attempts have been made to completely bypass endosomal pathways; subunits of toxins, such as *Diptheria* toxin (DT) and *Pseudomonas* exotoxin (PE) have been incorporated into DNA complexes to enhance transfection (Uherek *et al.,* 1998). However, this approach has been limited owing to the inherent toxicity and immunogenicity of the subunits.

#### 1.4.1.1 Delivery of protein toxins to the cytosol

With regard to the delivery of a drug to its target site, conjugation of the drug to a pH-responsive polymer could be useful in delivering drugs to target sites such as that

of the nucleus or cytosolic regions. It was thought that due to their pH responsive properties that the pseudopeptides investigated in this study could breach areas of low pH intracellularly such as that of endosomes (pH 5.0-6.0). The mechanism by which soluble, hydrophilic proteins are able to cross the barrier presented by the hydrophobic membrane is a fundamental problem in biology and protein toxins have developed various strategies to solve it (Falnes and Sandvig, 2000; Stayton *et al.*, 2000). Some of the protein toxins inherently have the machinery required for translocation, whereas others are strictly dependent on cellular components (Falnes and Sandvig, 2000). The activity of many protein toxins depends on an efficient mechanism for the delivery of the toxic domain to the cytosol (Plank *et al.*, 1998). The mechanisms by which toxins penetrate membranes is not well understood. Diptheria toxin (DT) is one of the most well studied with regard to its translocation properties and requires low endosomal pH (Falnes and Sandvig, 2000). The knowledge of its crystal structure and the availability of detailed knowledge about the DT receptor offers distinct advantages for the study of membrane translocation. DT is a single polypeptide with a molecular weight of 58,342 D (Umata and Mekada, 1998). It is proteolytically cleaved to two distinct fragments (A and B) in the presence of reducing agents. Fragment A ($M_r$ = 21,145) consists of the catalytic domain of the toxin and inhibits protein synthesis. Fragment B ($M_r$ = 37,240) is responsible for binding to the receptor and for mediating the translocation of fragment A into the cytoplasm (Umata and Mekada, 1998). The analysis of the crystal structure of DT has shown that fragment B consists of two structurally and functionally separable domains, referred to as T (transmembrane) and R (receptor-binding). The T domain is made up of nine α-helices, whereas the R domain is a β-barrel structure (Umata and Mekada, 1998). The translocation of fragment A of DT to the cytosol is initiated by binding of DT to a specific receptor on the cell surface

which has been shown to be identical to the membrane-anchored form of heparin-binding EGF-like growth factor (pro-HB-EGF; Umata and Mekada, 1998).

Previous research has shown that DT becomes internalised into endocytic vesicles via a receptor-mediated process. Several lines of evidence indicate that the acidic environment of the endocytic vesicle is required for the translocation of fragment A from the endosome to the cytosol (Raso *et al*, 1997; Umata and Mekada, 1998). In the acidic vesicle, a conformational change takes place of the toxin. This results in the insertion of the T domain into the endocytic vesicle membrane, and the enzymatically active fragment A translocates from the endocytic vesicle to the cytosol, where it exerts its toxicity (Umata and Mekada, 1998). In addition, transferrin has been exploited as a ligand to enhance the receptor mediated endocytosis of certain therapeutics (Wagner *et al*, 1994).

### 1.4.1.2 Viral fusion proteins

When carrier-plasmid complexes are taken up by either cell adsorption or by receptor mediated endosomes, the next limiting step is the release of plasmids from endosomes before their degradation takes place (Wagner, 1998). Viral genomes are released by activation of viral proteins upon acidification of the endosome. The active membrane sequences are located at the amino-terminus of such viral proteins and contain alternating clusters of hydrophobic and hydrophilic residues which form an α-helical structure. The mechanism of membrane destabilisation by endosomolytic peptides might involve either membrane rupture or pore formation (Plank *et al.,* 1998; Wagner, 1998). A number of α-helical peptides displaying pH-dependent fusogenic and endosomolytic activities have been described to facilitate lysosomal degradation before the contents of endosomes are delivered to lysosomes and thereby increase transfection

efficiency (Plank *et al.*, 1998; Wagner, 1998; Mahato *et al.*, 1999; Scheller *et al*, 1999). These peptides mimic the entry of viruses into cells and consist of random coils with no lytic activity at pH 7.0 but become endosomolytic at pH 5.0 by adopting an amphipathic α-helical conformation that interacts with the phospholipid membrane inducing fusion and lysis (Plank *et al.*, 1994; Lear and DeGrado, 1987).

Several viral fusion proteins, like the influenza virus hemagglutinin (HA) are activated by the low pH of endosomes (pH 5.0-6.0). The acidification triggers a conformational change of the protein. This results in the fusion peptide domain becoming extruded from its buried location within the protein. Commonly, the fusion peptide is located at the *N*-terminus of the protein and contains several acidic (glutamic or aspartic acid) residues. The protonation of these residues in the endosome are believed to enhance their membrane destabilising activity (Plank *et al.*, 1998).

The *N*-terminus of the influenza virus hemagglutinin subunit HA-2 has been well studied (Wiley and Skenel, 1987; Plank *et al.*, 1998). Structural information which has been gained from X-ray studies at neutral pH and at the pH of fusion indicate that, triggered by the endosomal pH, the fusion peptide is delivered at least 10 nm away from the viral surface, permitting the peptide to interact with membranes. When the peptide binds to the membrane it adopts an α-helical structure (Plank *et al.*, 1998). The low pH relieves the mutual repulsion of the acidic residues and seems to promote this transition to an α-helix, but in the presence of the lipid membrane this can also occur at neutral pH.

In this study it was envisaged that pseudopeptides may behave in a similar manner to that of previously described membrane destabilsing amphipathic peptides. Although the individual steps of membrane reorganisation are physically not well-understood, the membrane destabilising element can often be attributed to a short-

peptide domain of about 20-30 amino acids. Synthetic membrane-active peptides offer an attractive opportunity to enhance intracellular delivery of drugs by facilitating transmembrane transport. As such, many researchers have focused on the peptide-mediated endosomal escape of compounds following their endocytic uptake. For this purpose pH specific peptides can be used which destabilise endosomal membranes specifically. This means that they must not affect the integrity of the cell surface membrane as do for example the cytotoxic peptides.

The most commonly used synthetic fusogenic peptide is derived from the amino-terminal sequence of the $HA_2$ subunit of influenza hemagglutinin (INF; GLFEAIAGFIENGWEGMIDGGGC [amino acid single letter code]); Wagner *et al.*, 1992; Plank *et al.*, 1994). Another commonly used amphipathic peptide is GALA (WEAALAEALAEALAEHLAEALAEALEALAA; Parente *et al.*, 1990). INF peptides and GALA have been shown to increase the transfection efficiency when associated with poly-L-lysine-DNA, condensing peptide-DNA, cationic lipids, poly-ethyleneimine or polyamidoamine cascade polymers (Parente *et al.*, 1990; Wagner *et al.*, 1992; Zauner *et al.*, 1997). The hydrophobic face of another pore-forming peptide synthetic peptide, JTS1 (GLFEALLELLESLWLLEA) induces self-asociation and results in the formation of pores on one side of the endosomal membrane, leading to its rupture (Gottschalk *et al.*, 1996). Midoux *et al.*, (1998) have proposed a peptide, $H_5WYG$ which adopts an $\alpha$-helical structure at pH 7.0 and permeabilises cells as a random coil at pH 6.5.

Melittin, which is another membrane-active peptide, has been used to increase gene transfection (Ogris *et al.*, 2001, Ogris and Wagner, 2002). Melittin is a 26 amino acid peptide and is the main protein component of the venom of the European honey bee *Apis mellifera* and displays powerful haemolytic activity. Numerous studies have been undertaken to determine the mechanism of translocation, as well as incorporation,

of peptides and proteins into model biological membranes (Benachir and Lafleur, 1995). Melittin has been shown to produce potential-dependent ion-channels and an increase in the permeability and leakage of lipid vesicles. At micromolar concentrations melittin causes cell crenation, release of membrane fragments and lysis of red blood cells (RBCs). As such, melittin not only interacts with lipids but also with the protein components of membranes. Melittin itself is not pH-sensitive but has been shown to transfect DNA nanoparticles, possibly due to pore formation in the membrane. Membrane proteins may be included in melittin-induced leaky clusters and represent a constituent of a 'pore' or play a protective role by binding melittin and preventing its harmful interaction with the lipid bilayer. Recently, the membrane-active peptide, melittin was used for enhancing the intracellular delivery of a transgene (Ogris *et al.*, 2001). Cell culture experiments revealed that melittin enabled the efficient release of polyplexes from intracellular vesicles, and also uses a nuclear transport mechanism to enhance reporter gene expression in slowly or non-dividing cells.

#### 1.4.1.3 Synthetic endosomolytic polymers

The antimalarial drug, chloroquine is one of the classical endosomolytic agents which can prevent the acidification of endosomes, promote the swelling of the endosome vesicle and possesses membrane destabilising capability (Christie and Grainger, 2002). This molecule is capable of diffusing through the endosomal membrane in its uncharged state, however upon acidification in the endosome it becomes charged and is incapable of diffusing back out into the cytosol and becomes trapped inside the endosome. Tamoxifen, which behaves similarly to chloroquine, is a clinically applied breast cancer drug, and has been shown to promote lysosome escape of Adriamycin (ADR) in ADR-resistant cells (Altan *et al.*, 1999). ADR is sequestered

mainly in the acidic compartments of ADR-resistant cells, rendering the drug ineffective. The administration of Tamoxifen to cells in concentrations as low as 0.5 $\mu$M facilitated lysosome release of ADR and subsequent release into the cytosol and nucleus. In their free form, these drugs demonstrate efficacy *in-vitro*, however their use *in-vivo* to facilitate intracellular delivery is impractical. Adverse effects of tamoxifen treatment exist and include increased risks of liver disease which might be better addressed through polymer conjugation (Christie and Grainger, 2002).

Several synthetic constructs, for example poly (amido amines) which are endosomolytic polymers (Ferriti *et al*, 1998; Richardson *et al*, 1999; Ferruti *et al*, 2000) have been designed to work as proton sponges, that is, to prevent acidification of the endosome and promote rupture of the endosomal membrane, similar to the mechanism employed by chloroquine. Synthetic hydrophobically-modified polyelectrolytes have been used *in-vitro* to confer pH sensitivity to liposomes to enable the selective release of their contents (Thomas *et al.*, 1994;1995). Polymers possessing weak acidic side chains have been investigated for their abilities to destabilise lipid membranes (Murthy *et al.*, 1998). Lackey *et al.*, (1999) have extensively researched pH-sensitive polymers capable of lysing red blood cells (RBCs) at pH values similar to that found in endosomes (pH 5.0-6.0), while being non-disruptive at physiological pH (7.4). Poly(ethylacrylic acid) (PEAAc) and poly(propylacrylic acid) (PPAAc) have been compared for their membrane destabilising properties (Thomas and Tirrell, 1992). PEAAc, the first synthetic construct of this nature was designed to disrupt liposomal membranes and to facilitate the release of their contents in a pH-dependent manner (Thomas and Tirrell, 1992; Thomas *et al.*, 1994). The PPAAc polymer is constructed so that it incorporates shorter hydrophobic pendant side chain monomer units relative to PEAAc, which results in membrane association which is more sensitive to pH (Murthy

*et al.*, 1999). Both polymers demonstrate an increased level of haemolysis of red blood cells with increasing pH, with PPAAc showing haemolytic activity at higher pH. This can be attributed to a $pK_a$ shift of the carboxylate group in the lower dielectric biomembrane microenvironment. Polymers belonging to the alkyl acrylic acid family demonstrate greater membrane disruption capability than PEAAc (Murthy *et al.*, 1999). PPAAc demonstrates membrane-lytic activity in a pH-dependent manner (Lackey *et al.*, 1999). This polymer demonstrates minimum lytic activity towards RBCs at physiological pH with lytic activity increasing to a maximum at pH ~6.4. The pH at which membrane disruption occurred was also found to be dependent upon polymer concentration, ionic strength of the medium, tacticity and molecular weight of the polymer (Murthy *et al.*, 1999).

# CHAPTER 2

# MATERIALS AND METHODS

## 2.1 Materials

### 2.1.1 Chemicals

- MTT {3-(4,5-dimethylthiazol-2-yl)-2,5 diphenyltetrazolium bromide}(Sigma, Poole, Dorset, UK; Cat. No. M-5655).
- Trypan blue stain (0.4%; Sigma, Poole, Dorset, UK; Cat. No. T-8154).
- Dimethyl sulfoxide (DMSO; Sigma, Poole, Dorset, UK; Cat. No. T3924).
- *L*-lysine ethyl ester dihydrochloride (>99%; Sigma, Poole, Dorset, UK; Cat. No. T3924).
- Acetone (BP Chemicals, UK).
- *Iso*-phthaloyl chloride (98%; Sigma, Poole, Dorset, UK).
- *L*-lysine free base (97%; Sigma, Poole, Dorset, UK).
- Chloroform (99.9%; Sigma, Poole, Dorset, UK).
- Isopropanol (Sigma, Poole, Dorset, UK; Cat. No. 405-7).
- Methanol (Sigma, Poole, Dorset, UK; Cat. No. 82762).

### 2.1.2 Kits

- Cytotox 96® cytotoxicity assay (Promega, Southampton, UK; Cat. No. G1780).

### 2.1.3 Tissue culture media and supplements

- Dulbecco's minimum eagle medium (DMEM) (Invitrogen Life Technologies Ltd, Paisley, Scotland, UK; Cat. No. 21969-035).
- Nutrient mixture F-12 ham medium (Sigma, Poole, Dorset, UK; Cat. No. N4888).

- RPMI-1640 medium (Sigma, Poole, Dorset, UK; Cat. No. R7509).
- Foetal bovine serum (FBS; Sigma, Poole, Dorset, UK; Cat. No. F9665).
- Penicillin-streptomycin solution (100x; Sigma, Poole, Dorset, UK; Cat. No. P0781).
- L-glutamine solution (Sigma, Poole, Dorset, UK; Cat. No. G7513).
- Dulbecco's phosphate buffered saline (D-PBS; Sigma, Poole, Dorset, UK; Cat. No. D8537).
- Trypsin-EDTA solution (Sigma, Poole, Dorset, UK; Cat. No. T3924).

### 2.1.4 Dyes

- Cy3 bisamine fluorophore (Supplied by Amersham Biosciences, Cardiff, UK).
- Cy3 bisulphonic acid fluorophore (Supplied by Amersham Biosciences, Cardiff, UK).
- Fluorescent transferrin conjugate, FITC-Alexa Fluor 488 (Cambridge Bioscience, Cambridge, UK; Cat. No. T-13342).

### 2.1.5 Scintillation proximity assay (SPA) beads

- Hydrophobic SPA beads (Hydrophobic polymer laboratories, Essex Road, Church Stretton, Shropshire SY6 6AX, UK; Cat. No. SB4-SPA BEADS; Aldehyde).
- Hydrophilic SPA beads (Supplied by Amersham Biosciences, Cardiff, UK).
- FACT 111 microcarrier beads (sample supplied by Synthecon Inc., Houston, Texas, USA).

### 2.1.6 Buffers

All buffers were prepared by titrating D-PBS to various pH values with 0.1M HCl.

### 2.1.7 Electrophoresis reagents

- 12% Tris-HCl pre-cast polyacrylamide gel (Bio-Rad, Hemel Hempstead, Hertfordshire, UK; Cat. No. 161-1102).
- Native PAGE and HVPE Tris-glycine running buffer (10x); Trizma base (29g) and glycine (144 g) prepared in 1L of deionised $H_2O$. A stock solution (x10) was diluted 1 in 10 with deionised $H_2O$ (pH 8.3). The pH of the buffer (1x) was adjusted to pH 7.4 by titration with 0.1 M HCl.
- Loading buffer for native PAGE and HVPE; 20% glycerol in deionised $H_2O$.
- 3MM Whatman paper (Whatman Plc, Kent, UK).

## 2.2 Equipment

### 2.2.1 Tissue culture consumables

- Tissue culture grade flasks (75 $cm^2$; Corning, Bibby Sterilin, Staffordshire, UK).
- Sterile filters (0.2 $\mu$m; Sartorius, Epsom, Surrey, UK).
- Cryogenic vials (Fisher Scientific; Cat. No. TKV-200-128U).
- Costar 96-well microtitre plates (Corning, Bibby Sterilin Ltd., Staffordshire, UK).
- Wilco dishes (Intracel, Royston, UK; Cat. No. GWSt-1000).

### 2.2.2 Tissue culture equipment

- Boxer autoclave (Wolf Laboratories, Pocklington, York, UK).
- Sterile laminar flow hood (Nuaire Biological Safety Cabinet, Class II, obtained from Triple Red Limited, Thame, Oxfordshire, UK).
- NAPCO 6500 humidified incubator (Appleton Woods, Selly Oak, West Midlands, UK).
- Bright-line haemacytometer (Sigma, Poole, Dorset, UK; Cat. No. Z35,962-9).
- Counter tally (Fisher Scientific; Cat. No. CTL-350-B).
- Olympus CK2 light microscope (Olympus, London, UK).
- Bench-top centrifuge (Beckman Instruments, Buckinghamshire, UK).
- Anthos 2001 plate reader (Labtech International Ltd., Ringmer, East Sussex, UK).
- Nalgene's temperature controlled cooler (Mr. Frosty; Wessington Cryogenics, Tyne and Wear, UK).
- Cryogenic dewar (Fisher Scientific; Cat. No. CRY-850-130B).
- -80°C Freezer (Fisher Scientific; Cat. No. RFV-100-030J).
- Rotary cell culture system (RCCS; Synthecon Inc. Houston, Texas, USA).
- 50 ml disposable rotary cell culture system (RCCS; Synthecon Inc. Houston, Texas, USA; Part no. D-105).

### 2.2.3 Analytical equipment

- 2 ml disposable plastic cuvettes (supplied by Amersham Biosciences, Cardiff, UK).
- Quartz cuvettes (supplied by Amersham Biosciences, Cardiff, UK).
- Millipore miniplate (Millipore, Watford, UK).

- Automated Hiload (16/60) gel filtration chromatography (GFC) system fitted with a Superdex 75 column (supplied by Amersham Biosciences, Cardiff, UK).
- Fraction collector (FRAC 100; supplied by Amersham Biosciences, Cardiff, UK).
- Bio-Rad Mini-PROTEAN gel electrophoresis system (Bio-Rad, Hemel Hempstead, Hertfordshire, UK).
- Promega gel drying kit (Promega, Southampton, UK; Cat. No. G1780).
- LKB model 2117 multiphor11 electrophoresis unit adapted to be a cooled Metal Plate (Flat Bed) apparatus (supplied by Dr. P. Lambert, Dept., of Pharmacy, University of Aston, Birmingham, UK).
- Unicam UV1 UV-Vis spectrophotometer (supplied by Amersham Biosciences, Cardiff, UK).
- Aminco SPF-125 spectrofluorimeter (supplied by Amersham Biosciences, Cardiff, UK).
- YSI 2000 Glucose/Lactate analyser (YSI Limited, UK).

### 2.2.4 Imaging equipment

- Cytofluor® 4000 fluorescence multiwell plate reader (Applied Biosystems, Cheshire, UK).
- High definition fluorescence CCD image acquisition unit (Leadseeker™, Amersham Biosciences, UK).
- Typhoon 9410 imaging system (supplied by Amersham Biosciences, Cardiff, UK).
- Laser scanning confocal microscope (LSCM; Zeiss LSCM 410, supplied by Amersham Biosciences, Cardiff, UK).

- Metamorph™ image analysis software (supplied by Amersham Biosciences, Cardiff, UK).
- Fluorescence microscope (Olympus, London, UK).
- Adobe Photoshop version 5.0.
- Wallac-Victor 1420 fluorescent plate reader (Perkin Elmer Instruments, Beaconsfield, Buckinghamshire, UK).
- Olympus FV300 LSCM (supplied by Dr. Kaminski, Dept., of Chem Eng., University of Cambridge, UK).

### 2.2.4.1 Theory of fluorescence

The phenomenon of fluorescence is well documented. Electrons are capable of occurring in various energy states – a ground level of minimal energy and excitation states of higher energy. The higher energy states are reached through the absorption of energy, such as light radiation from an external source. The Jablonski diagram is depicted in Fig. 2-1 and represents the generation of fluorescence emissions where a photon of light is absorbed by the fluorophore, creating an excited singlet state ($S_1$').

The excited state lasts for approximately $1\text{-}10 \times 10^{9}$ seconds. Throughout this time period the fluorophore can undergo conformational changes and may be subjected to various possible interactions with its molecular environment. As such, the energy of the excited electron is partially redistributed, leading to a relaxed singlet state ($S_1$) from which fluorescence emission originates. Not all of the excited molecules return to the ground state ($S_0$) by fluorescence emission. Other processes are operating such as collisional quenching and fluorescence energy transfer, and the fluorescence quantum yield, or ratio of emitted photons of fluorescence to photons absorbed, depends on the extent of these processes.

Owing to the dissipation of energy during the excited state lifetime, the energy of the photon emitted to return the electron to its ground state is lower, and thus of longer wavelength than the excitation photon. The difference in energy or wavelength is termed the Stokes shift. This difference permits the detection of emission photons against a low background, isolated from excited photons.

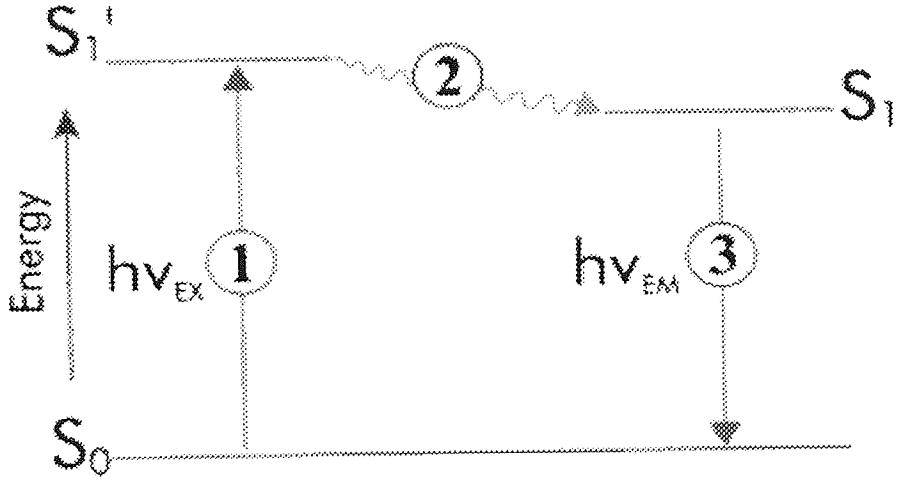


**Fig 2-1 represents the Jablonski diagram. This diagram illustrates the processes involved in the creation of an excited electronic singlet state by optical absorption and susbsequent emission of fluorescence.**

### 2.2.4.2 Confocal fluorescence microscopy

Various visual imaging techniques were employed in this study to elucidate if internalisation of PD20 was posible in CHO cells cultured *in-vitro* and to determine its subcellular fate subsequent to internalisation. Fluorescence microscopy was initially used to demonstrate that association of PD20 with the surface of the extra-cellular membrane of CHO cells varied relative to the pH values studied (pH 7.4 and 5.5).

Confocal fluorescent microscopy possesses a number of advantages over standard fluorescent microscopy. Confocal fluorescent microscopy can produce sharp,

clear images inside thick samples. High magnification lenses have very narrow focal planes. For samples which are more than a few microns thick, the majority of the light collected is unfocused and can blur the whole image. Confocal fluorescent microscopy can exclude most of the unfocused light yielding a clear image of the sample. Other advantages of confocal fluorescent microscopy over conventional fluorescent microscopy include increased effective resolution, improved signal-to-noise ratio, z-axis scanning, depth perception in Z-sectioned images and electronic magnification adjustment.

Fluorescence microscopy allows direct visualisation of the fluorescent probe only. It is often difficult to image biological samples as there can be a lack of contrast between various biological components. For example, the difference in the refractive index between the cytoplasm and the plasma membrane is small. Different contrast methods have been developed to image biological and other samples such as differential interference contrast and phase contrast.

A simplified schematic representation of the principles of fluorescent microscopy is shown in Fig. 2-2. Light from an excitation source such as a mercury lamp or laser is used to illuminate the fluorescently stained sample. When an excitation filter is placed between the light source and the dichroic mirror then the desired wavelengths of light are obtained. A dichroic mirror that reflects shorter wavelengths of light and transmits longer wavelengths is used to separate excitation from emission light. The shorter excitation wavelengths are reflected toward the sample where they excite the fluorescent molecules. These dyes fluoresce at longer wavelengths of light that are transmitted through the dichroic mirror towards the detector. The dichroic mirror reflects most of the excitation light that may be reflected or otherwise scattered by the sample. This reflection is typically ~90% efficient and an emission filter is

placed before the detector to further reduce light outside of the fluorescence wavelengths. The end result is an image of only the emitted fluorescent light indicating the location of the fluorescent marker.

In LSCM, a laser light beam is expanded to make optimal use of the optics in the objective (Pawley, 1995). Through an x-y deflection mechanism this beam is turned into a scanning beam, focussed to a small spot by an objective lens onto a fluorescent specimen. The mixture of reflected light and emitted fluorescent light is captured by the same objective and (after conversion into a static beam by the x-y scanner device) is focused onto a photodetector (photomultiplier) via a dichroic mirror (beam splitter). The reflected light is deviated by the dichroic mirror while the emitted fluorescent light passes through in the direction of the photomultiplier (Pawley, 1995). A confocal aperture (pinhole) is placed in front of the photodetector, such that the fluorescent light (not the reflected light) from points on the specimen that are not within the focal plane (the so called out-of-focus light) where the laser beam was focussed will be largely obstructed by the pinhole. In this way, out-of-focus information (both above and below the focal plane) is greatly reduced. This becomes especially important when dealing with thick specimens (Pawley, 1995). The spot that is focussed on the centre of the pinhole is often referred to as the confocal spot. A simple arrangement of a LSCM illustrating the confocal principle is shown in Fig. 2-3.

A 2-D image of a small partial volume of the specimen centered around the focal plane (referred to as an optical Section) is generated by performing a raster sweep of the specimen at that focal plane. As the laser scans across the specimen, the analog light signal, detected by the photomultiplier, is converted into a digital signal, contributing to a pixel-based image displayed on a computer monitor attached to the LSCM. The relative intensity of the fluorescent light, emitted from the laserhit point,

corresponds to the intensity of the resulting pixel in the image (typically 8-bit greyscale). The plane of focus (Z-plane) is selected by a computer-controlled fine-stepping motor which moves the microscope stage up and down. Typical focus motors can adjust the focal plane in as little as 0.1 micron increments. A 3-D reconstruction of a specimen can be generated by stacking 2-D optical Sections collected in series.

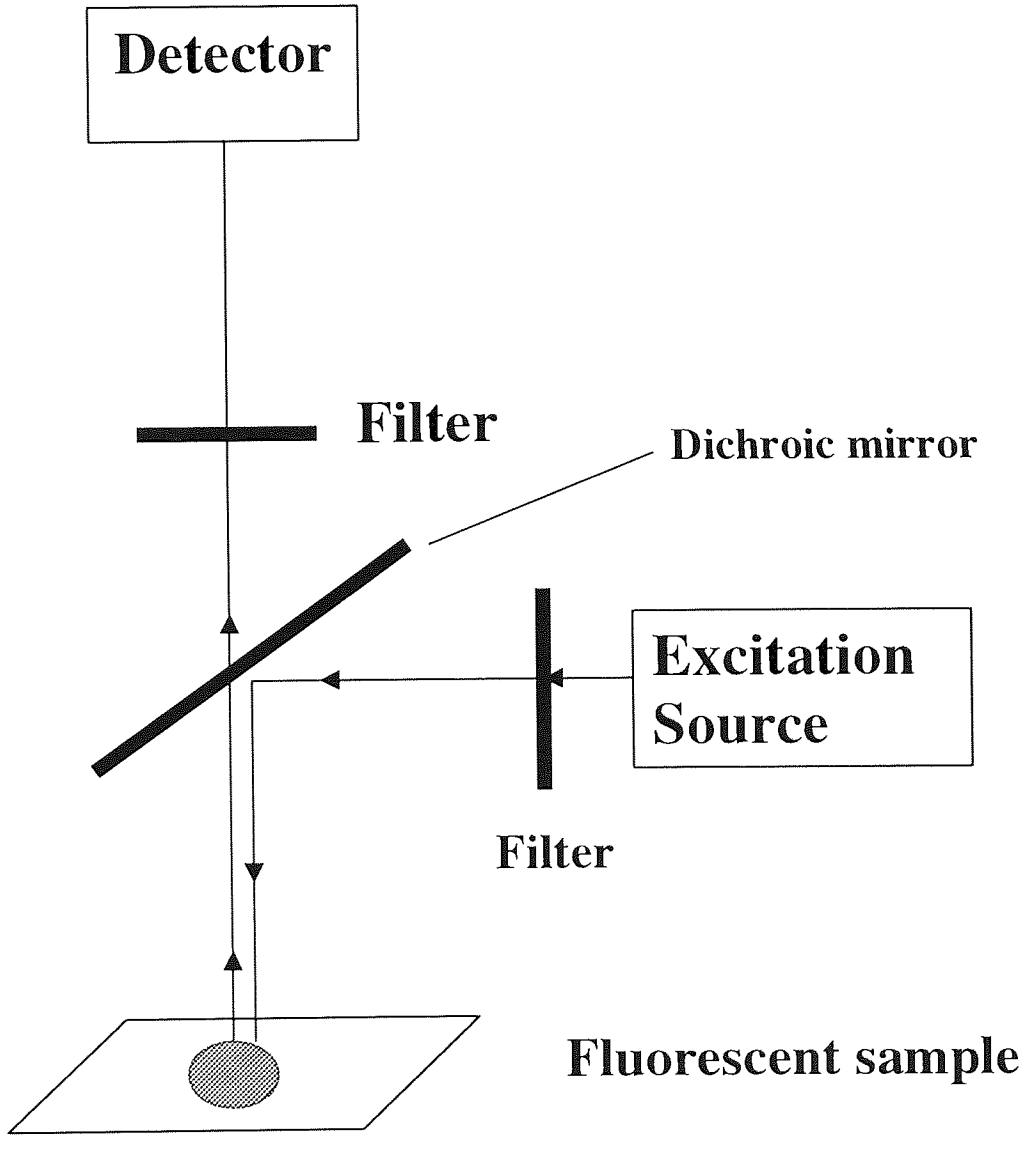


**Fig. 2-2 Simplified schematic representation of fluorescent microscopy (adapted from Pawley, 1995).**

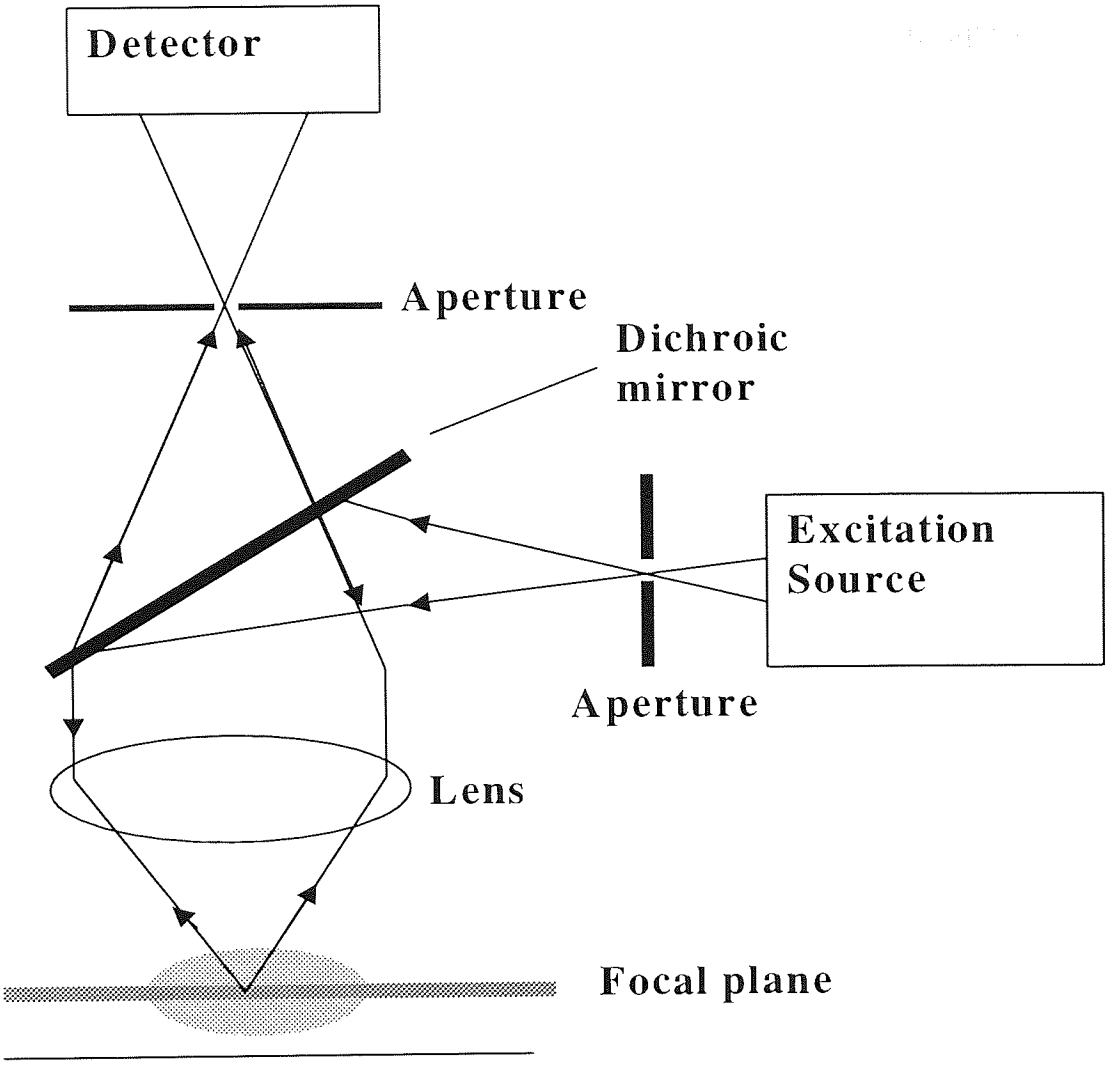


**Fig. 2-3 Simplified diagrammatic representation of the optics of a laser scanning confocal microscope (LSCM). The critical optics of a laser scanning confocal microscope in addition to the track of the fluorescent and transmitted light from the specimen to the photodetector are shown (adapted from Pawley, 1995).**

### 2.2.5 Cell lines

The cell lines employed in this thesis included:-

- C26; murine colon adenocarcinoma cell line.
- A2780; human ovarian carcinoma cell line.

- COS-1; African green monkey, kidney cell line.
- EBV-transformed B cell line; Epstein-Barr virus-transformed B cell line.
- LoVo; colorectal adenocarcinoma cell line.

All of the above cell lines were obtained from the Cancer Research Centre (CRC) at the University of Birmingham, Birmingham, UK.

- CHO; Chinese hamster ovarian cell line.
- HepG2; human hepatocyte carcinoma cell line.

Both CHOs and HepG2's were obtained from Amersham Biosciences, Cardiff, UK.

### 2.2.6 Pseudopeptides and Polydyes

#### 2.2.6.1 Pseudopeptides

Pseudopeptides prepared in this thesis were synthesised by Dr. Eccleston (Eccleston *et al.*, 2000) and are as follows:

- Poly (L-lysine *iso*-phthalamide).
- Poly (L-lysine ethyl ester co-L-lysine *iso*-phthalamide).
- Poly (L-lysine dodecanamide).

#### 2.2.6.2 Fluorophore labelled polymers (prepared by Dr. Eccleston)

Fluorophore labelled polymers (Polydyes, herein denoted as PD20, PD30, PD40, PD60 and PD80) were investigated in this thesis.

## 2.3 Methods

### 2.3.1 Culture conditions

All tissue culture manipulations were completed in sterile laminar flow hoods, using sterile disposable plasticware. Anything introduced into the culture vessels was either autoclaved or filter (0.2 $\mu$m) sterilised.

C26, COS-1 and HepG2 cell lines were grown in Dulbecco's minimum eagle medium (DMEM; refer to Appendices; Appendix II; C) containing 10% foetal bovine serum (FBS). CHO cells were grown in nutrient mixture F-12 ham medium (refer to Appendices; Appendix II; B) and A2780 cells were grown in RPMI-1640 medium (refer to Appendices; Appendix II; A). Both sets of medium for CHO and A2780 cell lines were supplemented with 10% FBS. All types of medium provide an isotonic solution of nutrients including amino acids, carbohydrate energy sources, vitamins, salts, and bicarbonate for buffering. RPMI medium is commonly used for growing suspension cells, and DMEM for adherent cells because of the relatively high concentration of calcium and magnesium in DMEM required for adherence via cadherins and integrins. RPMI-1640 medium was developed by Moore and Woods, (1976) at Roswell Park Memorial Institute, hence the acronym RPMI. Hams nutrient mixtures were originally developed to support clonal growth of several clones of CHO cells, as well as clones of HeLa and mouse L-cells. Hams F-12 has been used for the growth of primary rat hepatocytes and rat prostate epithelial cells. The contents of serum is not well defined, but is known to contain growth factors and hormones. Serum was supplied heat-inactivated to avoid the possibility of complement-mediated lysis of cultured cells. All media was supplemented with 100 U/ml penicillin and 100 $\mu$g/ml streptomycin to discourage the growth of micro-organisms. The medium in all cases was also supplemented with 200 mM L-glutamine. L-glutamine is an essential amino

acid that is required by virtually all mammalian cells in culture. All cell lines employed in this study were maintained in a humidified incubator at 37°C with 95% air and 5% $CO_2$.

The suspension cell lines (EBV-transformed B) and LoVo (colorectal adenocarcinoma) were routinely cultured in RPMI-1640 medium containing 10% FBS with 100 U/ml penicillin and 100 $\mu$g/ml streptomycin. They were subcultured twice weekly by simply re-suspending the cells and then replacing half the cell suspension with fresh medium.

Adherent cells were grown to 80% confluence in tissue culture grade flasks (75 $cm^2$) and were subcultured by discarding the spent medium, leaving the cells adhered to the bottom of the flask. The cells were then washed with 1x 5 ml of Dulbecco's phosphate buffered saline (D-PBS) and incubated at 37°C with 3 ml of trypsin-EDTA until the cells had detached from the bottom of the cell culture flask. The enzyme trypsin cuts adhesion molecules on the cell and EDTA chelates the calcium and magnesium ions esential for adhesion. Complete medium, 3 ml (containing 10% FBS, 2 mM L-glutamine and 100 U/ml penicillin and 100 $\mu$g/ml streptomycin) was added to neutralise the effects of trypsin, and typically one tenth of the cells were retained for further sub-culture.

### 2.3.2 Determination of cell concentration

The number of suspension or trypsinised adherent cells was estimated using a bright-line haemocytometer. When the cell suspension was introduced under the coverslip, it was possible to count the cells in a defined area using a microscope and a cell counter tally. A gap of 0.1 mm exists between the coverslip and the haemocytometer, so when the central 25 squares (1 $mm^2$) are counted, this represents an

area of 0.1 $mm^3$. The number of cells counted multiplied by $10^4$ equals the number of cells per ml ($cm^3$). All cell counts were made using a trans-illuminated Olympus CK2 microscope fitted with a x10 magnification lens and a x10 eyepiece.

### 2.3.2.1 Viable Cell Counts (trypan blue staining)

To distinguish between viable and non-viable cells on the haemocytometer, trypan blue staining was employed. Live cells can exclude the trypan blue stain, leaving them with a normal appearance under the microscope. Dead cells however take up the stain making them appear blue.

An equal volume of cell suspension and stain (0.4%) were mixed and applied to the bright-line haemocytometer. The number of cells counted (ignoring blue cells) is multiplied by $2x10^4$ to calculate cells/ml, thus taking into account the dilution factor upon addition of the trypan blue.

### 2.3.3 Freezing and Thawing Cells

All cell lines employed in this study (see Section 2.2.5) were frozen and stored in liquid nitrogen. Cells were cooled at a rate of 1°C per minute in a temperature controlled cooler (Nalgene's Mr. Frosty). Medium containing serum and DMSO were employed in the freezing process to prevent the formation of ice crystals inside cells that would otherwise cause cellular damage. Briefly, a Nalgene's temperature controlled cooler (Mr. Frosty) was filled with 100% isopropanol and cooled to 4°C. The adherent cell lines which were to be frozen were counted and 2 to $3x10^6$ cells were centrifuged at 1000 rpm (180 x*g*) in a bench-top centrifuge. The supernatant was discarded, and the cell pellet re-suspended in 1 ml of freezing mix (70% medium:20% FBS:10% DMSO). The cells were transferred to a cryogenic vial, put into the Mr. Frosty and placed in a -

80°C freezer overnight (24 h). The cryogenic vials were then transferred to liquid nitrogen (boiling point -196°C) for long-term storage. The suspension cell line, EBV-transformed B cell line was pelleted by centrifugation at 1000 rpm (180 x*g*) in a bench-top centrifuge. The supernatant was discarded and the pellet was re-suspended in freezing medium (50% FBS:40% medium:10% DMSO).

Cells which were preserved in liquid nitrogen were recovered for culture in the following way: (this procedure was carried out as quickly as possible, as DMSO is cytotoxic to cells); the cryogenic vials were removed from liquid nitrogen storage, and thawed by placing them in an incubator at 37°C for four minutes until the cell suspension had thawed. The cells were then mixed with 20 ml of pre-warmed medium (37°C) to dilute the DMSO, and centrifuged for 3 minutes at 3000 rpm. The supernatant was discarded, the pellet re-suspended in fresh medium (10 ml) and the cells cultured as usual. Subsequently, the cell culture flask was checked 24 h later for cell growth. Medium was changed if it contained substantial amounts of cell debris. Cells were sub-cultured twice prior to use.

### 2.3.4 Pseudopeptide and Polydye Synthesis

#### 2.3.4.1 Pseudopeptide synthesis

The pseudopeptides were synthesised according to the method described by Eccleston *et al.*, (2000). Polymers based on L-lysine and the aromatic diacid chloride iso-phthaloyl chloride were synthesised by a miscible mixed solvent technique using acetone as the solvent for the diacyl chloride and water as the solvent for the lysine. This method was also employed for the synthesis of partially-esterified copolymers whereby the initial reaction mixture contained a 4:1 molar ratio of L-lysine to L-lysine ethyl ester. The low hydrolytic stability of aliphatic dicarboxylic acids precluded the use

of a single acetone/aqueous phase reaction for these monomers. Polymers based on L-lysine and aliphatic diacyl chlorides were synthesised by an interfacial technique in which chloroform was employed as the solvent for the diacyl chloride.

The synthesis of poly (L-lysine *iso*-phthalamide) has been described in detail (Eccleston *et al.*, 2000). Briefly, a solution of *iso*-pthaloyl chloride in acetone (0.2 M) was added to a rapidly stirred, aqueous solution of L-lysine (0.2 M, 0 °C) and potassium carbonate (0.6 M) that acts as an acid acceptor. After 30 minutes the acetone was removed under vacuum. The crude polymer solutions were then concentrated to a volume of 100 ml using a Millipore miniplate™ containing a cellulose diafiltration membrane with a molecular weight cut off of 3 kD and then dialysed with deionised water to remove inorganic salts, low molecular weight oligomers and residual organic solvent. The purified polymers were then lyophilised to remove the potassium salt and stored at 4°C.

### 2.3.4.2 Polydye synthesis

Fluorophore labelled polymers (PD20, PD30, PD40, PD60 and PD80) were synthesised by Dr. Eccleston and were prepared by copolymerising L-lysine and a bisamine Cy3 cyanine fluorophore derivative with *iso*-phthaloyl chloride. The polymerisation technique was analagous to that of the unlabelled polymer, poly (L-lysine *iso*-phthalamide; Eccleston *et al.*, 2000). Using this polymerisation technique, there is no effect of dye substitution upon the molecular weights of the polydyes. Hence, the molecular weights of the polydyes do not decrease with decreasing dye substitution ratios. By way of an example, the synthesis of PD20 proceeded as follows; 1.462 g $L^{-1}$ L-Lysine (10 mM), 0.21 g bis-amine Cy3 (0.5 mM) and 4.29 g potassium carbonate (31 mM) were dissolved in 50 ml deionised water and cooled to 0 °C (note,

the polydye number denotes the molar ratio of L-Lysine to bis-amine Cy3 in the reaction mixture, in this case, 20:1). A solution of *iso*-phthaloyl chloride, 2.132 g (10.5 mM) was dissolved in 50 ml acetone, and pre-cooled (0°C). Thereafter, the organic solution was added to the rapidly stirred aqueous phase (Waring blender, full speed) and stirring was maintained for 30 minutes. The acetone was then removed under vacuum and the aqueous phase dialysed in an ultra filtration unit (Millipore, MW cut off 3 kD) with four volumes of deionised water to remove salts and oligomeric material. The resulting solution was then lyophilised to produce a deep purple solid. Polymers with higher molar ratios of L-Lysine to bisamine Cy3 were prepared analogously. It is noteworthy that in view of the marked difference in chemical structure and size of the L-lysine and bis-amine Cy-3 monomers the implicit assumption of stoichiometric incorporation of each monomer into the polymer may well be invalid. As an alternative approach, the fluorophore contents of the probes could have been estimated by employing Beer-Lambert calibrations using an extinction coefficient of 150 000 l $mol^{-1}$ $cm^{-1}$ for the polymerised fluorophore, the same as that for the free Cy3 bisamine fluorophore.

### 2.3.5 Cell viability at pH 7.4 - The MTT- tetrazolium based assay

The cytotoxic effects of the polymer, poly (L-lysine *iso*-phthalamide) and the copolymer, poly (L-lysine ethyl ester co-L-lysine *iso*-phthalamide) towards a C26 cell line (murine colorectal adenocarcinoma) were tested *in vitro* at a physiological pH (pH 7.4) by employing the hydrogen acceptor 3-(4,5-dimethylthiazol-2-yl)-2,5 diphenyltetrazolium bromide, MTT, to estimate cellular viability (refer to Chapter 3; Section 3.2.1). Aliquots (200 $\mu$l) of colon-C26 cells ($4x10^3$ cells/well) were dispensed into 96-well microtitre plates. The plates were incubated overnight in a humidified

incubator at 37°C with 95% air and 5% $CO_2$. The medium was then aspirated (200 $\mu$l) and serial dilutions of the polymers, poly (L-lysine *iso*-phthalamide) and the copolymer, poly (L-lysine ethyl ester co-L-lysine *iso*-phthalamide; 200 $\mu$l: final concentrations of 2-500 $\mu$g/ml) were added in quadriplicate (n = 4) to a final volume of 200 $\mu$l. Control wells were also prepared (n = 4) where only cells and medium (200 $\mu$l) were present. The plates were then incubated for 48 h in a humidified incubator at 37°C with 95% air and 5% $CO_2$. Using a slight modification of the protocol for the MTT assay originally described by Mossman (1983), the medium containing the polymer treatment was removed and the plates were washed once with D-PBS. A 100 $\mu$l solution of a 1 mg/ml MTT solution was added to each well and the plate was subsequently returned to the incubator (37°C) with 5% $CO_2$, for a further 4 h. Subsequently, the medium was aspirated (100 $\mu$l) using a fine needle, care was taken to not destroy the MTT crystals. Supernatant (100 $\mu$l) was carefully removed from each well and replaced with 100 $\mu$l of DMSO. Complete solubilisation of formazan crystals was achieved by repeated pipetting of the solution. The plates were then read on an Anthos 2001 plate reader and the amount of purple colour formed indicating the conversion of MTT by the redox activity of living cells was measured using a 550 nm filter. The means and standard deviations were determined for quadriplicate samples. The cytotoxic effect of the polymer, poly (L-lysine *iso*-phthalamide) and the copolymer, poly (L-lysine ethyl ester co-L-lysine *iso*-phthalamide) was expressed as the relative viability as a percentage of the control and was calculated in the following way:

Relative viability = [(experimental absorbance – background absorbance) ÷ absorbance of untreated controls – background absorbance)] × 100%.

### 2.3.6 Cell membrane disruption at pH 5.5 - Lactate Dehydrogenase (LDH) assay

The MTT assay cannot always be employed as the method of choice to demonstrate the cytoxicity profiles of certain therapeutics. It is a time-consuming assay and not all cells have the ability to metabolise MTT and others appear to lose the ability at high cell densities (Coley *et al.,* 1997). Subsequent to the MTT assay a shorter 30-minute coupled enzymatic assay, the lactate dehydrogenase (LDH; Decker and Lohmann-Matthes, 1998) assay was employed to determine the effect of each of the polymers being tested upon cellular viability following polymer dosing and acidification (pH 5.5) of cell culture supernatants. The Cytotox 96® cytoxicity assay was employed to determine LDH release profiles. The assay quantitatively measures LDH, a stable cytosolic enzyme that is released when cell lysis occurs. Released LDH in culture supernatant is measured with a 30-minute coupled enzymatic assay that results in the conversion of a tetrazolium salt (INT) into a red formazan product. The amount of colour formed is directly proportional the number of lysed cells. Visible wavelength absorbance data are collected using a standard 96-well plate reader. The assay can be used to measure membrane integrity for cell-mediated cytoxicity assays in which a target cell is lysed by an effector cell, or to measure lysis of target cells by bacteria, viruses, proteins, or chemicals.

#### 2.3.6.1 An assessment of the linearity of the LDH assay

Prior to the testing of the polymers, poly (L-lysine dodecanamide) and poly (L-lysine *iso*-phthalamide), and the copolymer, poly (L-lysine ethyl ester co-L-lysine *iso*-phthalamide) an assessment of LDH activity was carried out on the cell lines that were to be employed in the assay, namely COS-1 and A2780 cells. In independent experiments, both A2780 and COS-1 cell lines were plated into 96-well plates with

varying densities (0-20,000 cells/well) and incubated for 24 h in a humidified incubator at 37°C with 95% air and 5% $CO_2$. LDH activity was then measured in each well through the use of the Cytotox-96 assay kit. Tissue culture medium (200 $\mu$l) was removed from each of the 96-well plates containing both sets of the adherent culture cell lines, A2780 and COS-1 cell lines, respectively. Serum-free medium (200 $\mu$l) was then added into each well and the plates were placed in a -80°C freezer. The plates were then gradually thawed out at 37°C so as to allow subsequent cell rupture. Freeze-thaw lysis is a technique employed to disrupt cells without denaturing the cellular proteins within. Subsequently, using a multichannel pipette, aliquots of 50 $\mu$l from each well were dispensed in mirror fashion into fresh 96-well plates. To each well, 50 $\mu$l of the substrate reaction mixture from the Cytotox-96 assay kit was added and the colour reaction was allowed to develop for approximately 30 minutes in the dark at room temperature. Stop solution from the Cytotox-96 assay kit was then added to all wells (50 $\mu$l) and the absorbance was read within one hour at 492 nm using an Anthos 2001 plate reader.

### 2.3.6.2 LDH assay on COS-1 cells

In the initial experiments $5x10^3$ COS-1 cells (100 $\mu$l) were incubated at 37°C with 1-500 $\mu$g/ml of the polymers, poly (L-lysine dodecanamide) and poly (L-lysine *iso*-phthalamide) and the copolymer, poly (L-lysine ethyl ester co-L-lysine *iso*-phthalamide). After one hour, the cells were pelleted by centrifugation at 1000 rpm for 4 minutes and the amount of LDH released into the medium was measured. No toxicity was observed with any of the polymers used at a concentration of 100 $\mu$g/ml or lower. At a concentration of 500 $\mu$g/ml for each polymer some cytotoxic levels were observed. However, at this concentration of polymer all of the assay wells appeared turbid. This

could be attributed to increased absorbance values owing to the polymers precipitating out of solution at high concentration (500 $\mu$g/ml) upon addition of the acetic acid solution. Thereafter, a modified version of the LDH release assay was used to circumvent turbidity problems.

In the adapted protocol, cell viability was investigated following polymer dosing and acidification treatments. Subsequently, treated cells in addition to control ones (untreated) were lysed using a freeze-thaw cycle. Using this technique, the LDH assay was adapted to estimate the number of cells intact at the end of the assay (cell viability) following polymer dosing and acidication treatments, compared to untreated cells (controls). By performing the assay in this way, any factors that might have contributed to turbidity problems could be removed prior to the start of the assay.

COS-1 cells were employed in the adapted protocol (refer to Chapter 3; Section 3.2.2). COS-1 cells were trypsinised and a 100 $\mu$l cell suspension in complete medium was seeded into a 96-multiwell plate to a cell density of 10,000 cells per well. The cells were incubated overnight (24 h) in a humidified incubator at 37°C with 95% air and 5% $CO_2$. The spent medium (100 $\mu$l) was subsequently removed from each well and the cells were washed three times with D-PBS (100 $\mu$l) to remove any excess serum. A series of fresh serum-free medium samples were prepared, each containing a 1 mg/ml solution of the polymers, poly (L-lysine dodecanamide) and poly (L-lysine *iso*-phthalamide), and the copolymer, poly (L-lysine ethyl ester co-L-lysine *iso*-phthalamide). A sample (100 $\mu$l) of each polymer was added to the experimental wells in the 96-well plate (n = 4). Control wells were also prepared (n = 4) which contained COS-1 cells suspended in serum-free medium only (100 $\mu$l). The pH of each well was then adjusted immediately to pH 5.5, by titration with 0.1 M HCl. Previous titrations have shown that a shift to pH 5.5 could be achieved by adding 27.5 $\mu$l of 0.1 M HCl to a

100 $\mu$l solution of cell culture medium. Thereafter, cells were incubated in a humidified incubator at 37°C with 95% air and 5% $CO_2$ for the appropriate time-course (15, 30, 45 or 60 minutes). Following the appropriate incubation periods the spent medium (100 $\mu$l) was removed from each well and replenished with fresh serum-free medium (100 $\mu$l). The plate was then incubated in a -80°C freezer for 45 minutes to ensure 100% cell lysis. The plate was then thawed for 15 minutes in a humidified incubator (37°C with 95% air and 5% $CO_2$). The plate was then centrifuged for 4 minutes (1000 rpm). Meanwhile a flat-bottomed 96-multiwell plate was prepared containing control wells with medium (n = 4). The plate was then removed from the centrifuge and 50 $\mu$l of supernatant was transferred to each well of a newly prepared 96-multiwell flat-bottomed plate. Promega substrate mix (50 $\mu$l) was then added to each well. The plate was then wrapped in tin foil and left at room temperature for 30 minutes until the red colour product formed. Promega stop solution (50 $\mu$l) was then added to each well and the cells were then incubated at 37°C for 5 minutes to ensure a reduction in bubbles. The absorbance of each experimental well was measured at 490 nm using an Anthos 2001 plate reader and the results were presented as cell viabilities relative to control experiments, in which cells were acidified for equivalent periods of time with no polymer present.

### 2.3.6.3 LDH assay on A2780 cells

A modified version of the LDH assay was also completed by employing a different cell line, namely, A2780's (refer to Chapter 3; Section 3.2.2). The protocol that was used previously for COS-1 cells (see Section 2.3.6.2) was also employed for the A2780 cell line. However, some steps were changed appropriately. In this assay,

serum-free medium was prepared which contained a 1 mg/ml solution of the polymers, poly (L-lysine *iso*-phthalamide) and poly (L-lysine dodecanamide). A sample (100 $\mu$l; n = 4) of a solution of each polymer was added to the experimental wells. A2780 cells were incubated with the polymers in a humidified incubator (37°C with 95% air, 5% $CO_2$) for an initial period of 30 minutes. Following this, the polymers were removed and A2780's were re-suspended in fresh serum-free medium (100 $\mu$l) which was titrated to pH 5.5 using 0.1 M HCl. A2780's were then incubated in a humidified incubator at 37°C with 95% air and 5% $CO_2$ for the appropriate time course (15, 30, 45 or 60 minutes). Subsequent steps were carried out according to the method described previously for COS-1 cells (see Section 2.3.6.2).

### 2.3.7 Characterisation of polydyes

#### 2.3.7.1 Gel Filtration Chromatography (GFC)

A series of experiments were completed at the laboratories of Amersham Biosciences (Cardiff, UK) to determine if the Cy3 bisamine fluorophore moieties were conjugated into the backbone of the polymer, poly (L-lysine *iso*-phthalamide).

Gel filtration chromatography (GFC) is a liquid chromatography technique that separates molecules according to their size and it is sometimes referred to as size exclusion or gel filtration chromatography (Amersham Biosciences, Gel Filtration: Principles and Methods). Gel filtration can be used for group separations, fractionation or size analysis. In most forms of liquid chromatography, molecules are separated depending on their relative abilities to permeate into the pores of the solid-phase material. In GFC the molecules are separated according to their molecular weights, with the larger molecules eluting first as they do not penetrate into the pores of the adsorbent particles.

An automated Hiload chromatography system (Hiload 16/60) was used with a Superdex 75 column prepacked to a bed height of 60 cm and an internal diameter of 1.6 cm. The Superdex 75 column was first equilibrated overnight by passing 0.1 M phosphate buffer, pH 7.4, containing 0.1 M NaCl, through the column at a flow rate of 1 ml/min. The following day PD20 (1 mg/ml) and Cy3 bisamine fluorophore (0.05 $\mu$g/ml), both in 0.1 M phosphate buffer, were passed through the column in two independent runs (refer to Chapter 4; section 4.2.1). The column was run for 150 minutes at a flow rate of 1 ml/min. Samples (75x2 ml) were collected at regular time intervals using a (FRAC 100) fraction collector. Samples (100 $\mu$l) from each fraction collected (2 ml) were then transferred to a black Costar 96-multiwell plate with clear bottoms and the fluorescence intensity of each well was determined with a CytoFluor® 4000 fluorescence plate reader. The excitation and emission wavelengths for the Cy3 bisamine fluorophore were 530/25 nm and 590/20 nm respectively.

### 2.3.7.2 Native Polyacrylamide Gel Electrophoresis (PAGE) of the polydyes

Native PAGE of PD20, PD40, PD60 and PD80 was conducted to separate the samples on the basis of charge and size (refer to Chapter 4; Section 4.2.2). Native and SDS-PAGE are common analytical techniques used to separate and characterise proteins (Hames and Rickwood, 1990).

In SDS-PAGE the molecular weight is the principle means of fractionation. The sieving effect in gel electrophoresis is different from that in gel-filtration chromatography. In gel filtration, molecules are excluded from the interiors of the gel beads according to their size so that the largest molecules elute first. In gel electrophoresis, the gel matrix is a mesh-like membrane rather than a bead, and therefore it acts as a sieve. The mobility of larger molecules is restricted relative to that

of smaller molecules. Therefore, larger molecules travel more slowly than small molecules. In summary, the charge density, and the size and shape of a native macromolecule all affect the electrophoretic migration rates.

The electrophoretic mobility of macromolecules is also affected by the gel concentration. Higher percentage gels are more suitable for the separation of smaller proteins and peptides. Polyacrylamide gels can be prepared to have a gradient of gel concentrations. Typically the top of the gel (under the sample wells) has a concentration of 4%, increasing linearly to 20% at the bottom. Gradient gels can be useful in separating protein mixtures that cover a large range of molecular weights. Whilst gels of uniform concentration are better suited for separating proteins within a narrow molecular weight range.

Sodium dodecyl sulfate (SDS) was omitted from the native PAGE studies and PD20, PD40, PD60 and PD80 were separated using native PAGE. SDS is an amphipathic detergent with an anionic headgroup and a lipophilic tail. It binds non-covalently to proteins, with a stoichiometry of approximately one SDS molecule per two amino acids. SDS causes proteins to denature and dissociate from each other (excluding covalent cross-linking) and confers negative charge, hence in the presence of SDS, the intrinsic charge of a protein is masked. SDS is therefore used to coat the proteins so that there is an equal distribution of charge per length of protein and the rate of migration of SDS-treated proteins is effectively determined by the molecular weight of the protein. In these set of experiments SDS was omitted in the preparation as it was intended to separate the negatively charged samples of PD20, PD40, PD60 and PD80 owing to the overall negative charge conferred on the polymer, poly (L-lysine *iso*-phthalamide) at pH 7.4, and the Cy3 bisamine fluorophore (positively charged) all on the basis of charge and size (refer to Chapter 4; Section 4.2.2; Fig. 4-2; image A).

Native PAGE of various samples was conducted including PD20, the un-conjugated Cy3 bisamine fluorophore mixed with a sample of the naked polymer, poly (L-lysine *iso*-phthalamide). Controls were also run in an equivalent manner which included the Cy3 bisamine fluorophore (positively charged). In a separate native PAGE study all samples were run in an equivalent manner with the direction of the electrical current was reversed as necessary (refer to Chapter 4; Section 4.2.2; Fig. 4-2; image B).

Native PAGE was completed using a Bio-Rad Mini-PROTEAN gel electrophoresis system. A 12% Bio-Rad Tris-HCl pre-cast polyacrylamide gel with a 4% stacking gel was used. Prior to each run, the sample wells were washed first with distilled water followed by the running buffer (1x Tris-glycine buffer, pH 7.4). Samples (10 $\mu$l) of PD20, PD40, PD60 and PD80 at a concentration of 1 g $l^{-1}$ were mixed with an equal volume of loading buffer (20% glycerol) and loaded into the wells of the gel. The free Cy3 bisamine fluorophore and a mixture of the free Cy3 bisamine fluorophore with polymer, poly (L-lysine *iso*-phthalamide) were run as controls. The gel was then run at 200 V in running buffer (1x Tris-glycine buffer) at pH 7.4 until completion. It is noteworthy that the concentration of the free Cy3 bisamine fluorophore used in the Native PAGE studies was unknown. The concentration of the fluorophore could have been estimated by employing Beer-Lambert calibrations using an extinction coefficient of 150 000 l $mol^{-1}$ $cm^{-1}$ which is appropriate for the free Cy3 bisamine fluorophore.

A separate native PAGE study was completed in which the direction of the electrical current was reversed (anode to cathode) using samples and controls which were analysed previously. In this experiment a native PAGE run was undertaken whereby all samples were run in a reversed electric field (+ve; anode towards –ve; cathode) Gels were removed from the Biorad (Mini-PROTEAN II cell) gel electrophoresis kit following the completion of each run. Subsequently, gels were

imaged with a high definition fluorescence CCD image acquisition unit by employing excitation and emission wavelengths appropriate for the free Cy3 bisamine fluorophore ($\lambda_{ex}$535 nm $\lambda_{em}$595 nm, with 10 nm band widths on the excitation filter). Following imaging the gels were dried using a Promega gel drying kit. Each gel was placed between two moistened sheets of clear cellulose film (dampened with tap water), clamped between the frames provided and allowed to dry overnight. Gels dried in this way were easily viewed and could be stored for subsequent analysis.

### 2.3.7.3 High Voltage Paper Electrophoresis (HVPE) of polydyes at different pH values

HVPE was employed to separate PD20, PD40, PD60 and PD80 on the basis of their charge and size at various pH values (7.4, 6.4 and 4.8). HVPE of PD20, PD40, PD60 and PD80 was conducted at different pH values (pH 7.4, 6.4 and 4.8) to investigate the effect of changing the environmental pH upon the charge of PD20, PD40, PD60 and PD80 (refer to Chapter 4; Section 4.2.3; Fig. 4-3).

HVPE is a rapid and reproducible method for the separation and identification of small molecules such as amino acids, peptides, indoles, phenols, purines, pyrimidines, nucleotides and imidazoles. There are perceived advantages over paper and thin-layer chromatography, notably speed and the lack of any need to desalt the samples, except when the salt concentration is much higher than physiological conditions or a very large sample is to be applied. Since 1-10 kV at 50-400 mA is generally used, the main technical problems are heat dissipation and prevention of evapouration of buffer from the paper electropherogram. Two main types of apparatus have been developed to overcome these difficulties. In the first, the electropherogram is pressed down onto a water-cooled metal plate by means of a sheet of plastic foam to ensure complete and

even contact and hence uniform cooling of the paper. In the second approach, the paper is immersed in a cooled, water-immiscible organic solvent. Both techniques produce extremely similar results and the choice of technique is entirely a matter of personal preference.

An LKB model 2117 multiphor11 electrophoresis unit was adapted to be a cooled Metal Plate (Flat Bed) apparatus so that HVPE of PD20, PD40, PD60 and PD80 could be carried out at different pH values (pH 7.4, 6.4 and 4.8). The 1x Tris-glycine running buffer was titrated to various pH values (7.4, 6.4 and 4.8) using 0.1 M HCl. The point of application or origin at which the sample is applied depends on the nature of the compounds to be separated or the pH of the buffer, but it must always be located within the area of the plate. For example, all amino acids, except cysteic acid, move towards the cathode at pH 2 and so the origin should be placed near the anode end. Conversely, all organic acids move towards the anode in appropriate buffers and so the origin should be near the cathode. Mixtures containing both anions and cations should be placed near the midpoint if it is desired to examine all the components present. Since PD20, PD40, PD60 and PD80 display an overall net negative charge at physiological pH (7.4), and the free Cy3 bisamine fluorophore, a positive charge a midpoint origin was chosen in order to achieve HVPE of all the samples investigated. The origin line was drawn in pencil across 3MM Whatman paper. Samples of PD20, PD40, PD60 and PD80 at a concentration of 1 g $l^{-1}$ were mixed with an equal volume of loading buffer (20% glycerol) and loaded onto the marked pencil areas. The free Cy3 bisamine fluorophore was used as a control. All samples were run in running buffer (1x Tris-glycine buffer) which was titrated to various pH values (pH 7.4, 6.4 and 4.8) using 0.1 M HCl. PD's sample size conducted at pH 7.4 on HVPE was 10 $\mu$l whereas the sample size at pH 6.4 and 4.8 was 20 $\mu$l due to limited sample volume. A 1%

bromophenol blue solution was used as a marker since it is negatively charged and moves towards the anode. The transparent lid was then closed and a voltage of 300 V was applied for 2 h. At the end of the experiment the 3MM Whatman paper was removed from the HVPE apparatus, held by bulldog clamps and dried using a domestic hairdryer. This was completed for each pH investigated (pH 7.4, 6.4 and 4.8). Subsequently, HVPE samples were then imaged using a Typhoon 9410 imaging system with excitation and emission wavelengths set for the free Cy3 bisamine fluorophore ($\lambda_{ex}$535 nm and $\lambda_{em}$595 nm respectively).

### 2.3.8 The fluorescence intensity (I) of polydyes in the presence and absence of serum

Albumin is the most abundant plasma protein *in-vivo* and it is generally accepted that once a drug is administered some kind of interaction will occur with this molecule (Esposito and Najjar, 2002). Hence, it was considered to be important to study the interaction of the polymer, poly (L-lysine *iso*-phthalamide) with this protein. Experiments were designed to determine if the fluorescence of the polydyes (PD20, PD40, PD60 and PD80) was affected in the presence of serum (refer to Chapter 4; Section 4.2.4). Separate stock solutions of each of the polydyes (PD20, PD40, PD60 and PD80) were prepared in D-PBS buffer in the absence and presence of serum (10%) and were titrated to the different pH values (pH 4.0-7.4) using 0.1 M HCl.

Initially, 100 $\mu$l samples (n = 3) of a known concentration (60 $\mu$g/ml) of each of the polydyes (PD20, PD40, PD60 and PD80) at the various pH values (pH 4.0-7.4) in either serum free D-PBS or D-PBS which contained serum to a final concentration of 10% were prepared in 96-multiwell black costar plate with clear bottoms and the fluorescence was compared as function of pH (pH 4.0-7.4; refer to Chapter 4; Fig. 4-4).

Subsequent to the initial study, various concentrations of PD20 were prepared (5-100 $\mu$g/ml) in either D-PBS buffer with and without serum (10%) at pH 7.4 to determine if different concentrations of PD20 (5-100 $\mu$g/ml) in the presence of the same final concentration of serum (10%) displayed an effect upon the fluorescence (refer to Chapter 4; Fig. 4-6). Samples (100 $\mu$l; n = 3) of the various concentrations of PD20 (5-100 $\mu$g/ml) at pH 7.4 in either serum free D-PBS or D-PBS which contained serum to a final concentration of 10% were prepared in 96-multiwell black costar plate with clear bottoms and the fluorescence was compared as function of concentration (5-100 $\mu$g/ml) as described above.

In a further set of studies the effect of varying the concentration of serum (0-40%) upon the fluorescence of PD20 was determined (refer to Chapter; Fig. 4-7). Samples (100 $\mu$l; n = 3) of PD20 (60 $\mu$g/ml) in D-PBS buffer at pH 7.4 with varying concentrations of serum (0-40%) were prepared in 96-multiwell black costar plate with clear bottoms and the fluorescence of PD20 was compared as function of varying the concentration of serum (0-40%).

The average fluorescence intensity (I) of all samples was measured on a Wallac-Victor$^2$ 1420 fluorescent multiwell plate reader with the exciatation and emission wavelengths set for the detection of the free Cy3 bisamine fluorophore ($\lambda_{ex}$535 nm, $\lambda_{em}$590 nm).

### 2.3.9 UV-Vis absorption spectroscopy of the free Cy3 bisamine fluorophore prepared in various media compared to that of PD20

UV-Vis absorption spectroscopy profiles of the free Cy3 bisamine fluorophore in various cell culture media and PD20 were obtained to determine if there was a shift in the maximum absorption values subsequent to conjugation into the backbone of the

polymer, poly (L-lysine *iso*-phthalamide). Samples of the free Cy3 bisamine fluorophore (unknown concentration due to availability) were prepared in two types of tissue culture media namely F12 Nutrient Ham Mixture, and DMEM without phenol red. UV-Vis absorption spectra were obtained by scanning the UV-Vis spectrum between 350-700 nm on a Perkin-Elmer UV-Vis spectrophotometer (refer to Chapter 4; Section 4.2.5; Fig. 4-8). Control scans were completed in an equivalent manner for each tissue culture medium preparation without the free Cy3 bisamine fluorophore.

UV-Vis absorption and fluorescence spectroscopy of PD20 was assessed to determine if first, there was a shift in the maximum absorbance of PD20 following conjugation of the Cy3 bisamine fluorophore into the backbone of the polymer, poly (L-lysine *iso*-phthalamide) compared to that of the free Cy3 bisamine fluorophore. And second to study the effect of varying the pH and the solvent polarity in the surrounding medium of PD20 upon its absorption values.

In the initial study, various samples of PD20 were prepared in serum-free medium and titrated to pH 7.4, 5.08 or 4.8 using 0.1 M HCl. Separate samples of PD20 were prepared in medium at physiological pH (7.4) containing serum (10%). A further sample of PD20 was prepared in methanol. All PD20 samples tested were prepared to a concentration of $1.9 \times 10^{-2}$ $gL^{-1}$. A scan of the UV-Vis spectrum of all samples of PD20 was completed between 350 and 700 nm using a Perkin-Elmer UV-Vis spectrophotometer (refer to Chapter 4; Section 4.2.5; Fig. 4-9). All samples were further characterised and excitation and emission profiles of each were obtained using an Aminco SPF-125 spectrofluorimeter ($\lambda_{ex}$ 556 nm $\lambda_{em}$ 579 nm; refer to Appendix 2; Fig. A).

The samples of PD20 tested previously for their excitation and emission profiles were further characterised for their fluorescence output (refer to Appendix II; Fig. B).

The previously investigated samples of PD20 with the exception of PD20 in methanol were prepared so that they were of an equivalent absorption unit (0.09+/-0.001) by employing the Perkin-Elmer UV-Vis spectrophotometer. These samples were then analysed for their fluorescence output and an excitation and emission spectra was produced for each sample by employing the Aminco SPF-125 spectrofluorimeter ($\lambda_{ex}$ 556 nm $\lambda_{em}$ 579 nm; refer to Appendix II; Fig. B).

### 2.3.10 The association of PD20 with scintillation proximity assay (SPA) beads

Hydrophobic and hydrophilic SPA beads were used as test substrates to determine if the association of PD20 with hydrophobic beads at low pH (5.0) would increase owing to the association of carboxyl groups along the polymer backbone resulting in increased hydrophobicity at this pH. The aim of this experiment was to determine if there was an effect upon the fluorescence of PD20 in the presence of either hydrophobic or hydrophilic SPA beads (refer to Chapter 4; Section 4.2.6). A sample of hydrophobic SPA beads (10 $\mu$l; quantity of 100 g at 104 mg/g in PBS/azide) and PD20 (500 $\mu$l) were prepared in D-PBS buffer which was titrated to various pH (5.0, 5.5, 6.0 and 7.4) using 0.1 M HCl. A sample of each was added to separate Wilco dishes (n = 4; pH 5.0, 5.5, 6.0 and 7.4). Sample dishes (n = 4; pH 5.0, 5.5, 6.0 and 7.4) were placed on the laser scanning confocal microscope (LSCM; Zeiss 410). The hydrophobic SPA beads were allowed to settle in the Wilco dishes for a period of 10 minutes. Images were then obtained of PD20 binding to the beads at the various pH values being studied (pH 5.0, 5.5, 6.0 and 7.4). Images were then quantified for their average grey value total fluorescence intensity (I) values through the use of Metamorph™ software (refer to Chapter 4; Fig. 4-10; B). Hydrophilic SPA beads were also assessed in the same manner to assess their binding properties to PD20 at a more wider range of pH values (pH 4.8,

5.0, 5.5, 6.0, 6.5 and 7.4; refer to Chapter 4; Fig. 4-10; A) than those investigated previously for the hydrophobic SPA beads (pH 5.0, 5.5, 6.0 and 7.4).

### 2.3.11 Fluorescence microscopy of PD20 with CHO cells at pH 7.4 and pH 5.5

Fluorescence microscopy was undertaken to determine if PD20 would associate with the extracellular membrane of CHO cells cultured *in-vitro* at physiological pH (pH 7.4) and at a low pH value of 5.5 (refer to Chapter 5; Section 5.2.1). A CHO cell suspension (2 ml of 100,000 cells/ml) was seeded into Wilco dishes and incubated overnight (24 h) in a humidified incubator at 37°C with 95% air and 5% $CO_2$. The following day, the supernatant in the Wilco dishes containing the CHO cells was removed, and the cells were washed (3x) with 2 ml of D-PBS (pH 7.4) to remove the presence of any excess serum proteins. Subsequently, a 2 ml volume of either PD20 (1 mg/ml) at pH 7.4 or PD20 (1 mg/ml) at pH 5.5 was added to independent Wilco dishes. Both dishes were then incubated in a humidified incubator at 37°C with 95% air and 5% $CO_2$ for a period of 30 minutes. PD20 treatments (2 ml) were subsequently removed from independent Wilco dishes, and the cells were washed (x3) with D-PBS (2 ml) which was either titrated to pH 7.4 or 5.5. CHO cells were then re-suspended (2 ml) in the appropriate buffers (pH 7.4 or 5.5). The cells were visualised using a fluorescence microscope with a x20 magnification eyepiece. The excitation and emission wavelengths were set at the excitation and emission wavelengths appropriate for the detection of the free Cy3 bisamine fluorophore ($\lambda_{ex}$ 535 nm and $\lambda_{em}$570 nm). Fluorescent photomicrogram images of CHO cells cultured *in-vitro* and the association of their extracellular membranes with PD20 at pH 7.4 and pH 5.5 were determined (refer to Chapter 5; Fig. 5-1; A and B). A phase contrast image of CHO cells was obtained and was used to highlight the association of PD20 with the extracellular

membrane of CHO cells cultured *in-vitro* at pH 7.4 (refer to Chapter 5; Fig. 5-1, image A). A fluorescent image of CHO cells cultured *in-vitro* and association of PD20 with the surface of the extracellular membrane at pH 5.5 (refer to Chapter 5; Fig. 5-1, image B) was overlaid onto the previously obtained phase contrast image to highlight the fluorescence of CHO cells cultured *in-vitro* at pH 5.5.

### 2.3.12 Laser scanning confocal microscopy (LSCM) images of CHO cells cultured *in-vitro* demonstrating the subcellular fate of PD20 at pH values of 7.4 and 5.0.

Experiments were designed using laser scaning confocal microscopy (LSCM) to determine if internalisation of PD20 (1 mg/ml) by CHO cells cultured *in-vitro* (160,000/ ml) at pH values of 7.4 and 5.0 was possible (refer to Chapter 5; Sections 5.2.2.1 and 5.2.2.2 repectively). CHO cells (80,000/ml) were seeded into Wilco dishes and incubated in a humidified incubator at 37°C with 95% air and 5% $CO_2$. The following day, medium containing serum was removed from independent Wilco dishes and CHO cells were washed (3x) with D-PBS (2 ml) to remove the presence of any excess serum proteins. Subsequently, CHO cells were incubated with a 2 ml volume of PD20 (1 mg/ml) prepared in serum-free medium (F12 Nutrient Ham Mixture) which had been titrated previously using 0.1 M HCl to pH values of 7.4 and 5.0. The CHO cells were then incubated in a humidified incubator at 37°C with 95% air and 5% $CO_2$ for 10 minutes. Subsequently, the supernatant in the Wilco dishes was removed and CHO cells were washed (3x) with D-PBS (2 ml) which had been pH'd to the various pH values under study (pH 7.4 and 5.0). CHO cells cultured *in-vitro* were then placed in the appropriate serum free medium (2 ml volumes at pH 7.4 or 5.0). The dishes were placed on a heater stage (37°C) and LSCM images were obtained. CHO cells were imaged

using a LSCM for a period of 10 to 60 minutes following the initial incubation period (10 minutes at 37°C) with PD20 (1 mg/ml). LSCM (Zeiss 410) was used to visualise the time-dependent internalisation or adsorption to the extracellular membrane of PD20 (1 mg/ml) by CHO cells (160,000/ml) at various time points following the initial incubation period of 10 minutes at 37°C at pH values of 7.4 and 5.0 (refer to Chapter 5; Fig. 5-2 and Fig. 5-4 respectively). The excitation and emission wavelengths were 535 nm and 570 nm which is appropriate for the detection of the free Cy3 bisamine fluorophore. To clearly display the time-dependent internalisation of PD20 in CHO cells cultured *in-vitro*, the cells were imaged for 60 minutes (the cells were imaged at 10-minute intervals to reduce photobleaching and cell exposure to the laser) following the initial incubation period (10 minutes at 37°C). Subsequent to LSCM, the average grey value toal fluorescence in each of the images obtained previously were quantified using Metamorph™ image analysis software (refer to Chapter 5; Fig. 5-3 and Fig. 5-5). Adobe Photoshop version 5.5 was employed to visualise the LSCM images obtained.

A similar study was completed to determine where the free Cy3 bisamine fluorophore trafficked to following internalisation at pH 7.4 (refer to Chapter 5; Section 5.2.3). CHO cells were cultured *in-vitro* according to the method described above and were incubated (10 minutes) with a sample of the Cy3 bisamine fluorophore which was prepared to be of an equimolar concentration (139 $\mu$g/ml) to that of the previously tested sample of PD20 (1 mg/ml). LSCM images were obtained (refer to Chapter 5; Fig. 5-6) according to the method described previously for PD20.

### 2.3.13 Co-localisation of PD20 with FITC-Alexa fluor 488

To determine where PD20 (1 mg/ml) was trafficking to following internalisation at pH 7.4, simultaneous uptake studies of PD20 (1 mg/ml) and a fluorescent transferrin

conjugate, FITC-Alexa Fluor 488 was completed (refer to Chapter 5; Section 5.2.4). FITC-Alexa Fluor 488 is an endosomal marker has greatly aided the investigation of the process of endocytosis. HepG2 cells were selected to study the colocalisation of PD20 with the FITC-Alexa Fluor 488 conjugate as they express the transferrin receptor.

HepG2 cells (80,000/ml) were seeded into Wilco dishes, and incubated overnight at 37°C. The following day, HepG2 cells were incubated in a humidified incubator at 37°C with 95% air and 5% $CO_2$ for a period of 15 minutes with a sample mixture comprised of both PD20 and FITC-Alexa Fluor 488, so that the final concentration of PD20 addition was 1 mg/ml and that of the FITC-Alexa Fluor 488 was equivalent to 50 $\mu$g/ml. Both solutions of PD20 and FITC-Alexa Fluor 488 were prepared in serum free medium appropriate for HepG2 cells (Dulbecco's modified eagle medium) at pH 7.4. The supernatant (2 ml) was removed and the cells were washed 3x in the appropriate serum free medium (2 ml). Cells were then re-plenished with a 2 ml volume of the appropriate serum free medium and placed on a heater stage (37°C) on the LSCM (Zeiss 410). Subsequently, HepG2 cells were imaged using LSCM. For the detection of PD20, the excitation wavelength was 535 nm and the emission wavelength was 570 nm, which are appropriate settings for the detection of the Cy3 bisamine fluorophore. For detection of FITC-Alexa Fluor 488 an excitation wavelength of 495 nm and an emission wavelength of 518 nm was employed. Adobe Photoshop version 5.0 was employed to visualise the LSCM images obtained (refer to Chapter 5; Section 5.2.5; Fig. 5-7).

### 2.3.14 The subcellular fate of PD30 in CHO cells cultured *in-vitro*

To investigate if greater nuclear localisation of polydye could be achieved in CHO cells cultured *in-vitro,* a polydye (PD30) was synthesised to be of a lower

molecular weight than that of the previously described PD20. Two separate short studies were set up to investigate the internalisation and internal trafficking of PD30 in both CHO and HepG2 cells cultured *in-vitro* (refer to Chapter 5; Section 5.2.5).

Both CHO and HepG2 cells (80,000 cells/ml) were seeded into independent Wilco dishes and incubated overnight at 37°C with 95% air and 5% $CO_2$. Subsequently, both sets of cells were washed 3x with D-PBS (2 ml at pH 7.4) to remove the presence of any excess serum proteins. Into separate Wilco dishes, containing CHO and HepG2 cells (160,000 cells/ml) cultured *in-vitro*, a 2 ml volume of PD30 (1 mg/ml) was added and both sets of cells were incubated for 10 minutes in a humidified incubator at 37°C with 95% air and 5% $CO_2$. The supernatant (2 ml) was removed and the cells were washed three times (2 ml) in the appropriate serum free medium. Cells were then replenished with a 2 ml volume of the appropriate serum free medium and placed on a heater stage (37°C) on the Olympus FV300 LSCM. LSCM images were obtained thirty minutes post the initial incubation period (10 minutes at 37°C; refer to Chapter 5; Fig. 5-8 and Fig. 5-9). In both cases, control experiments were set up, so that the mode of association of the free Cy3 fluorophores (Cy3 bisamine and Cy3 bissulphonic acid) with CHO and HepG2 cells cultured *in-vitro* could be determined.

### 2.3.15 Time dependent internalisation of PD30 in CHO cells cultured *in-vitro*

A short-term time-dependent internalisation study of PD30 was completed in CHO cells cultured *in-vitro* (refer to Chapter 5; Section 5.2.6) following the initial short study described previously (see Section 2.3.14) to determine if the intracellular localisation of PD30 changed over time (20-60 minutes) following an initial incubation period of 10 minutes.

CHO cells (80,000/ml) were seeded into a Wilco dish and incubated in a humidified incubator at 37°C with 95% air and 5% $CO_2$. The following day, medium containing serum was removed from the Wilco dish and CHOs were washed (3x) with D-PBS (2 ml) to remove the presence of any excess serum proteins. Subsequently, CHO cells were incubated with a 2 ml volume of PD30 (1 mg/ml) prepared in serum-free medium (F12 Nutrient Ham Mixture) at pH 7.4. The CHO cells were then incubated in a humidified incubator at 37°C with 95% air and 5% $CO_2$ for 10 minutes. Subsequently, the supernatant in the Wilco dishes was removed and CHOs were washed (3x) with D-PBS (2 ml) at pH 7.4. CHO cells cultured *in-vitro* were then re-plenished in the appropriate serum free medium (2 ml volume at pH 7.4). The dish was placed on a heater stage (37°C) and LSCM images were obtained. CHO cells were imaged using a LSCM for a period of 20 to 60 minutes following the initial incubation period (10 minutes at 37°C) with PD30 (1 mg/ml). LSCM (Olympus FV300) was used to visualise the time-dependent internalisation of PD30 (1 mg/ml) by CHO cells (160,000/ml) cultured *in-vitro* at various time points (20-60 minutes) following the initial incubation period of 10 minutes at 37°C at pH 7.4 (refer to Chapter 5; Fig. 5-10). The excitation and emission wavelengths were 535 nm and 570 nm respectively which is appropriate for the detection of the free Cy3 bisamine fluorophore. Adobe Photoshop version 5.5 was employed to visualise the LSCM images obtained.

It was thought that greater nuclear localisation of PD30 could be determined if it was incubated with CHO cells cultured *in-vitro* over a more extensive incubation period (24 h at 37°C, pH 7.4; refer to Chapter 5; Section 5.2.6). CHO cells were cultured *in-vitro* according to the method described above and incubated with 1 mg/ml of PD30 at pH 7.4 for 24 h at 37°C with 95% $CO_2$ and 5% air. The following day, the PD30 treatment was aspirated from the Wilco dish containing CHO cells, washed (x3) with D-

PBS (pH 7.4) and re-suspended in fresh serum free medium. LSCM (Olympus FV300) was used to visualise the internalisation of PD30 (1 mg/ml) by CHO cells following a 24 h incubation period (refer to Chapter 5; Fig. 5-11). The excitation and emission wavelengths were 535nm and 570nm respectively which is appropriate for the detection of the free Cy3 bisamine fluorophore. Adobe Photoshop version 5.5 was employed to visualise the LSCM images obtained.

### 2.3.16 Cultivation of suspension cells in the rotary cell culture system (RCCS)

#### 2.3.16.1 Cultivation of LoVo suspension cells in the RCCS and uptake of the copolymer, poly(L-lysine ethyl ester co L-lysine *iso*-phthalamide)

To demonstrate uptake of the copolymer, poly(L-lysine ethyl ester co L-lysine *iso*-phthalamide), a clumpy aggregate of an adenocarcinoma cell line, LoVo was cultivated on FACT 111 microcarrier beads in the rotary cell culture system (RCCS; refer to Chapter 3; Section 3.2.3). The RCCS is depicted in Fig. 2-1.

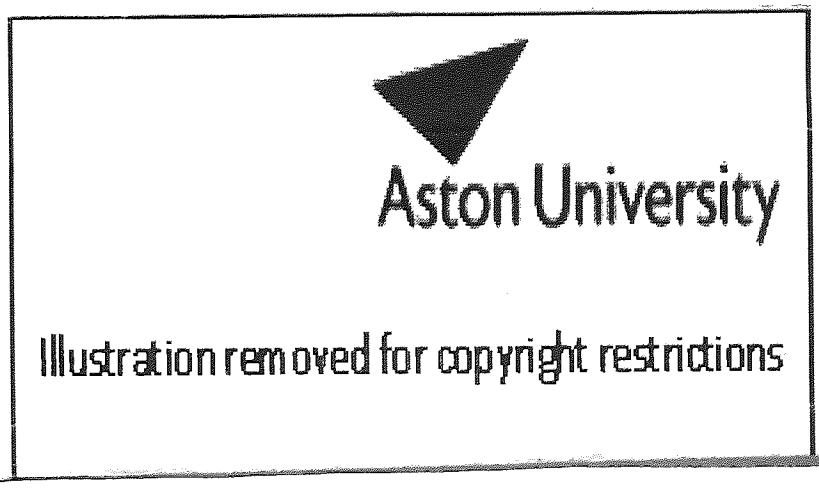


**Fig. 2-4 reproduced image of the experimental set up for the RCCS.**

Fast attachment collagen-treated (FACT 111) microcarrier beads (4 g) were suspended in deionised $H_20$ and autoclaved at 121°C for 15 minutes. Subsequently, the autoclaved liquid was discarded and the beads were rinsed in a 10 ml suspension of specialised RPMI-1640 media containing 10% FBS, 100 U/ml penicillin and 100 $\mu$g/ml streptomycin to rinse away the autoclaving liquid and to condition the beads. The microcarrier solution was then placed in a $CO_2$ incubator for a period of 30 minutes. The media was discarded and the beads were re-suspended in 20 ml of fresh warm media. It was estimated that for a 50 ml culture, $5x10^6$ LoVo cells were required. LoVo cells were obtained from the log phase of growth and added to the microcarrier suspension and enough warm media was added to obtain a 30 ml suspension of cells. The cell suspension was stirred slowly to prevent a bead or cell slurry from forming a static layer on the bottom of the stir flask. The spinner flask was stirred and incubated overnight (24 h). Subsequently, the cell suspension was prepared to 50 ml with fresh, warm media. LoVo cells were then introduced into the RCCS according to the method described in Section 2.3.16.3 yielding a final concentration of 5 mg/ml FACT 111 microcarrier beads resulting in a ratio of 10 cells per bead. A culture of LoVo cells was maintained for a period of 12 days. As growth of LoVo cells progressed a medium exchange was completed on day 4 (refer to Section 2.3.16.4). Measurements of glucose and lactate levels in the cell culture were obtained throughout the 12 day period by obtaining a 1 ml suspension of cell culture from the RCCS and placing it in a YSI 2000 Glucose-Lactate analyser which gave a readout of glucose and lactate measuements in mmol/L. A measurement of tumour metabolic activities was obtained pre- and post copolymer, poly(L-lysine ethyl ester co L-lysine *iso*-phthalamide) dosing (0.63 mg/ml on day 7 and 6.3 mg/ml on day 10; refer to Chapter 3; Section 3.2.3; Fig. 3-5).

### 2.3.16.2 Cultivation of the EBV-transformed B suspension cell line in the RCCS and uptake of PD20

A short study was conducted to determine if diffusion of PD20 into a cellular aggregate of an EBV-transformed B cell line was possible (refer to Chapter 5; Section 5.2.7). Following 21 days of the growth period of the EBV-transformed B cell line an aggregate of approximately 5 mm was formed (refer to Chapter 5; Fig. 5-12). A study was conducted to determine if uptake of PD20 (1 mg/ml) by the aggregate of EBV-transformed cell line was possible. A solution of PD20 (1 mg/ml) was prepared in serum-free medium (DMEM) and added to the RCCS in the same manner used for a medium change (refer to Section 2.3.16.3). Following a 24 h incubation period the aggregate was removed from the vessel in a sterile manner and transferred to a vial containing 4% formalin (fixing solution). This vial was then transferred to a refrigerator (4°C) and fixed in 4% formalin for two days. The aggregate was subsequently placed into a vial containing D-PBS (pH 7.4) and stored at 4°C until LSCM images were obtained by employing an Olympus FV300 LSCM. The excitation wavelength was set at 530 nm and the emission wavelength was set at 570 nm which was appropriate for the detection of PD20.

### 2.3.16.3 RCCS - Experiment start up

The following cell culture procedure was employed in setting up the growth of suspension cells. The RCCS vessel was transferred to a sterile laminar flow hood. The end caps of the 50 ml disposable rotary cell culture system (RCCS) were removed and placed in sterile petri dishes. Using a sterile pipette (10 ml), the vessel was filled to 50% of the total volume with medium without serum, allowing space to load the cells (serum

addition at this time increases foaming and leads to difficulties in removing the air bubbles later on). The suspension cells were removed from tissue culture flasks (75 $cm^2$). Cells were counted according to the method described previously (see Section 2.3.2). EBV-transformed cells were diluted in medium to yield a final concentration of 2-3x$10^5$ cells/ml. Using a 10 ml pipette, the cell suspension was loaded into the 50 ml disposable vessel through the ½ inch port. The appropriate amount of FBS (10% of total volume) was added and the vessel was topped up with medium. The port was wiped with a solution of ethanol (70%), the cap was tightened and the syringe port valves were closed. A 20 ml syringe was then filled with serum free medium. One syringe port was wiped with ethanol (70%) and the syringe was attached. The other syringe port was wiped with ethanol (70%) and an empty 5-10 ml syringe was attached. Both syringe ports were then opened. The vessel itself was then inverted gently and the sides of the vessel were tapped to expel air bubbles from under the ports. The air bubbles were manoeuvred under the empty syringe. With both valves open, the syringes were pushed gently so as to replace the air bubbles with medium. Both syringes were then removed, ports were closed and fitted with 0.2 $\mu$m sterile filters and the end caps were replaced. The vessel was then attached to the rotator base in a humidified $CO_2$ incubator making sure that the unit was level. The power was turned on and an initial rotation speed of 6 to 8 rpm was employed for the suspension cell culture.

### 2.3.16.4 Media exchange in the RCCS

A change of medium was employed once every three days throughout the 21 day culture of the EBV virus transformed B suspension cell line and on day 4 throughout the 12 day culture growth of LoVo cells. The following procedure was used to change the medium in the vessel. The power was switched off, and the vessel was immediately

removed from the base and transferred to a sterile laminar flow hood. The suspension cells/aggregates were then allowed to settle to the bottom with the valves and the ½ inch port rotated upwards. The end caps and sterile filters (0.2 $\mu$m) were removed, valves opened and wiped with ethanol (70%). An empty 10 ml syringe was attached and was carefully used to withdraw medium from the vessel. Usually half of the conditioned medium was left in the vessel. A 10 ml syringe was filled with pre-warmed medium (37°C) and fresh medium was injected into the syringe port. Care was taken not to disturb the aggregate particles. A 20 ml syringe was filled with serum free medium. One syringe port was wiped with ethanol (70%) and the syringe was attached. The other syringe port was wiped with ethanol (70%) and an empty 5-10 ml syringe was attached. Both syringe ports were then opened. The vessel was gently inverted and the sides of the vessel were tapped to remove air bubbles from under the ports. The air bubbles were then manoeuvred under the empty syringe. With both valves open, the syringes were pushed gently so as to replace the air bubbles with medium. When all air bubbles were removed, the syringe valves were closed and both syringes were discarded. The ports were wiped with ethanol (70%). Fresh 0.2 $\mu$m filters were attached to the ports and the caps were replaced. The vessel was then attached to the rotator base in a humidified $CO_2$ incubator making sure that the unit was level. The power was turned on and an initial rotation speed of 6 to 8 rpm was employed for the suspension cell culture.

# CHAPTER 3

# BIOLOGICAL CHARACTERISATION OF PSEUDOPEPTIDES – CYTOTOXIC AND CELL MEMBRANE DESTABILISING MECHANISMS

## 3.1 Introduction

The aim of the work presented in this chapter was to establish whether previously synthesised synthetic amphiphilic pseudopeptides based on L-lysine and its esterified derivatives with aromatic diacid chlorides (Eccleston *et al.,* 1999; see Fig. 3-1) displayed similar pH-disruptive cell membrane characteristics to that of the previously described viral fusion proteins (see Chapter 1; Section 1.3.1.2). Hydrophobically modified polyelectrolytes (Eccleston *et al.,* 1999) were investigated which displayed pH-mediated conformational changes between an extended rod-like

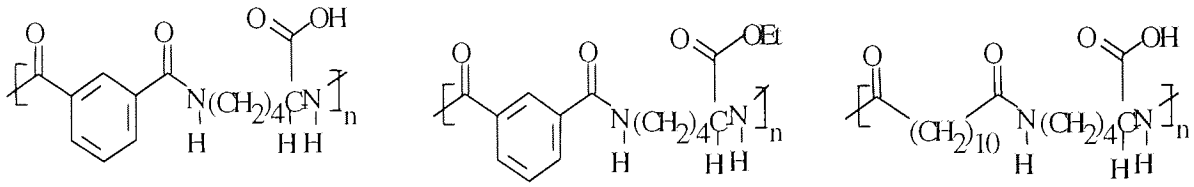

A B C

**Fig. 3-1 The repeat unit structures of polycondensates of L-lysine with aromatic and aliphatic di-acid chlorides. A, B and C represents the polymers poly (L-lysine *iso*-phthalamide), poly (L-lysine ethyl ester *iso*-phthalamide) and poly (L-lysine dodecanamide) respectively. The copolymer, poly (L-lysine ethyl ester co L-lysine *iso*-phthalamide) can be represented by a combination of structures A and B.**

conformation and a collapsed hydrophobically associated coiled conformation at low pH (see Chapter 1; Fig. 1-3). A change in conformation of the polymer was achieved by combining hydrophobic and weakly charged hydrophilic moieties within the backbone. When the carboxylic acid moieties are charged they cause dissolution of the polymer and when they are fully associated the hydrophobic moieties result in precipitation (in an aqueous solution) (Eccleston *et al.*, 1999). The amphiphilic macromolecules studied here contain charged carboxyl groups together with pendant hydrophobic groups and change conformation in response to their local pH. They adopt an extended chain conformation at pH values (typically pH > 6.0) where the carboxyl groups are charged. At lower pH values < 5.2 loss of charge causes intra-molecular hydrophobic association and the polymer chain progressively collapses to a compact, insoluble conformation. In this way, a conformation dependent functional property can be made to switch on or off in response to small changes in the environment. Furthermore, partial esterification of the polymer poly(L-lysine *iso*-phthalamide) was employed to increase the average distance between the carboxylic acid groups along the polymer backbone. It was thought that replacement of the carboxylic acid groups with hydrophobic ethyl ester groups, would lead to decreased repulsion between the carboxylic acid groups along the polymer backbone and result in an increase in both cell membrane interaction and permeabilising activities.

It was proposed that in their extended state, these pseudopeptides would interact with cell membranes and become internalised by cells. Following internalisation, it was proposed that if they encountered an acidic vesicle such as that of an endosome greater association of the hydrophobic groups would take place leading to possible fusion with the endosomal membrane and subsequent rupture and release into the cytosol. The pseudopeptides investigated here were tested for their cytoxicity towards a colorectal

adenocarcinoma cell line, namely C26 cells. The initial approach precluded the use of a well known cytoxicity assay, namely, the MTT (3-(4,5-dimethylthiazol-2-yl)-2,5-diphenyltetrazolium bromide) assay which was completed on C26 cells following their incubation (48 h) with various concentrations (2-500 $\mu$g/ml) of the polymer, poly (L-lysine *iso*-phthalalamide), and the copolymer, poly (L-lysine ethyl ester co L-lysine *iso*-phthalamide) at physiological pH (7.4). The MTT assay was selected to determine detrimental intracellular effects on mitochondria and metabolic activity. Subsequently, a shorter 30-minute coupled enzymatic assay, the lactate dehydrogenase (LDH) assay was completed to test the cell membrane disruption properties of the polymers, poly (L-lysine dodecanamide), poly (L-lysine *iso*-phthalamide) and the copolymer poly (L-lysine ethyl ester co L-lysine *iso*-phthalamide), at a concentration of 1 mg/ml towards two well known cell lines (A2780s and COS-1 cells) at the lower pH value of 5.5. The LDH assay can be used to determine membrane damage by quantifying the release of a cytosolic enzyme lactate dehydrogenase (LDH). In addition, an aggregate of a colorectal adenocarcinoma cell line (LoVo) was cultured *in-vitro* in the rotary cell culture system (RCCS) to demonstrate if cell uptake of the copolymer, poly (L-lysine ethyl ester-co-L-lysine *iso*-phthalamide) was possible at physiological pH (pH 7.4).

## 3.2 Results and Discussion

### 3.2.1 Polymer cytoxicity at pH 7.4

Initially the cytotoxicity of the polymer, poly (L-lysine *iso*-phthalamide) and the copolymer, poly (L-lysine ethyl ester co L-lysine *iso*-phthalamide) was assessed using the 3-{4,5-dimethylthiazol-2-yl}-2,5-diphenyltetrazolium bromide (MTT) assay (see Chapter 2; Section 2.3.5). The mitochondrial dehydrogenase activity using the 3-{4,5-dimethylthiazol-2-yl}-2,5-diphenyltetrazolium bromide (MTT) assay has gained

widespread favour as a reliable method for the quantitation of cell viability (Abe and Matsuki, 2000). The MTT assay measures the conversion of MTT into a purple coloured formazan by the redox activity of living cells, whereby a decrease in cellular MTT reduction is an index of cell damage (Abe and Matsuki, 2000).

The MTT assay was used to evaluate the cytotoxicity profiles of the polymer, poly (L-lysine *iso*-phthalalamide), and the copolymer, poly (L-lysine ethyl ester co L-lysine *iso*-phthalamide), towards a C26 (colorectal adenocarcinoma) cell line at

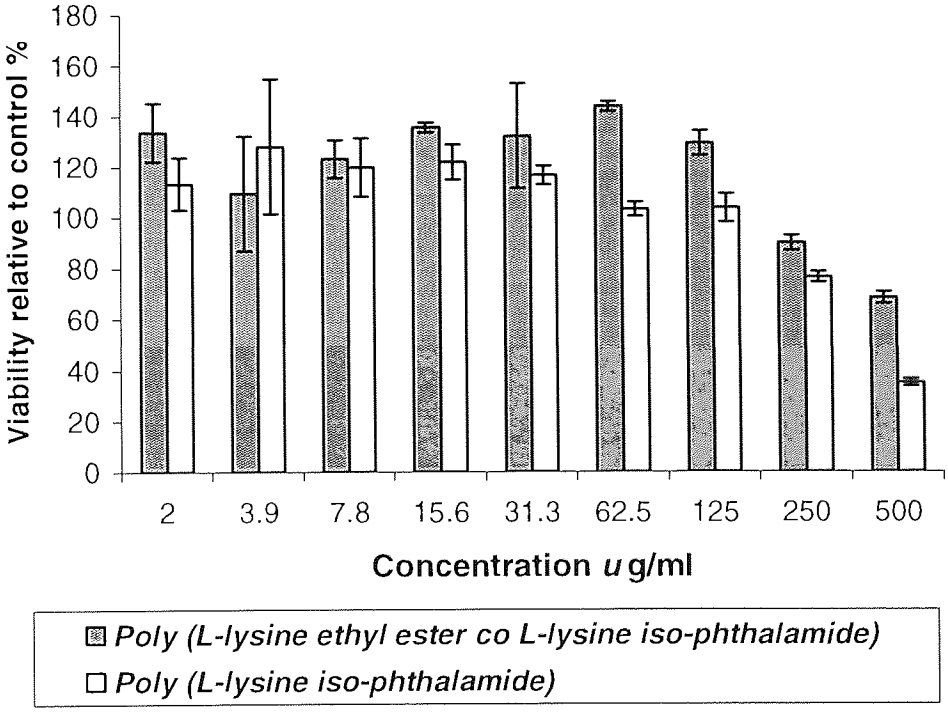


**Fig. 3-2 Cell viability relative to control values (%) of C26 cells following an MTT assay at physiological pH (pH 7.4). C26 cells (200 $\mu$l of 4x10$^3$ cells/well) were dosed with the polymer, poly (L-lysine *iso*-phthalamide) and the copolymer, poly(L-lysine ethyl ester co L-lysine *iso*-phthalamide) at concentration values between 2-500 $\mu$g/ml and incubated for 48 h. Subsequently, an MTT assay was completed (see Chapter 2; Section 2.3.5).**

physiological pH (7.4) and the results are shown in Fig. 3-2. C26 cells were treated with various concentrations (2-500 $\mu$g/ml) of the aforementioned polymers at physiological pH of 7.4 and an MTT assay was conducted according to the method described previously (see Chapter 2; Section 2.3.5).

The results indicated that both polymers were well tolerated in solution at physiological pH (pH 7.4) within the concentration range of 2-125 $\mu$g/ml. An increase in cell proliferation was observed when poly (L-lysine *iso*-phthalalamide), and poly (L-lysine ethyl ester co L-lysine *iso*-phthalamide) were dosed to C26 cells at concentrations in the range of 2-125 $\mu$g/ml. This could be attributed to cells utilising low molecular weight oligomers present in the unfractionated samples as a nutrient source.

At concentrations above 125 $\mu$g/ml, both poly (L-lysine *iso*-phthalalamide) and poly (L-lysine ethyl ester co L-lysine *iso*-phthalamide) demonstrated a cytotoxic effect towards C26 cells. Following dosing with poly (L-lysine *iso*-phthalamide), C26 cell viability relative to control values was found to decrease by 24% in the presence of 250 $\mu$g/ml of polymer and cell viability fell by a further 65% in the presence of 500 $\mu$g/ml. Similarly, when C26 cells were dosed with poly (L-lysine ethyl ester co L-lysine *iso*-phthalamide), at concentration values of 250-500 $\mu$g/ml, the cell viability of C26 cells decreased by 10.2% and 32% respectively relative to controls. Thus, both polymers were found to be relatively non-toxic when C26 cells were treated with concentrations of either polymer up to a concentration value of 125 $\mu$g/ml. However, at higher concentrations of 250 and 500 $\mu$g/ml, the cell viability of C26 cells was found to be significantly reduced with poly (L-lysine *iso*-phthalamide), demonstrating a greater cytotoxic effect towards C26 cells than that obtained with poly (L-lysine ethyl ester co L-lysine *iso*-phthalamide).

### 3.2.2 Cell membrane disruption at pH 5.5

Prior to the testing of the cell membrane disruptive properties of the polymers, poly (L-lysine dodecanamide), poly (L-lysine *iso*-phthalamide) and the copolymer poly (L-lysine ethyl ester co L-lysine *iso*-phthalamide), an assessment of LDH activity was carried out on the cell lines that were to be employed in the assay (see Chapter 2; Section 2.3.6.1). This study was conducted to determine the optimum cell density for

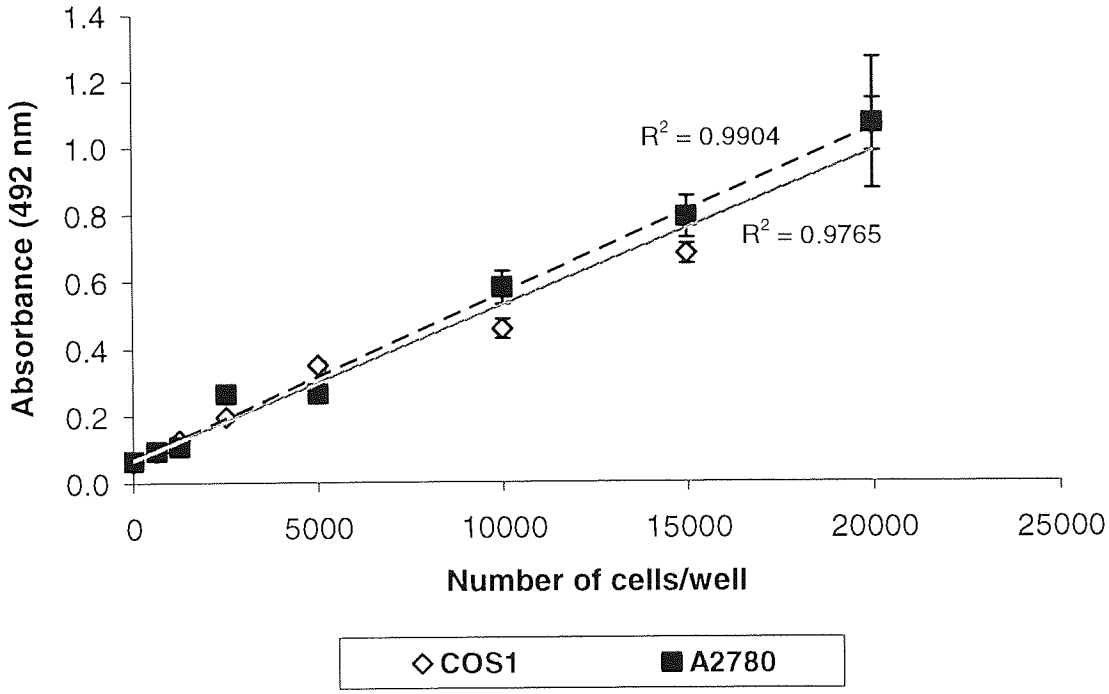


**Fig. 3-3 Graph representing the linear relationship between optical density and cell number for the LDH assay for both cell lines employed, A2780 and COS-1 respectively. Data points are shown for individual experiments each representing the mean of 8 wells per experiment. In independent experiments both A2780 and COS-1 cell lines were plated onto 96-well plates at varying densities (0-20,000 cells/well) and incubated for 24 h in an humidified $CO_2$ incubator at 37°C with 0.5% $CO_2$. LDH activity was then measured for each well using the Cytotox-96 assay kit (see Section 2.3.6.1).**

use in the LDH assay. The absorption due to conversion of the tetrazolium salt (INT) into a red formazon product was plotted versus cell number (0-20,000 cells per well) for A2780 and COS-1 cells (see Chapter 2; Section 2.3.6.1). The plot was linear up to an absorption value of 1.1 optical density at a wavelength of 492 nm for both A2780 and COS-1 cells. The lines obtained for both A2780 and COS-1 cells (Fig. 3-3) were shown to be linear and gave $r^2$ values of 0.990 and 0.977 respectively.

The similarity between extracellular and liposomal membranes prompted a study to investigate whether synthetic hypercoiling pseudopeptides described here could disrupt cell membranes in an acidic environment. Thus, the cell membrane lytic properties of the polymers, poly(L-lysine *iso*-phthalamide) and poly(L-lysine dodecanamide) and of a copolymer, poly(L-lysine ethyl ester co L-lysine *iso*-phthalamide) were investigated at pH 5.5, using a less time-consuming assay than that of the previously employed MTT assay, that is, a 30-minute coupled enzymatic assay established cytotoxicity assay, the lactate dehydrogenase (LDH) assay (see Chapter 2; Sections 2.3.6.2 and 2.3.6.3). Eccleston *et al.*, (2000) established previously that these pseudo-polypeptides were capable of inducing the haemolysis of red blood cells (RBC's). Haemolysis was found to be strongly pH-dependent, with neglible lysis at pH 7.4 and maximum lysis occurred as the pH decreased to pH 5.0.

The LDH assay represents an alternative method for assaying the loss of membrane integrity, by measuring the release of the intracellular enzyme LDH upon damage to the plasma membrane into the cell culture medium (Abe and Matsuki, 2000). The aim of the LDH assay here was to complete further investigations of the pseudopeptides and their interactions with cell membranes at low pH (pH 5.5). The LDH assay was carried out on COS-1 and A2780 cells according to methods described previously (see Chapter 2; Sections 2.3.6.2; 2.3.6.3).

The aim of this assay was to confirm the observations that these amphipathic polymers display striking structural and functional similarities to the amino-terminal peptide of viral hemagglutinins. These peptides are involved in the internalisation of viruses by promoting cell membrane rupture within the reduced pH environment of endosomal compartments within the cell (Wagner *et al.,* 1992; Plank *et al.,* 1994). Endosome rupture has also been demonstrated for the amphipathic GALA-like peptides (Subbarao *et al.,* 1987; Parente *et al.,* 1988; Haensler and Szoka, 1993), a property which has been envisaged for the polymers studied here. Furthermore, the functionally similar poly-2-ethylacrylic acid (PEAA) has been shown to provide a pH-sensitive trigger for the release of hydrophilic compounds entrapped in liposomes (Thomas and Tirrell, 1992).

It was established whether the polymers displayed any cell toxicity in their fully dissociated state. The cell lysis behaviour of the polymers, poly (L-lysine dodecanamide), poly (L-lysine *iso*-phthalamide) and the copolymer, poly (L-lysine ethyl ester co L-lysine *iso*-phthalamide), towards COS-1 cells after co-incubation for 60 minutes under normal cell culture conditions in the absence of serum was determined. No toxicity was observed with any polymer at a concentration of 100 $\mu gml^{-1}$ or less. Cytotoxicities of 14.95% (poly (L-lysine dodecanamide), 6.7% (poly (L-lysine ethyl ester-co-L-lysine *iso*-phthalamide), and 13.7% (poly (L-lysine *iso*-phthalamide), were measured at a polymer concentration of 500 $\mu gml^{-1}$ (data not shown). However, at this concentration all the wells appeared turbid, possibly due to precipitation of the polymer on addition of acetic acid used to quench the enzymatic conversion of the tetrazolium salt. This effect interfered with the absorbance readings obtained. A modified version of the LDH assay was employed in order to avoid interference of turbidity at high polymer concentrations.

A modified version of the LDH assay was completed to determine whether exposure of two sets of cell lines, COS-1's and A2780's to each of the polymers tested, followed by a reduction of the culture pH to that at which hypercoiling occurs, would lead to cell lysis (see Chapter 2; Sections 2.3.6.2; 2.3.6.3). This approach was selected to simulate the low pH environment that is encountered within the intracellular endosomal compartment of the cell (pH 5.0-6.0). Polymer toxicity was investigated following dosing of poly (L-lysine dodecanamide), poly (L-lysine ethyl ester-co-L-lysine *iso*-phthalamide), and poly (L-lysine *iso*-phthalamide), to COS-1 and A2780 cell lines. In the initial assay, COS-1 cells were treated with 1 mg/ml of each polymer to be tested and the pH was immediately dropped to pH 5.5 by titration with 0.1 M HCl and the cells were incubated at 37°C for 15, 30, 45 and 60 minutes (see Chapter 2; Section 2.3.6.2). Control wells were also prepared containing COS-1 cells without polymer with the pH of the surrounding medium was titrated in an equivalent manner to that of polymer treated cells. Following the required incubation periods the cell supernatant was removed from each well and replaced with fresh serum-free medium (100 $\mu$l). LDH released into the cell culture supernatant was removed from each of the wells. Cells which had survived the various polymer treatments and acidification (pH 5.5) were lysed using a freeze-thaw method and LDH activity of the cells intact at the end of the assay was determined and compared to control cells which were acidified in the same manner but not treated with polymer (see Chapter 2; Sections 2.3.6.2; 2.3.6.3).

A further LDH assay was carried out using A2780 cells whereby they were pre-incubated (37°C) with either 1 mg/ml of poly (L-lysine dodecanamide), or poly (L-lysine *iso*-phthalamide), at pH 7.4 for 30 minutes at 37°C (see Chapter 2; Section 2.3.6.3). This was completed to investigate if an initial association period of polymer with cells was required in order to achieve greater cell rupture than that seen when a pH

drop was carried out immediately following addition of polymer treatments (see Chapter 2; Section 2.3.6.2). Following the initial pre-incubation period of 30 minutes, the polymer treatments were removed, the cells were re-suspended in fresh serum free medium and the pH of the supernatant in each well was dropped to pH 5.5 by addition of 0.1 M HCl (27.5 $\mu$l). At the appropriate time intervals (15, 30, 45 and 60 minutes) the acidified supernatant was removed from each well and replaced with fresh serum-free medium (100 $\mu$l). Subsequently, an LDH assay was carried out according to the modified method described earlier for COS-1 cells (see Chapter 2; Section 2.3.6.2).

The data obtained following measurements of the pH dependent LDH release upon dosing of poly (L-lysine dodecanamide), poly (L-lysine ethyl ester-co-L-lysine *iso*-phthalamide), and poly (L-lysine *iso*-phthalamide), to COS-1 cells is displayed in Fig. 3-4(a). It was found that the cell toxicity of polymers was markedly increased when acidification was conducted below the respective $pK_a$ of the polymers (pH 5.5). In each case the viability of cells relative to the control fell with time with a relative minimum viability of only 4% for treatment with poly (L-lysine dodecanamide), after 60 minutes. A2780 cells also showed a pH sensitivity to poly (L-lysine dodecanamide), and poly (L-lysine iso-phthalamide), upon acidification. However the relative loss of cell viability was less than that obtained for COS-1 cells. This finding is possibly due to the removal of polymer treatments prior to acidification (pH 5.5) when A2780 cells were assessed rather than acidification (pH 5.5) in the presence of polymer when COS-1 cells were employed. This data demonstrates that the polymers exert greater cell membrane disruption properties more efficiently at low pH (pH 5.5) than at physiological pH.

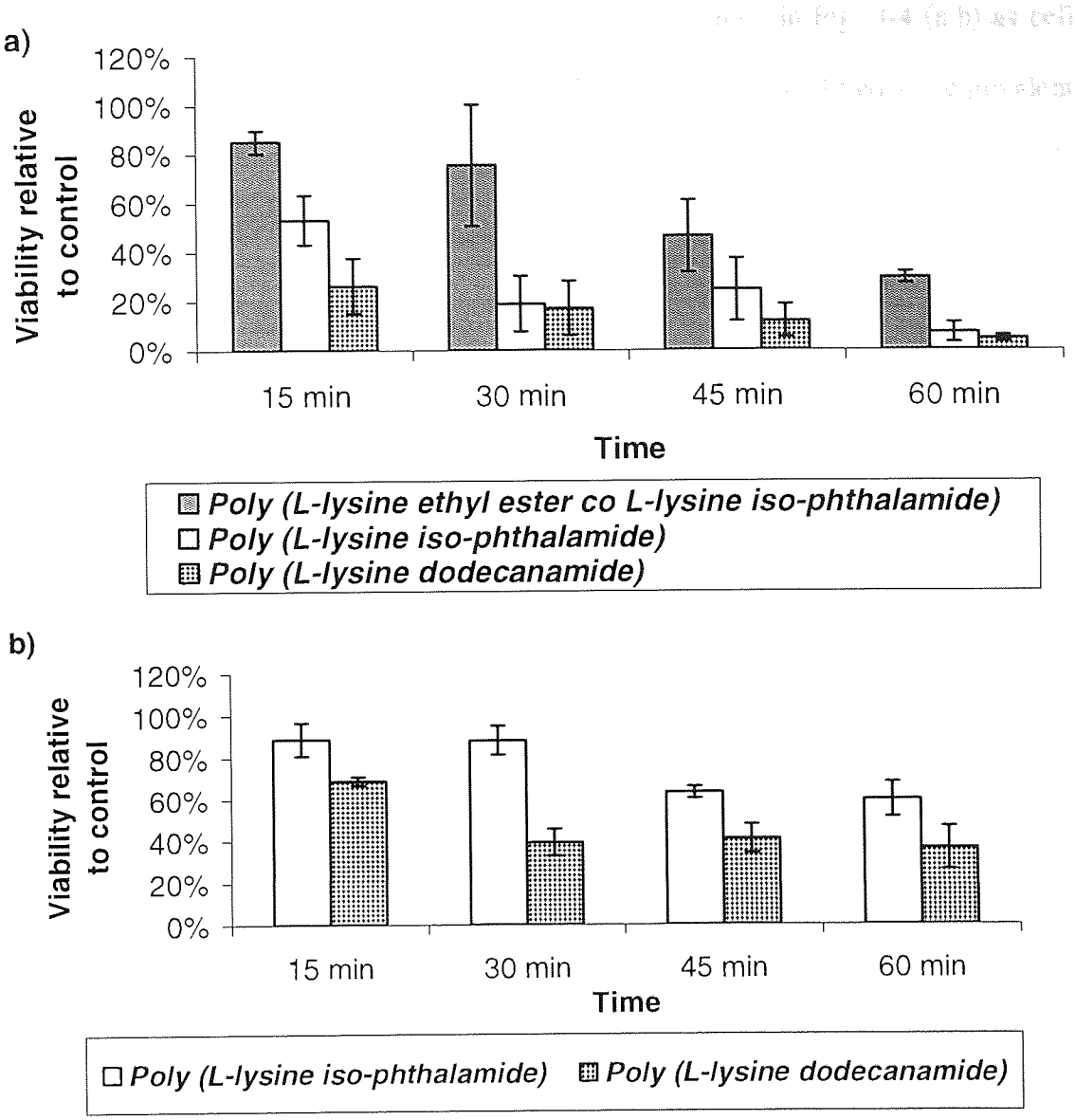


Fig. 3-4 represents the viability of (a) COS-1 and (b) A2780 cells relative to control cells following dosing with 1 mg/ml of the polymers with time, poly (L-lysine *iso*-phthalamide), and poly (L-lysine dodecanamide) and the copolymer, poly (L-lysine ethyl ester co L-lysine *iso*-phthalamide) at pH 5.5. The Cytotox 96® assay quantitatively measures LDH which is a stable cytosolic enzyme that is released upon cell lysis. The released LDH in culture supernatants can be measured within a 30-minute coupled enzymatic assay that results in the conversion of the tetrazolium salt to a red formazon product. The amount of colour formed (measured at an absorbance reading of 490 nm) is proportional to the number of cells lysed. Cell viability is expressed as a percentage of the control wells (untreated cells).

The results for both COS-1 and A2780 cells are presented in Fig. 3-4 (a;b) as cell viabilities relative to control experiments in which cells were acidified for equivalent periods of time with no polymer present. The overall viability of COS-1 cells (Fig. 3-4;a) dropped markedly for cells incubated at pH 5.5 for 60 minutes but clear differences both with the control (no polymer) and each other were observed in the presence of all polymers. Poly (L-lysine dodecanamide), appeared to be the most toxic with a cell viability of 0.8% after 60 minutes. Poly (L-lysine ethyl ester co L-lysine *iso*-phthalamide), appeared to be the best tolerated and poly (L-lysine dodecanamide) the least. A2780 cells (Figure 3-4:b) were similarly insensitive to polymer treatment at pH 7.4 but showed a pH dependent sensitivity to polymers poly (L-lysine dodecanamide), and poly (L-lysine *iso*-phthalamide), upon acidification (though the relative loss of viability was now approximately 50 % after 60 mins exposure).

### 3.2.3 Cultivation of LoVo cells in the rotary cell culture system (RCCS) and polymer uptake

It is well established that tumour cells proliferate much faster than normal cells. As such they have an increased metabolism, requiring more glucose which in turn leads to greater lactate production (McSheehy *et al*, 2000). Glucose uptake and lactate release (mmol/L) by a human colon adenocarcinoma cell line, designated LoVo was investigated before and after copolymer, poly (L-lysine ethyl ester co L-lysine *iso*-phthalamide) incubation through the use of a Glucose/Lactate YSI 2000 analyser (see Chapter 2; Section 2.3.16.1).

The rotary cell culture system (RCCS) is a horizontally rotated, bubble free culture vessel with membrane diffusion gas exchange (Mitteregger *et al.*, 1999). The culture medium, cells and cell aggregate particles rotate with the vessel and do not collide with the vessel walls or any other damaging objects. Destructive shear forces are

markedly reduced since this system has no impellers, air lifts, bubbles or agitators. As such cells, cell aggregates or tissue particles establish a uniform, very low shear, fluid suspension orbit within the horizontally rotating culture vessels. As the cell aggregates or tissue particles grow, the rotation speed is adjusted to compensate for increased sedimentation rates. The absence of damaging stress forces allows three dimensional aggregation of large cell masses. Normal, neoplastic, mono and co-cultures of fragile, human, anchorage dependent and suspension cells have been grown *in-vitro* (Mitteregger *et al.,* 1999).

One of the main advantages of the RCCS over conventional systems is its ability to grow tissue cultures which differentiate or mimic the structure and function of the parent tissue (Mitteregger *et al.,* 1999). The culture can be seeded with the same mixture of cells that are normally present in the parent tissue. These cells then grow and organise themselves into a 3-dimensional structure that is similar to that of the parent type. This growth has been made possible owing to the lack of destructive turbulence and collision forces within the RCCS. As such the RCCS can be employed to grow very complex, fragile tissue cultures, which can be used to mimic the parent tissue as aggregates form a 3-dimensional structure. As such, the effect of changes in the growth of the cell culture caused by addition of chemotherapeutic agents can be closely monitored.

An adenocarcinoma cell line (LoVo) was cultivated on FACT 111 microcarrier beads (sample supplied by Synthecon Inc.) *in-vitro* in the RCCS (see Chapter 2; Section 2.3.16.1). Glucose and lactate (mmol/L) levels in the medium were measured over a 12 day period and the results are shown in Fig. 3-5. Glucose and L-lactate levels (mmol/L) were measured from the time of inoculation (Day 0) up to day six in the absence of polymer treatment. At the start of inoculation period (Day 0) glucose and lactate values

were found to be 11.1 and 0 mmol/L respectively. However as clumps of LoVo cells started to appear in the culture vessel (Day 4) glucose and lactate values were measured to be 6.8 and 7.71 mmols/L respectively. On day four a medium exchange was conducted according to the method described previously (see Chapter 2; Section 2.3.16.3). By day 7 larger clumps of LoVo cells started to appear and the culture vessel was dosed with 0.63 mg/ml of the copolymer, poly (L-lysine ethyl ester co L-lysine *iso*-phthalamide) and glucose and L-lactate measurements (mmol/L) were obtained three days later. By day 10 (three days post-polymer dosing of 0.63 mg/ml) glucose and lactate levels were measured (5.9 and 8.25 mmol/L respectively). On day ten the culture vessel containing LoVo aggregates was inoculated with a higher dose of polymer (6.3 mg/ml) and by day twelve it was demonstrated that both glucose and L-lactate release (mmol/L) had began to level off and that the metabolic activity of the clumpy cell line had normalised.

### 3.3 General Conclusions

The aim of the work described in this chapter was to investigate the cell membrane disruptive properties of previously described pseudopeptides (see Fig. 3-1). *In-vitro* experiments were designed to determine if these pseudopeptides behaved in a similar manner to the previously described proteins of the hemagglutinin virus (HA). Initial experiments were completed using the MTT assay to investigate the toxicity of poly (L- lysine *iso*-phthalamide) and the copolymer, poly (L-lysine ethyl ester co L-lysine *iso*-phthalamide) towards a C26 (colorectal adenocarcinoma) cell line at physiological pH (7.4). The initial tests demonstrated that with extended exposure (48 h) both polymers were well tolerated by C26 cells at physiological pH (7.4) at

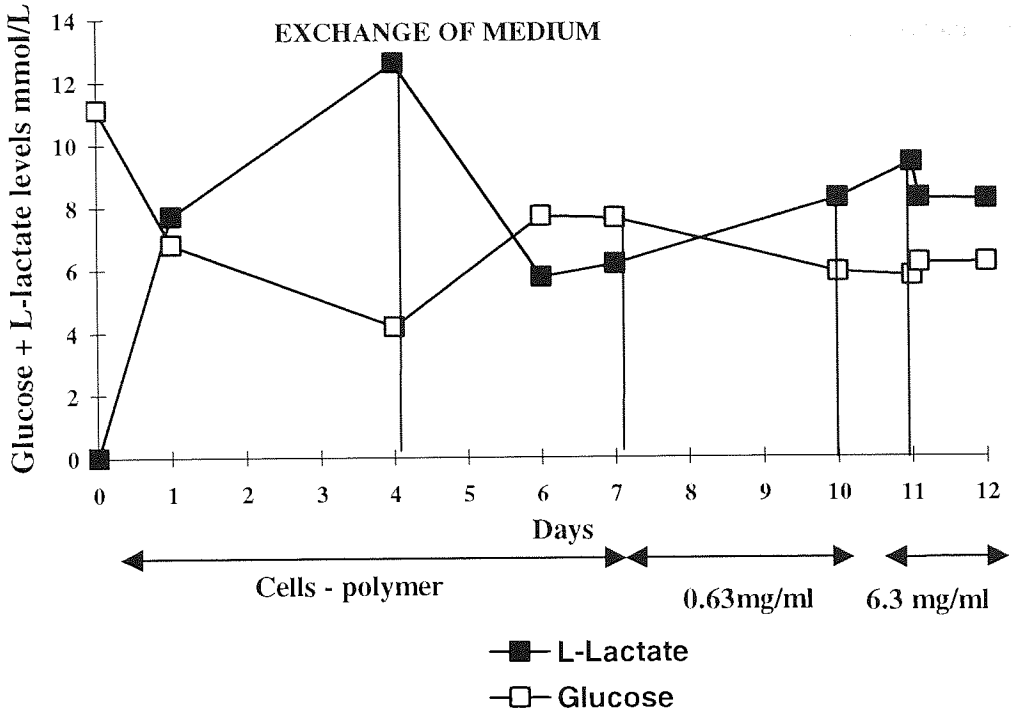


**Fig. 3-5 representation of the L-lactate and glucose levels (mmol/L;obtained using a Glucose/Lactate YSI 2000 analyser) to measure the tumour metabolic activity of LoVo (colon adenocarcinoma) cells cultured in a RCCS (Synthecon Inc.). On day 0 5 mg/ml of FACT III microcarrier beads having a ratio of 10 cells per bead were seeded into the RCCS ($5x10^6$ Lovo cells). Following 7 days of clumpy cell growth the copolymer, poly(L-lysine ethyl ester co L-lysine *iso*-phthalamide) was dosed into the RCCS at a concentration of 0.63 mg/ml. Subsequently, at day 11 the copolymer was added at a concentration of 6.3 mg/ml.**

concentrations between 2-125 $\mu$g/ml. At concentrations above 125 $\mu$g/ml, both polymers caused a decrease in cellular viability relative to control values. C26 cell viability was found to decrease by 24% in the presence of poly (L-lysine *iso*-phthalamide) and fell a further 65% in the presence of 500 $\mu$g/ml of the same polymer. Dosing with poly (L-lysine ethyl ester co-L-lysine *iso*-phthalamide) at concentration values between 250-500 $\mu$g/ml led to a decrease in C26 cellular viability relative to

control values of 10.2% and 32% respectively. Thus, it was determined that poly (L-lysine iso-phthalamide) displayed greater cytotoxic effects than the copolymer poly (L-lysine ethyl ester co-L-Lysine *iso*-phthalamide).

Data presented here suggests that hypercoiling pseudopeptides can integrate with cell membranes and exhibit pH mediated cell membrane disruption, the extent of which can be varied by careful choice of polymer structure. At pH 5.5 a significant increase in toxicity for all polymers is seen. At pH 5.5 poly (L-lysine *iso*-phthalamide) appears to be approximately twice as toxic as poly (L-lysine ethyl ester co L-lysine *iso*-phthalamide) at the lower pH value (pH 5.5) and this correlates with the more extreme hypercoiling transition of the un-esterified polymer.

The results presented here pertain to the investigation of pH responsive pseudopeptides. Previously, it was demonstrated that these polymers are capable of lysing the membranes of sheep erythrocytes at pH values observed in endosomal compartments of the cell (pH 6.0), while being non-disruptive at physiological pH (Eccleston *et al.*, 2000). As such these results bear striking similarities to those found by Thomas and Tirrell (1992) for the membrane disruptive properties of poly (2-ethylacrylic acid); PEAAc. This polymer has been shown to have pH-dependent membrane disruptive properties in liposomes (Thomas and Tirrell, 1992). They have demonstrated that a pH-triggered conformational change occurs at pH 6.3 and below (Borden *et al.*, 1987; Eum *et al.*, 1989). Under such low pH conditions, PEAAc appears to permeabilise phosphatidylcholine (PC) membranes, disrupts the lamellar structure of lipid bilayers, and forms mixed micelles composed of polymer and lipid. This process has been shown to have a high efficiency, and the disruption of PC membranes in liposomes is general as PEAAc disrupts distearoyl, dipalmitoyl, dimyristoyl, dilauroyl and dioleoyl PC at low pH values (Thomas and Tirrell, 1992). Such observations have

led to suggestions that these polymers may be useful as a new class of drug delivery formulation components that enhance delivery of biomolecules to the cytoplasm. Murthy *et al.*, (1998) have also demonstrated that PEAAc and PPAAc efficiently induce red blood cell haemolysis at low pH values such as those which exist in endosomes. In order for PEAAc and PPAAc to be effective in assisting the endosomal release of therapeutics they must also retain their haemolytic activity when they are conjugated to a protein. Lackey *et al.*, (1999) prepared complexes of PPAAc and streptavidin at stoichiometries of 1:1 and 3:1 polymer to protein. It was demonstrated that PPAAc hemolyses RBCs with the same efficiency whether as a free polymer or complexed via biotin to the protein streptavidin. The haemolysis was found to be strongly pH-dependent with the transition from neglible lysis to maximum lysis occurring as the pH decreased over a narrow pH range from pH 6.9 to 6.3 (Lackey *et al.*, 1999). Thus linkage of PPAAc to the protein does not affect the pH-dependent conformational and physical change of the polymer and its ability to disrupt the RBC membrane. They envisage that the ability of the PPAAc-streptavidin complexes to disrupt RBC membranes at lowered pH values, such as those present in endosomes, suggest that these unusual pH-responsive polymers represent a new avenue to facilitate endosomal release and to improve the intracellular delivery of protein or DNA therapeutics.

In conclusion, the development of synthetic, biocompatible polymers which are capable of pH dependent precipitative targeting towards tumour cells or acidic regions within tumours would offer the potential of diagnostic imaging tools of drug delivery devices. The most significant results pertaining to the study of these pH-responsive polymers, poly (L-lysine dodecanamide), poly (L-lysine ethyl ester co L-lysine *iso*-phthalamide), and poly (L-lysine *iso*-phthalamide), include data which displays their pH dependent interaction with cellular membranes, their ability to rupture membranes at

low pH values, that is, similar to that of endosomes (pH 5.0 to 6.0), and to lyse cells upon hypercoiling. It was therefore envisaged that a more suitable approach was to use these polymers as potential synthetic chaperones for the endosomal internalisation of conjugated molecules, since the polymers appear to behave in a similar manner to that of proteins of viral hemagglutinins and bear structural similarities with respect to the molecular arrangement of pendant carboxylic acid and hydrophobic moieties.

The polymers described here, demonstrated an ability to rupture cell membranes in an acidic environment (pH 5.5) similar to that of an endosomal compartment. It was therefore envisaged that their subcellular fate in CHO cells cultured *in-vitro* and localisation thereafter could be visualised through the use of laser scanning confocal microscopy (LSCM; refer to Chapter 5) following conjugation of a fluorescent probe, Cy3 bisamine fluorophore into the backbone of the polymer, poly (L-lysine *iso*-phthalamide; refer to Chapter 4).

# CHAPTER 4

# PHYSICAL CHARACTERISATION OF CY3 BISAMINE CONJUGATED POLY (L-LYSINE *ISO*-PHTHALAMIDE) POLYMERS

## 4.1 Introduction

Subsequent to the initial characterisation of the unlabelled amphiphilic poly (L-lysine *iso*-phthalamide) polymer (see Chapter 3 and Eccleston *et al.*, 2000), a range of amphiphilic poly (L-lysine co-bis-amine-Cy-3 *iso*-phthalamide) polymers were synthesised having Cy3 bisamine fluorophores conjugated into the backbone of the polymer. The intended application of fluorescently labelled polymers was to serve as a fluorescent label allowing the location and trafficking of the polymer, poly(L-lysine *iso*-phthalamide) to be visualised in cells cultured *in-vitro* (refer to Chapter 5).

The aim of the work detailed in this chapter was to characterise the amphiphilic poly (L-lysine co-bis-amine-Cy-3 *iso*-phthalamide) polymers (see Chapter 2; section 2.3.4.2). These polymers were synthesised having Cy3 bisamine fluorophores conjugated into the backbone of the polymer. Initial ratios of lysine:Cy3 bisamine of 20:1, 40:1, 60:1 and 80:1 were employed in the synthesis of the four polydyes (PD20, PD40, PD60 and PD80). Since the rate of Cy3 bisamine monomer incorporation into the polymer might be different from that of lysine, the possibility exists that the relative molecular weights of the fluorophore-conjugated polymers might vary with fluorophore loading. In addition, the distribution of the fluorophores in the polymers may be non-random, with local incorporation of multiple fluorophores leading to fluorescence quenching even in extended polymer chains. To reduce the probability of such effects extremely low levels of fluorophore incorporation were used such that the maximum

mean level of dye incorporation in the fluorescent polymers corresponded to just one Cy3 bisamine monomer per 20.6kD of polymer (PD20). To examine if the relative molecular weights of fluorophore-incorporated copolymers varied with the degree of fluorophore to polymer ratios gel filtration chromatograms (GFC) were obtained from RAPRA technologies for PD30 and PD40 (see Table 4-1). GFC data was not obtained for PD20 owing to the lack of availability of analytical equipment. However, the expected number average molecular weight was thought to be between that of PD30 and PD40.

| | **Mw: Weight average molecular weight (D)** | **Mn: Number average molecular weight (D)** | **Mz: z average molecular weight (D)** | **Pd: polydispersity = Mw/Mn** |
|---|---|---|---|---|
| ***PD40*** | 100,900 | 89,360 | 118,800 | 1.13 |
| ***PD30*** | 18,230 | 15,220 | 22,000 | 1.20 |

**Table 4-1 The relative molecular weight distributions for PD30 and PD40 determined from aqueous gel filtration chromatograms (GFC) in pH 7.0 phosphate buffer (obtained from RAPRA technologies).**

In this chapter, the initial experiments were designed to determine if the Cy3 bisamine fluorophore was conjugated into the backbone of the polymer, poly (L-lysine *iso*-phthalamide). A number of techniques were employed including gel filtration chromatography (GFC; see Chapter 2; Section 2.3.7.1), native polyacrylamide gel electrophoresis (PAGE; see Chapter 2; Section 2.3.7.2) and high voltage paper

electrophoresis (HVPE; see Chapter 2; Section 2.3.7.3). In a different study, the fluorescence intensity of the polydyes was investigated in the presence and absence of serum (see Chapter 2; Section 2.3.8). This initial testing was completed to demonstrate the increased enhancement in fluorescence when the polydyes were mixed with serum at different pH values. This experiment was used to highlight the ability of the polydyes to bind to other proteins. In a further set of studies UV-Vis absorption and fluorescence techniques were employed to determine if there was a shift in the absorption and fluorescence of PD20 compared to that of the free Cy3 bisamine fluorophore (see Chapter 2; Section 2.3.9).

A further study was completed using laser scanning confocal microscopy (LSCM) and Metamorph™ image acquisition analysis techniques to determine the association of both hydrophilic and hydrophobic scintillation proximity assay (SPA) beads with PD20 at various pH values (pH 4.8 - 7.4; see Chapter 2; Section 2.3.10). This experiment was completed to show the change in polymer conformation and the increase in hydrophobicity at low pH (4.8).

## 4.2 Results and Discussion

### 4.2.1 Gel filtration chromatography

Gel filtration chromatography was completed to investigate if the Cy3 bisamine fluorophores were copolymerised with lysine and *iso*-phthaloyl chloride into the backbone of the polymer (see Chapter 2; Section 2.3.7.1). The gel filtration chromatogram of PD20 and the free Cy3 bisamine fluorophore following independent runs on a Superdex-75 gel filtration column is shown in Fig. 4-1. The gel filtration chromatogram indicated the presence of three peaks, the first distinct one being PD20 which started to appear after 30 ml of eluent had passed through the column and is

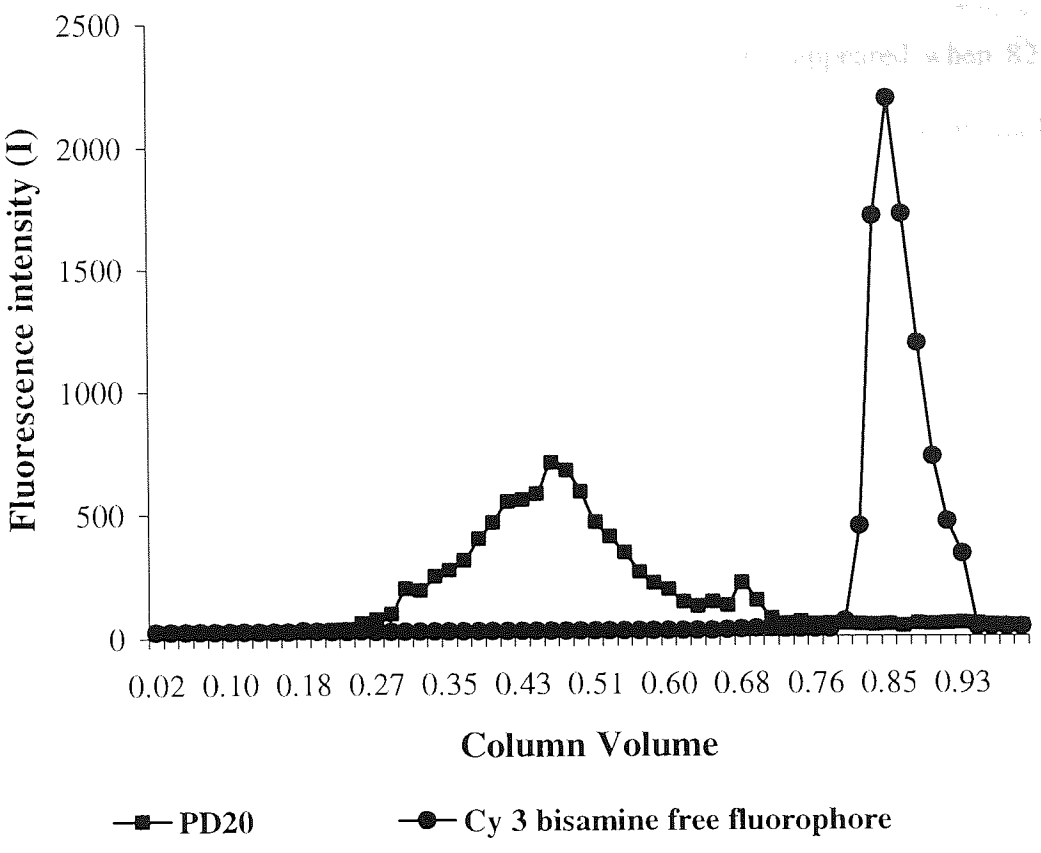


Fig. 4-1 The gel filtration chromatography profiles of PD20 and the free Cy3 bisamine fluorophore. An automated Hiload chromatography system (Hiload 16/60) was employed with a settled bed volume of 120.7 ml to determine if the Cy3 bisamine fluorophore moieties were conjugated into the backbone of the polymer, poly (L-lysine *iso*-phthalamide). In independent runs a 1 mg/ml solution of PD20 and a sample of Cy3 bisamine fluorophore (0.05 $\mu$g/ml) was passed through the column with 0.1 M phosphate buffer (pH 7.4) for 150 minutes with a flow rate of 1 ml/min. Samples (75 x 2 ml) were collected and 100 $\mu$l samples of each were transferred to a black Costar 96-multiwell plate with clear bottoms. A CytoFluor® 4000 Fluorescence Multi-Well Plate Reader was employed to obtain the fluorescent intensity (I) values of each well ($\lambda_{ex}$530 nm and $\lambda_{em}$590 nm, bandwidth (excitation) = 25 nm, bandwidth (emission) = 20 nm).

associated with the PD20 molecule and was evident until 86 ml of buffer eluent had run through the column. (see Fig. 4-1). The second peak which appeared when 82 ml of buffer eluent had run through the column could be due to the presence of low molecular weight oligomeric polymer which may have been present in the PD20 sample. The appearance of the third and final peak represents that of the free Cy3 bisamine fluorophore and indicates a sharp peak which initially appeared when 96 ml of buffer had eluted from the column and appeared to cease when 114 ml in total of buffer had been passed through the column.

The elution profile of PD20 demonstrates a broad band which indicates that the PD20 molecule displayed a broad range of molecular weight oligomers. The appearance of a peak for PD20 so early on in the gel filtration run, when only 30 ml of buffer passed through the column indicates that some of the PD20 molecule could have been running into the voids of the column. This suggests that the PD20 fraction contained samples greater than the 80 kD molecular weight cut off. However, this could be attributed to aggregation of the PD20 molecule resulting in the presence of apparently higher molecular weight fractions.

When the PD20 sample was passed through the column, no peak corresponding to the free Cy3 bisamine fluorophore was detected suggesting that there was no free dye associated with the PD20 sample. However, this technique did not provide conclusive evidence that the Cy3 bisamine fluorophore was covalently conjugated into the polymer, poly (L-lysine *iso*-phthalamide) either due to electrostatic interactions or that conjugation into the polymer backbone had been achieved. Further work to establish this conclusively would involve higher salt elutions (to break any electrostatic association) and elutions in the presence of a surfactant (to break any hydrophobic association). Furthermore, it would have been interesting to have obtained a GFC

chromatogram of a sample of the free Cy3 bisamine fluorophore mixed with PD20 to check for the effect of non-covalent associations between dye and the polymer.

### 4.2.2 Native polyacrylamide gel electrophoresis (PAGE) of the polydyes

The electrophoretic behaviour of the unconjugated fluorophore, Cy3 bisamine, the unlabelled polymer, poly (L-lysine *iso*-phthalamide) mixed with free Cy3 bisamine fluorophore and PD20, PD40, PD60 and PD80 were characterised by native PAGE (see Chapter 2; Section 2.3.7.2). Native PAGE of the various samples was conducted to separate the samples upon the basis of charge and size (see Chapter 2; Section 2.3.7.2). Samples of PD20, PD40, PD60 and PD80 were run in a 1x Tris-glycine base buffer at pH 7.4. Samples of the free Cy3 bisamine fluorophore was mixed with the naked polymer, poly (L-lysine *iso*-phthalamide). Control samples of the free Cy3 bisamine fluorophore which displays a net positive charge was run in an equivalent manner. A further native PAGE study was completed in which the direction of the electrical current was reversed (see Chapter 2; Section 2.3.7.2).

The various samples, PD20, PD40, PD60 and PD80 were subjected to native PAGE. At pH 7.4, the net charge conferred upon PD20, PD40, PD60 and PD80 was negative, consequently, PD20, PD40, PD60 and PD80 samples migrated down the gel from the sample wells towards the positive electrode.

The results of native PAGE of the unconjugated dyes, unlabelled polymer mixed with free dye and dye conjugated polymer are shown in Fig. 4-2 (images A and B). The electrophoretic mobilities of PD20, PD40, PD60 and PD80, and the free Cy3 bisamine, and a mixture of the unlabelled polymer, poly (L-lysine *iso*-phthalamide) with the free Cy3 bisamine fluorophore is depicted in Fig. 4-2; image A. PD20, PD40, PD60 and PD80 displayed smeared bands at pH 7.4 but a clear distinction could be made between

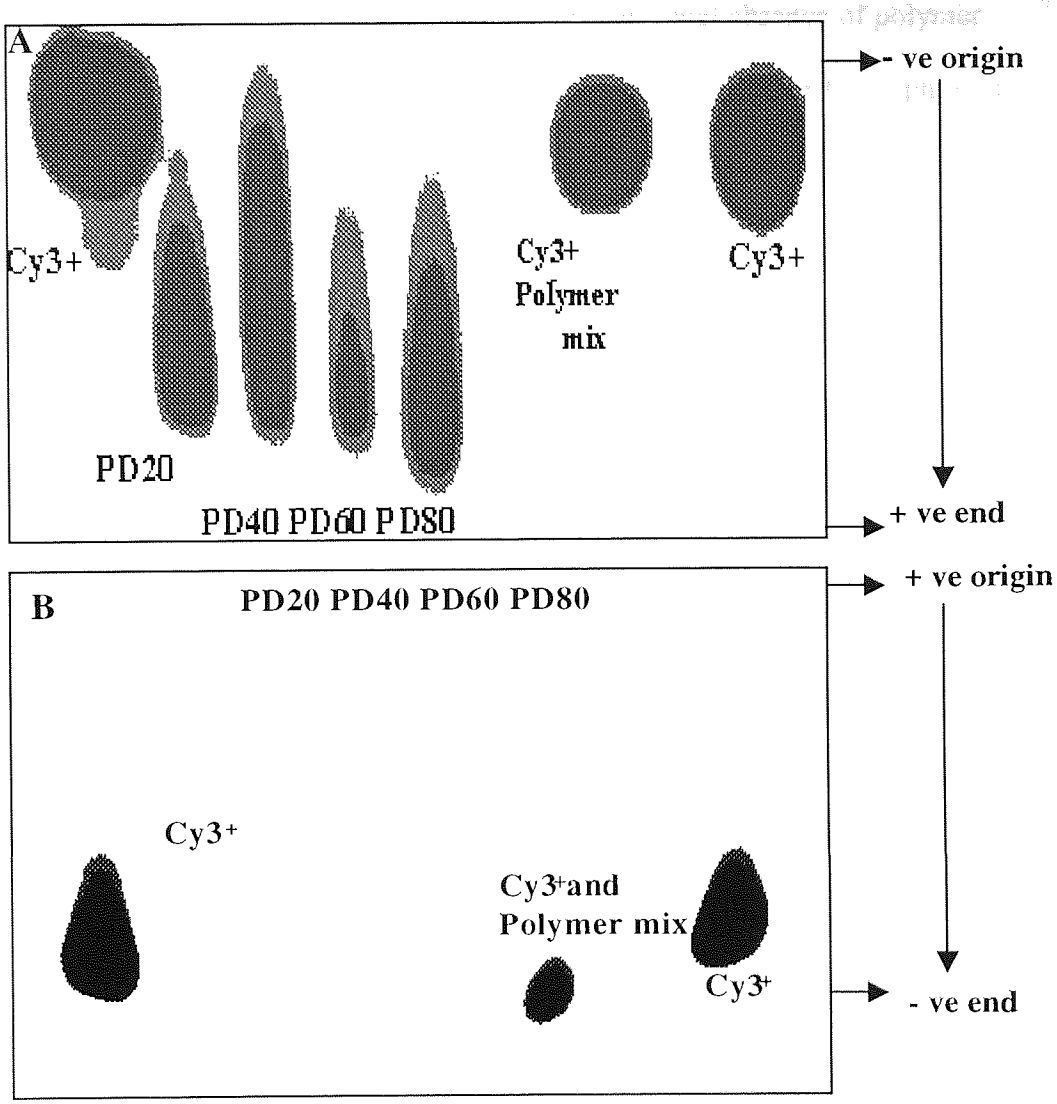


Fig. 4-2 (images A and B) represent the fluorescent images obtained following native polyacrylamide acrylamide gel electrophoresis (PAGE) of PD20, PD40, PD60 and PD80, the free Cy3 bisamine fluorophore and the free Cy3 bisamine fluorophore mixed with the unlabelled polymer, poly (L-lysine *iso*-phthalamide). Image A represents native PAGE of the samples in a negative to positive direction whereas Image B represents that of the samples in a reversed field native PAGE (positive to negative). Images A and B indicate the relative electrophoretic mobilities of the Cy3 bisamine fluorophore in free solution (in the absence and presence of polymer) and of the fluorophore conjugated dyes (PD20, PD40, PD60 and PD80). Fluorescent images of each were imaged with a high definition fluorescence CCD image acquisition unit ($\lambda_{ex}$535 nm, $\lambda_{em}$595 nm, bandwidths; exciation and emission = 10 nm).

the samples that moved towards the anode, and the Cy3 bisamine fluorophore control sample that moved towards the cathode both in the presence and absence of polymer (see Fig. 4-2; image A). The samples of either the free Cy3 bisamine fluorophore and that of the free Cy3 bisamine fluorophore mixed with a sample of unlabelled polymer, poly (L-lysine *iso*-phthalamide) did not appear on the gel as the positive charge migrated off the gel towards the cathode. Furthermore, there was no evidence of association of the unlabelled polymer, poly (L-lysine *iso*-phthalamide) to the free Cy3 bisamine fluorophore when the mixed sample was run. In the case of PD20, the long tail suggests the presence of a broad, polydisperse molecular weight range of polymers which, from the overlap of this band with those for unconjugated Cy3 bisamine, might include low molecular weight polymer material and unconjugated dye that was not removed during dialysis (see Chapter 2; Section 2.3.4.2).

The results of the reversed field native PAGE (see Chapter 2; Section 2.3.7.2) are shown in Fig. 4-2; image B. PD20, PD40, PD60 and PD80 samples were drawn off the gel toward the anode, thus demonstrating their net negative charge at pH 7.4. The electrophoretic mobilities of the free Cy3 bisamine fluorophore, and the mixture of unlabelled polymer, poly (L-lysine *iso*-phthalamide) with the free Cy3 bisamine fluorophore are also shown in Fig. 4-2; image B. These samples moved towards the cathode, thus demonstrating their net positive charge at pH 7.4. Samples of the free Cy3 bisamine fluorophore mixed with unlabelled polymer moved to the anode and were drawn off the gel, confirming the net negative charge of the polydyes at pH 7.4. The electrophoretic mobilities of these samples are in agreement with the normal field native PAGE mobilities (Fig. 4-2; image A) in that there was no evidence of association of the unlabelled polymer, poly (L-lysine *iso*-phthalamide) with the free Cy3 bisamine fluorophore when the mixed sample was run. It was concluded that clear separation of

dye from the polydyes (PD20, PD40, PD60 and PD80) in all channels strongly suggests that Cy3 bisamine moieties were conjugated into the polymer backbone. This data also provides strong evidence that there was no free or associated Cy3 bisamine fluorophore moieties following conjugation into the polymer backbone.

### 4.2.3 HVPE (High Voltage Paper Electrophoresis) of polydyes

High voltage paper electrophoresis (HVPE) experiments were completed to investigate the effect on the electrophoretic mobilities of PD20, PD40, PD60 and PD80 as their environmental pH was shifted from pH 7.4 to that at which hypercoiling of the naked polymer, poly (L-lysine *iso*-phthalamide) takes place (~pH 4.8; see Chapter 2; Section 2.3.7.3).

The fluorescent images of HVPE are shown in Fig. 4-3 following sample runs of PD20, PD40, PD60 and PD80, and control runs of free Cy3 bisamine fluorophore at different pH values (Fig. 4-3: image A; pH 7.4, image B; pH 6.4 and image C; pH 4.8). In contrast to the native PAGE experiment (Fig. 4-2; image A), most of the polydye samples (PD20, PD40, PD60 and PD80) analysed by HVPE displayed smeared bands at pH 7.4 (Fig. 4-3; image A). HVPE analysis of the samples revealed that the electrophoretic mobilities of PD20, PD40, PD60 and PD80 were affected by the pH of the buffer employed (Fig. 4-3: image A; pH 7.4, image B; pH 6.4 and image C; pH 4.8). The images shown in Fig. 4-3 (A, B and C) indicated that PD20, PD40, PD60 and PD80 displayed less electrophoretic mobilities and hence moved less towards the anode at pH 4.8 (Fig. 4-3; image C) than they appeared to at pH values of 7.4 and 6.4 (Fig. 4-3; images A and B respectively). This data could be used to demonstrate the effect of pH upon the charge of the unlabelled polymer, poly (L-lysine *iso*-phthalamide) backbone. The pH of the running buffer was decreased in HVPE experiments from that of pH 7.4,

in which the polymer exists in its extended conformation and is negatively charged, to pH 4.8 whereby the unlabelled polymer exists in a coiled conformation and is in a less negatively charged, hydrophobic state, whereby it has no charge due to the interaction of carboxylic acid groups within the polymer backbone. At pH 4.8 (see Fig. 4-3; image C) the negative charge on the polymer is reduced as progressive association of the carboxylic acid groups takes place. Thus, the electrophoretic mobilities of PD20, PD40, PD60 and PD80 are lower than at pH 7.4 (Fig. 4-3; image A) or pH 6.4 (Fig. 4-3; image B). At pH 6.4 the polymer exists in a transition state between an extended conformation at pH 7.4 and a coiled conformation at pH 4.8 with an overall negative charge. It is

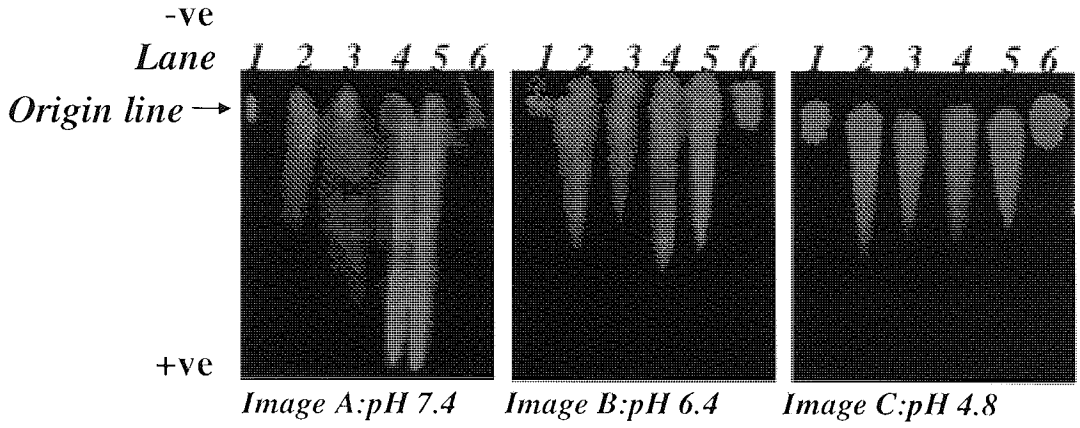


**Lane 1 Cy3 bisamine free fluorophore**
**Lane 2 PD20**
**Lane 3 PD40**
**Lane 4 PD60**
**Lane 5 PD80**
**Lane 6 Cy3 bisamine free fluorophore**

**Fig. 4-3 Fluorescent images depicting HVPE of the free Cy3 bisamine fluorophore, PD20, PD40, PD60 and PD80 indicating the relative electrophoretic mobilities of the fluorophore in free solution and of the fluorophore conjugated dyes at different pH values (pH 7.4; image A, pH 6.4; image B, and pH 4.8; image C). Fluorescent images were obtained using the Typhoon 9410 imaging system ($\lambda_{ex}$535 nm, $\lambda_{em}$595 nm, bandwidths; exciation and emission = 20 nm; see Chapter 2; section 2.3.7.3).**

noteworthy that the migration of PD60 and PD80 was greater than that of PD20 and PD40 when HVPE of all polydye samples was conducted at pH 7.4 (Fig. 4-3; image A). These results indicate that PD60 and PD80 consisted of a broader range of molecular weights compared to PD20 and PD40.

### 4.2.4 The fluorescence of polydyes in the presence and absence of serum

It has been widely reported that albumin can be exploited to serve as a transport carrier for drugs (Krieglstein *et al.*, 1972). Albumin is the most abundant plasma protein and it is generally accepted that a drug administered *in-vivo* will present some kind of interaction with this macromolecule, which would affect its bioavailability and toxicology (Esposito and Najjar, 2002). Bovine seum albumin (BSA) can be used to increase the plasma duration of certain drug molecules as the BSA molecule is not captured by macrophages in the liver and is not excreted by normal kidney excretion pathways (Shinoda *et al.*, 1998). In this study, it was considered to be important to study the interactions of the polymer, poly (L-lysine *iso*-phthalamide) with this protein particulary if it was to be conjugated to a therapeutic drug. The effectiveness of the pseudopeptides investigated in this study as potential polymer drug conjugates depends on their binding ability to other proteins. Bovine serum albumin (BSA) is a constituent of serum containing various amino acids (refer to Table 4-2), both positively and negatively charged, in addition to hydrophobic amino acids.

A study was completed to determine if the fluorescence of PD20, PD40, PD60 and PD80 would be affected in the presence of serum (FBS) due to their charge interactions (see Chapter 2; Section 2.3.8). Samples of known concentration (60 $\mu$g/ml) of each of the polydyes (PD20, PD40, PD60 and PD80) were prepared in either serum-

free buffers or buffers which contained serum (10%) titrated to various pH values (pH 7.4, 6.86, 6.4, 6.0, 5.0, 4.8 and 4.0) using 0.1 M HCl (see Chapter 2; Section 2.3.8).

The fluorescence of PD20, PD40, PD60 and PD80 as a function of pH (4.0-7.4) in buffers with and without serum (10%) is depicted in Fig. 4-4. When the fluorescence of PD20, PD40, PD60 and PD80 was investigated in buffers (pH 4.0-7.4) without serum it was found that PD40 yielded the highest average fluorescence intensity, followed by

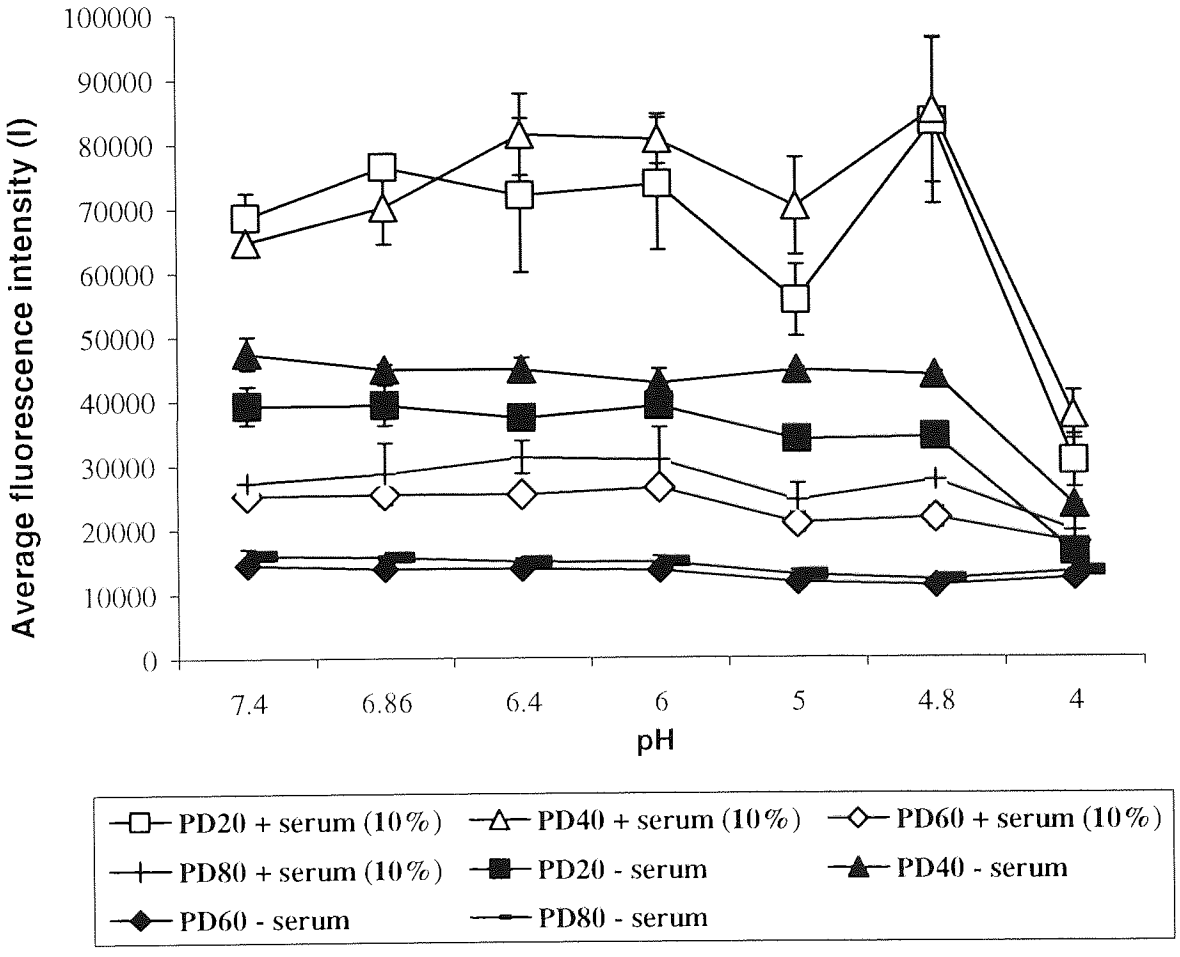


Fig. 4-4 Representation of the variation in the fluorescence intensity of PD20, PD40, PD60, and PD80 (60 $\mu$g/ml) as a function of pH (4.0 to 7.4) in the absence and presence of serum (10%). Fluorescent readings were obtained using the Wallac-Victor$^2$ 1420 plate reader set at the excitation and emission wavelengths for the Cy3 bisamine fluorophore ($\lambda_{ex}$535 nm, $\lambda_{em}$590 nm, bandwidths; excitation and emission = 10 nm). The average fluorescence intensity (I) was obtained by averaging values obtained (n = 3) for each of the polydyes tested in the absence or presence of serum (10%).

PD20, PD80 and PD60. PD60 and PD80 yielded the lowest average fluorescence of all four PD's examined in buffers (pH 4.0-7.4) without serum and their fluorescence was found to be similar without any significant change overall in fluorescence at each pH value tested. When the fluorescence of PD20, PD40, PD60 and PD80 was measured in buffers (pH 4.0-7.4) which contained serum (10%), it was demonstrated that the fluorescence of each was greater than the corresponding PD's which were measured in serum-free buffers (pH 4.0-7.4). It was apparent from Fig. 4-4 that PD40 yielded greater fluorescence than PD20 at each pH value examined (pH 4.0-7.4). However, it was initially envisaged that PD20 would yield the greatest fluorescence as it was initially intended to have a greater ratio of Cy3 bisamine fluorophore:lysine in the backbone of the polymer, poly (L-lysine *iso*-phthalamide). The observation that PD20 exhibited lower average fluorescence intensity (I) values than PD40 could be attributed to the possibility that in the case of PD40, the free Cy3 bisamine fluorophores were not conjugated into the backbone at the initially intended ratios of lysine:Cy3 bisamine dye of 40:1 and that it was possibly of a higher molecular molecular weight than that of the other polydyes.

It was established previously from potentiometric titration that poly (L-lysine *iso*-phthalamide) undergoes a hypercoiling transition between pH 4.0 and 5.0 (Eccleston *et al.*, 1999). Such a transition is characterised by the collapse of the polymer conformation into a tight coil that is stabilised by hydrophobic association. Thus, at low pH (pH 4.8) conjugated fluorophores are brought into closer proximity, effectively increasing their local concentration. It was anticipated that the collapse in polymer conformation at the onset of hypercoiling would be accompanied by a decrease in the fluorescence intensity, due to an increase in the local concentration of fluorophores (refer to Fig. 4-5). A rapid decrease in the fluorescence intensity of all four PD samples

was obtained at pH 4.8 in the absence and presence of serum (10%; see Fig. 4-4). The rapid decrease in fluorescence at this pH (pH 4.8) could be due to the polymer hypercoiling (refer to Fig. 4-5).

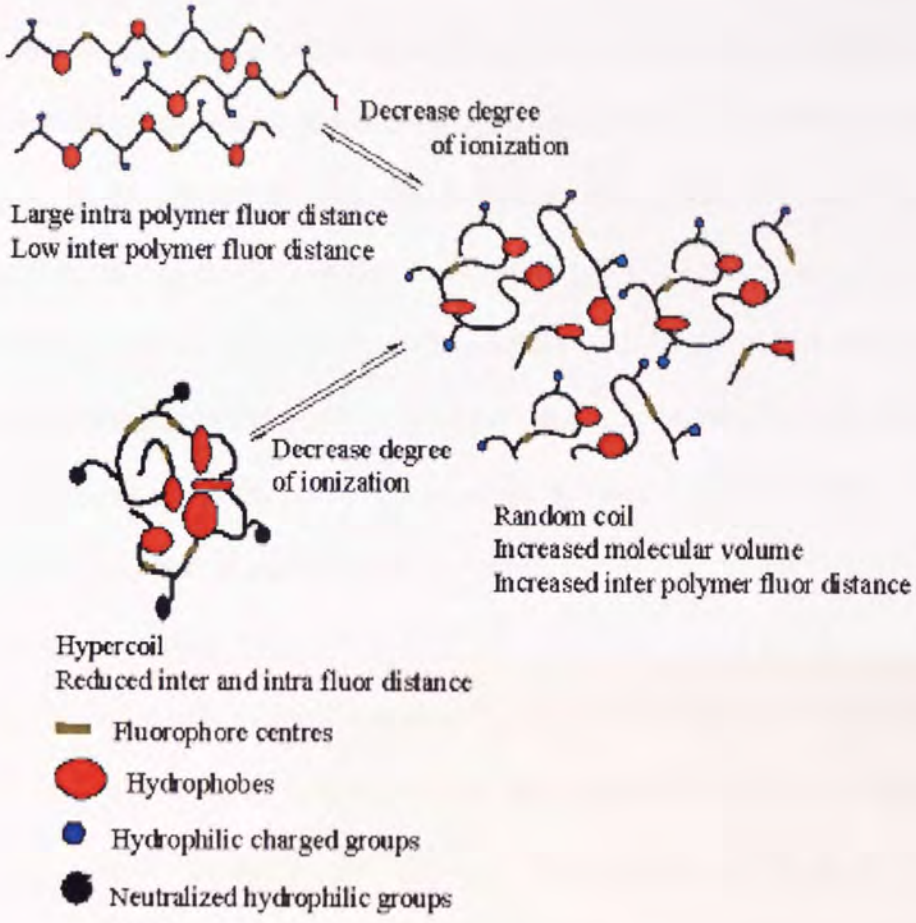


**Fig. 4-5 The degree of intra-polymer fluor-fluor distance and the inter-polymer fluor-fluor distance as PD20, PD40, PD60 and PD80 progress from an extended conformation at pH 7.4, to that of a random coil conformation at intermediate pH (pH 5.0 to 6.0) to that at which hypercoiling occurs (pH 4.8). The degree of quenching experienced by the fluorophores could be controlled by the pH of the aqueous solution of the polymerised dyes (PD20, PD40, PD60 and PD80).**

The enhanced fluorescence of all four PD samples in the presence of serum at all pH values tested (pH 4.0-7.4) is possibly due to the PD samples associating with the amino acids present in bovine serum albumin (BSA) which is a constituent of serum. The concentration of BSA in this particular sample of serum is 1.85 mg/ml (see Chapter 2; Section 2.1.3). The amino acids which are present in BSA are listed in Table 4-2 and show the positive and negative charged amino acids in addition to the hydrophobic ones. It is noteworthy that the isoelectric point of BSA may have affected the fluorescence of all PD samples shown in Fig. 4.4. BSA has an isoelectric point of 4.7 which is almost equivalent to the hypercoiling pH of the naked polymer, poly(L-lysine *iso*-phthalamide). Hence, it is possible that a reduction in the fluorescence of the polydyes in the presence of serum at pH 4.8 was a result of BSA precipitating from solution and loss of binding to the polydyes.

The initial results indicated that the fluorescence of PD20, PD40, PD60 and PD80 was greater in the presence of serum (10%) than that of the corresponding PD samples which were investigated in the absence of serum. A separate study was completed to determine the effect of concentration of PD20 (5-100 $\mu$g/ml) upon fluorescence in the presence of serum (10%; see Chapter 2; Section 2.3.8). The fluorescence of PD20 in buffer at pH 7.4 with and without serum (10%) is presented in Fig. 4-6. At a concentration of 100 $\mu$g/ml, the fluorescence of PD20 in buffer containing serum was almost double that of the value in buffer without serum. These results indicate that as the concentration of PD20 increases the fluorescence becomes greater. The results also indicate that the presence of serum (10%) resulted in higher fluorescence intensities of the PD samples. These results confirmed previous observations that PD20 interacts with amino acids present in BSA, one of the main constituents of serum (see Table 4-2).

| Amino Acid | % number of residues | Hydrophobic | Anionic | Cationic |
|---|---|---|---|---|
| Aspartic acid | 7 | | ✓ | |
| Glutamic acid | 10.1 | | ✓ | |
| Proline | 4.8 | ✓ | | |
| Alanine | 7.9 | ✓ | | |
| Valine | 6.2 | ✓ | | |
| Methionine | 0.7 | ✓ | | |
| Isoleucine | 2.4 | ✓ | | |
| Leucine | 10.5 | ✓ | | |
| Phenylalanine | 4.6 | ✓ | | |
| Lysine | 10.1 | | | ✓ |
| Histidine | 2.9 | | | ✓ |
| Tryptophan | 0.3 | ✓ | | |
| Arginine | 4 | | | ✓ |
| **% Total no. of residues** | **71.5** | **37.4** | **17.1** | **17** |

**Table 4-2 The amino acid composition of bovine serum albumin showing the % number of amino acid residues highlighting the hydrophobic, negatively and positively charged amino acid residues (adapted from Peters, 1985).**

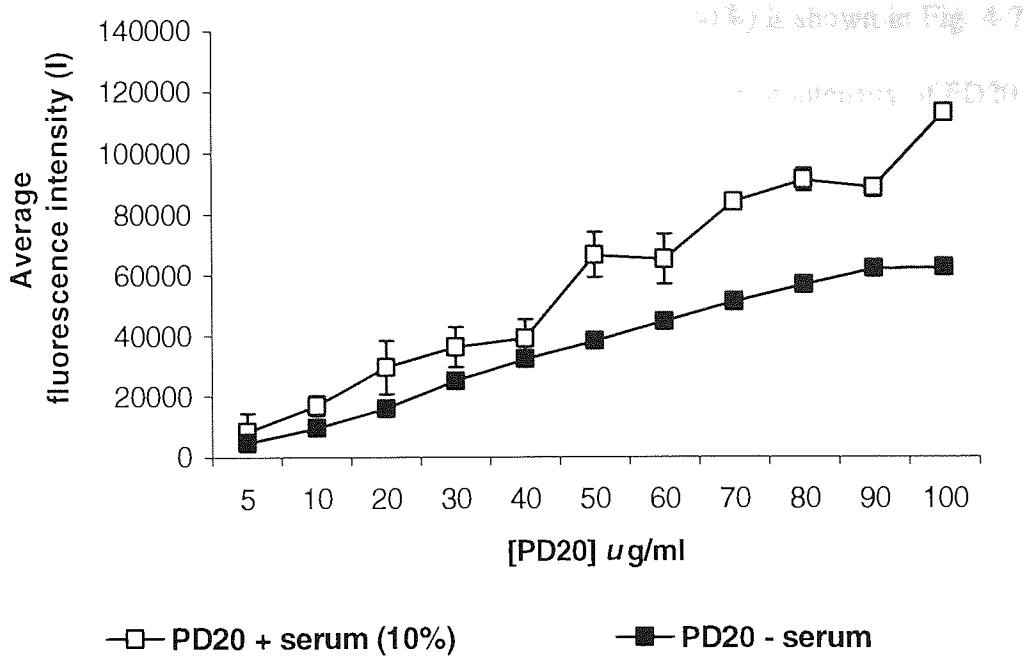


**Fig. 4-6 The variation in fluorescence intensity (I) of PD20 at various concentrations (5-100 $\mu$g/ml) in the presence and absence of serum (10%) at pH 7.4. Fluorescent readings were obtained using a Wallac-Victor$^2$ 1420 plate reader set at the excitation and emission wavelength for Cy3 bisamine fluorophore ($\lambda_{ex}$535 nm $\lambda_{em}$590 nm).**

A further study was completed to investigate the effect of the concentration of serum upon the fluorescence of PD20. Samples of PD20 were prepared in buffer (pH 7.4) at 60 $\mu$g/ml. Serum was added to each stock solution to yield samples of PD20 containing the required concentration of serum (0-40%; see Chapter 2; Section 2.3.8). Subsequently, 100 $\mu$l samples of each (n = 3) were transferred to a black costar 96 multiwell plate and the fluorescence of each sample was obtained using the Wallac-Victor$^2$ 1420 fluorescent plate reader ($\lambda_{ex}$535 nm, $\lambda_{em}$590 nm, bandwidths; excitation and emission = 10 nm; see Chapter 2; Section 2.2.8). The fluorescence of PD20 at 60

$\mu$g/ml in the presence of different concentrations of serum (0-40%) is shown in Fig. 4-7. The results show that there was an initial increase in the fluorescence intensity of PD20

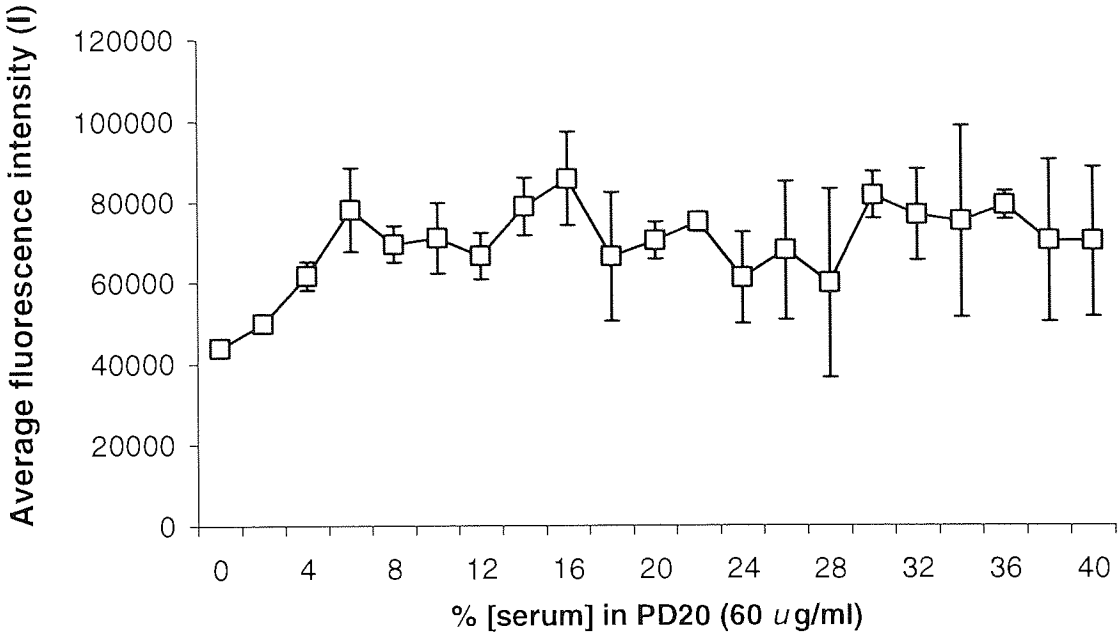


**Fig. 4-7 The variation in fluorescence intensity (I) of PD20 (60 $\mu$g/ml) with different concentrations of serum (0-40%) in D-PBS buffer (pH 7.4). Fluorescent readings were obtained using the Wallac-Victor$^2$ 1420 plate reader set at the excitation and emission wavelength for the Cy3 bisamine fluorophore ($\lambda_{ex}$535 nm $\lambda_{em}$590 nm with bandwidths of 10 nm).**

when the concentration of serum was increased from 0 to 6%. Subsequently, the fluorescence intensity of PD20 remained relatively constant. The results suggest that when the concentration of serum increases above 6%, there was an apparent equilibrium suggesting that the BSA molecule had saturated the available binding sites present on PD20 (see Table 4.1).

### 4.2.5 UV-Vis absorption of free Cy3 bisamine fluorophore

The UV-Vis absorption spectrum of the free Cy3 bisamine fluorophore was measured to determine if there was a shift in the maximum absorption values subsequent to conjugation into the backbone of the polymer (see Chapter 2; Section 2.3.9). Upon attachment to certain biomolecules, for example oligonucleotides, shifts in excitation and emission spectra of Cy3 have been observed. However, no effects have been observed in the presence of 10% DMSO or under a range of pH conditions (Amersham Biosciences, UK).

Samples of the free Cy3 bisamine fluorophore (unknown concentration due to limited sample availability) were prepared in various cell culture media (F12 Nutrient Ham Mixture, and DMEM without phenol red) and UV-Vis absorption spectra were determined (see Chapter 2; Section 2.3.9). UV-Vis absorption spectra were also obtained for each of the media preparations in the absence of the Cy3 bisamine fluorophore. The results of this study are shown in Fig. 4-8 and indicate that the Cy3 bisamine fluorophore in different types of media absorbed maximally at a wavelength of 540 nm following a UV-Vis scan between 350 and 700 nm. No absorption peak was detected when samples of F12 Nutrient Ham Mixture and DMEM (phenol red free) were similarly tested. It is noteworthy that UV-Vis absorption of the free Cy3 bisamine fluorophore prepared in both types of tissue cell culture medium (F12 Nutrient Ham Mixture and DMEM without phenol red) produced a shoulder at 510 nm. This may be due to aggregation of the Cy3 bisamine fluorophore. No corresponding absorption peak was evident in the control samples tested. It is noteworthy that the concentration of the fluorophore could have been estimated by employing Beer-Lambert calibrations using an extinction coefficient of 150 000 l $mol^{-1}$ $cm^{-1}$ which is appropriate for the free Cy3 bisamine fluorophore.

UV-Vis absorption techniques permitted further characterisation of PD20 and the effect of solvent polarity and pH on the UV-Vis absorption of PD20 was determined. Samples of a known concentration ($1.9x\ 10^{-2}\ gl^{-1}$) of PD20 were prepared in either serum-free medium (F12 Nutrient Ham Mixture) titrated to various pH values (pH 7.4, 5.08 and 4.8) with 0.1 M HCl, in medium (F12 Nutrient Ham Mixture) containing serum (10%) or in a solution of methanol (see Chapter 2; Section 2.3.9).

The UV-Vis absorption spectra of the various samples of PD20 are shown in Fig. 4-9 and can be compared to the UV-Vis absorption profile of the Cy3 bisamine fluorophore depicted in Fig. 4-8. It was found that the maximum absorption wavelength for all samples was 556 nm. The absorption values of each sample at a wavelength of 556 nm was found to be enhanced in methanol. This could be due to the polarity of

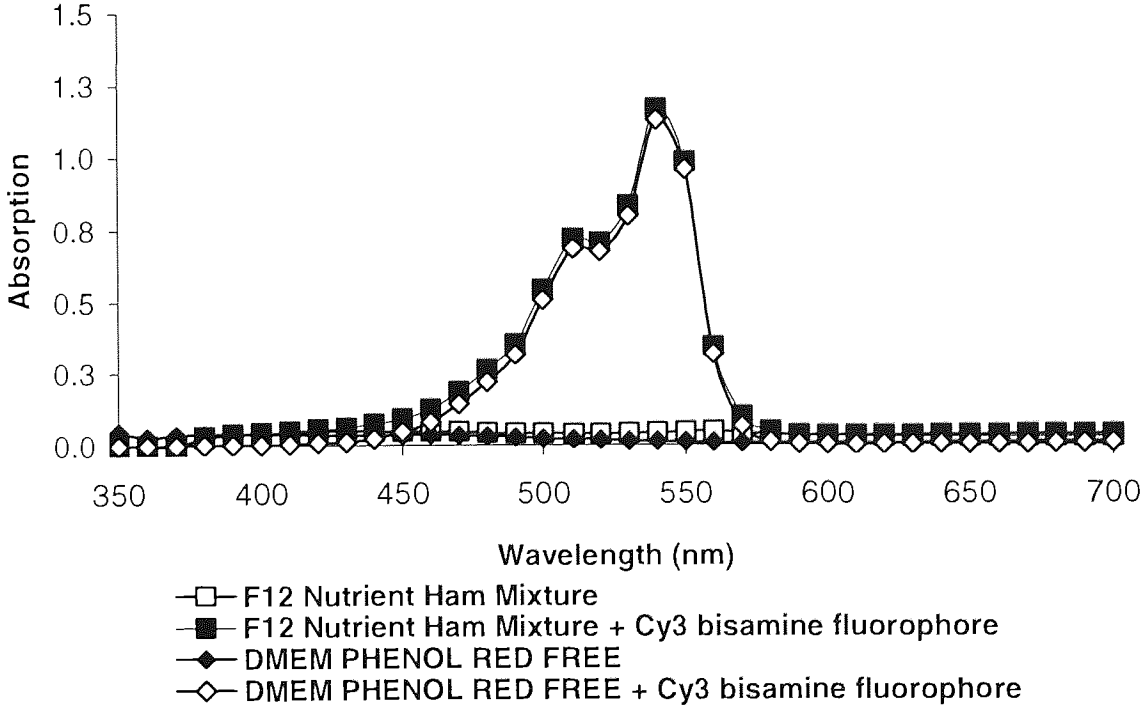


**Fig. 4-8 The UV-Vis absorbance of samples of various cell culture media (F12 Nutrient Ham Mixture and DMEM (phenol red free) in the presence and absence of Cy3 bisamine fluorophore.**

methanol which leads to greater rigidisation of PD20 resulting in an enhanced absorption value. The presence of 10% serum resulted in enhanced absorption values of PD20 at pH 7.4 (refer to Fig. 4-9). The absorption of PD20 was also found to be greater at pH 4.8 and 5.08 than that at pH 7.4 without serum (refer to Fig. 4-9). The lowest absorption value obtained was for the sample of PD20 which was prepared in medium at physiological pH (pH 7.4). These results indicate that the absorption of PD20 is affected by the polarity of different solvents. Similar to results found for the Cy3 bisamine fluorophore (Fig. 4-8) that there was an absorption band present at lower wavelengths in each case that could be attributed to the aggregation of dye molecules. Hence, the presence of a shoulder in Fig. 4-9 for all samples measured by UV-Vis absorption could be due to aggregation of PD20. The UV-Vis absorption profiles of PD20 was compared to that of the free Cy3 bisamine fluorophore. Fig. 4-8 represents the absorption spectra of the free Cy3 bisamine fluorophore, with maximum absorption at 540 nm. Therefore, when the absorption of PD20 was assessed there appeared to be a slight shift in comparison to the free Cy3 bisamine fluorophore, from 540 to 556 nm. The shift in absorption to a higher wavelength could be due to rigidisation or increased local viscosity of the dye upon conjugation into the backbone of the polymer, poly (L-lysine *iso*-phthalamide). It is noteworthy that there was uncertainty concerning the final ratios of dye to lysine following conjugation of the Cy3 bisamine fluorophore into the polymer, poly (L-lysine *iso*-phthalamide) backbone. It was initially intended that the polymer would have ratios of lysine:Cy3 bisamine of 20:1, 40:1, 60:1 and 80:1 following conjugation. One could have assumed a constant value of extinction coefficient following incorporation of Cy3 bisamine into the backbone of the polymer. The ratio of dye:polymer could possibly have been estimated from the absorbance of a solution of a known mass of polydye and the molecular weights shown in Table 4-1.

In addition to the UV-Vis absorption profiles the PD20 samples ($1.9\times10^{-2}$ $gL^{-1}$) were further analysed to determine its excitation and emission spectra at pH 7.4 (in the

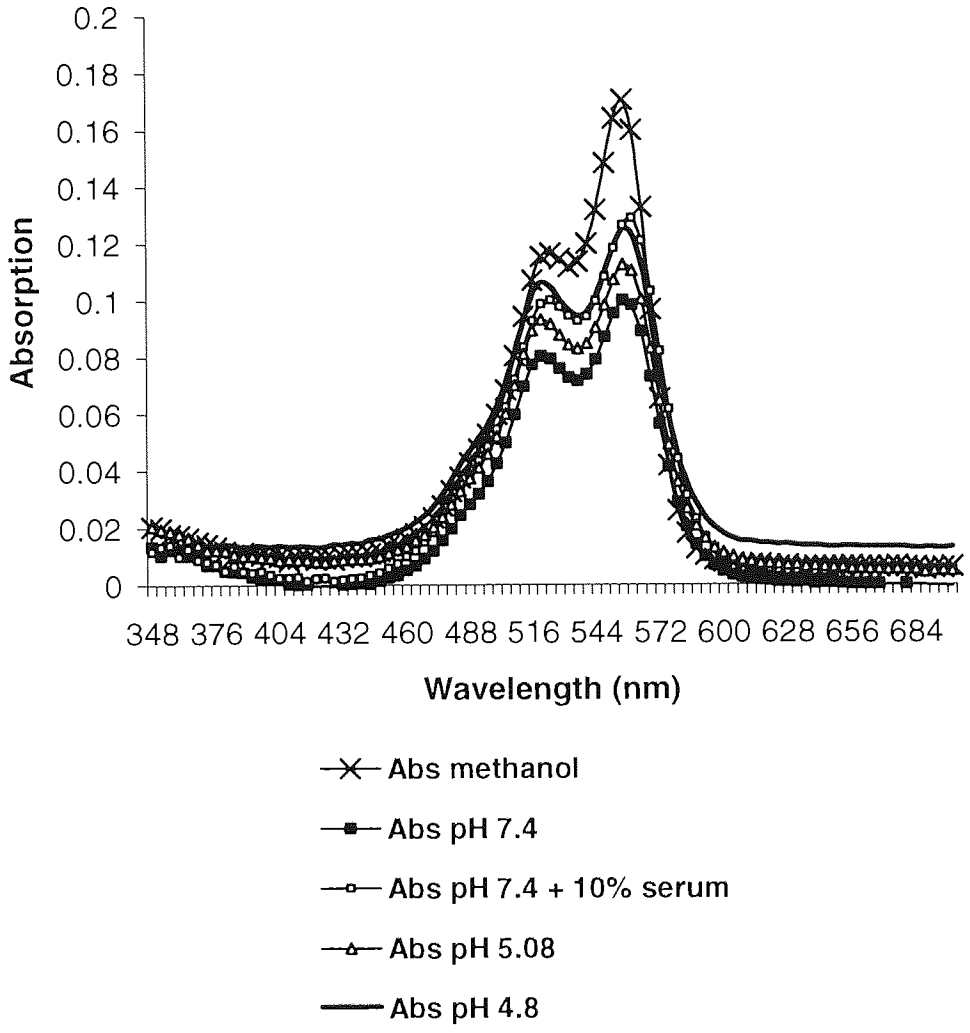


**Fig. 4-9 The UV-Vis absorption spectra of PD20 ($1.9\times10^{-2}$ $gL^{-1}$) at pH 7.4, pH 7.4 (10% serum), pH 5.08 and 4.8 and in methanol.**

absence and presence of 10% serum), pH 5.08 and 4.8 (refer to Appendix II; A). The excitation and emission spectra were measured on a spectrofluorimeter ($\lambda_{ex}$556 nm, $\lambda_{em}$579 nm). Following this, the same set of samples of PD20 were made up to the same absorption values (0.09 +/-0.001) and an excitation and emission spectra was obtained

in the same manner (Amnico luminescence spectrofluorimeter; $\lambda_{ex}$ 556 nm, $\lambda_{em}$ 579 nm; refer to Appendix II; B). The excitation and emission spectra obtained showed similarities to that of the UV-absorption profiles of PD20 obtained previously (see Fig. 4-9). It was established that the excitation and emission spectra of PD20 varied according to the pH in which PD20 was tested (refer to Appendix II; A and B). In addition, the excitation and emission spectra for the free Cy3 bisamine fluorophore is shown in Appendix III (data supplied by Amersham Biosciences, Cardiff, UK).

This data can be used as a signature of the response of PD20 to its surrounding pH. At pH 7.4, PD20 exists in its extended conformation whereby fluorophore mobility is greatly reduced. As the pH (pH 4.0 - 5.0) of the surrounding medium of PD20 is reduced the polymer, poly (L-lysine *iso*-phthalamide) changes conformation, loses it charge and hypercoils. A clear pH-dependence of the fluorescence intensity of PD20 was observed which was also shown in the corresponding absorption spectra (Fig. 4-9). It can be concluded that in contrast to the parent dye (Cy3 bisamine) the resulting conjugate, PD20 is sensitive to variations in pH owing to the conformational changes that take place within the backbone of the unlabelled polymer, poly (L-lysine *iso*-phthalamide) when the pH is reduced. This phenomenon is related to the conformational changes which take place within the polymer, poly (L-lysine *iso*-phthalamide) backbone as the surrounding pH environment decreases from pH 7.4 to that at which hypercoiling occurs (pH 4.8). It was deduced earlier (see Fig. 4-4) that there was a slight increase in the fluorescence intensity of PD20 followed by a sharp decrease when samples of PD20 were tested for their fluorescence behaviour at the hypercoiling pH (pH 4.8; see Section 4.2.4). It is noteworthy that UV-Vis absorption experiments were not conducted whereby serum was titrated into the polydye solution to investigate if an increase in absorbance at 510-530 nm would have resulted in greater fluorescence at 590 nm.

### 4.2.6 The association of PD20 with hydrophobic and hydrophilic SPA beads at various pH values

Scintillation proximity assay (SPA) beads of both a hydrophilic and hydrophobic nature were used as a model substrate to determine the effect of changing the environmental pH of the polymers surroundings from one in which the polymer exists in a negatively charged extended conformation (pH 7.4) to that at which the polymer loses its charge owing to the association of carboxylic acid groups along the polymer backbone and an increase in hydrophobicity (pH 4.8). The effect of mixing samples of PD20 with either hydrophobic or hydrophilic SPA beads at different pH values (5.0, 5.5, 6.0 and 7.4) upon fluorescence was determined (see Chapter 2; Section 2.3.10). This was carried out through the use of laser scanning confocal microscopy (LSCM) so that images of PD20 and its association with both types of SPA beads could be visualised and the average grey value total fluorescence was quantified through the use of Metamorph™ image analysis software. The term grey value is a measure of the intensity of the image in a particular pixel. The average grey value total can be described as the average fluorescence in the total number of pixels per image.

The fluorescence of PD20 and its association with hydrophobic beads at various pH values is depicted in Fig. 4-10 (B). This data indicates that there was a marked increase in the fluorescence intensity of PD20 when hydrophobic SPA beads were mixed with PD20 at lower pH values (5.5 and 5.0). At low pH (5.0 - 5.5) the exposure of hydrophobic groups within the PD20 molecule results in a stronger interaction with the hydrophobic beads and this results in an increase in fluorescence. It is noteworthy that it would not have been possible for the aldehyde groups present on the hydrophobic SPA beads to react with the amine groups present on the polymer as they are uncharged. As such, it is highly unlikely that PD20 associated with the aldehyde groups but

associated with the SPA beads owing to the increased hydrophobicity of the amphiphilic polymer, poly (L-lysine iso-phthalamide) at the lower pH values. The

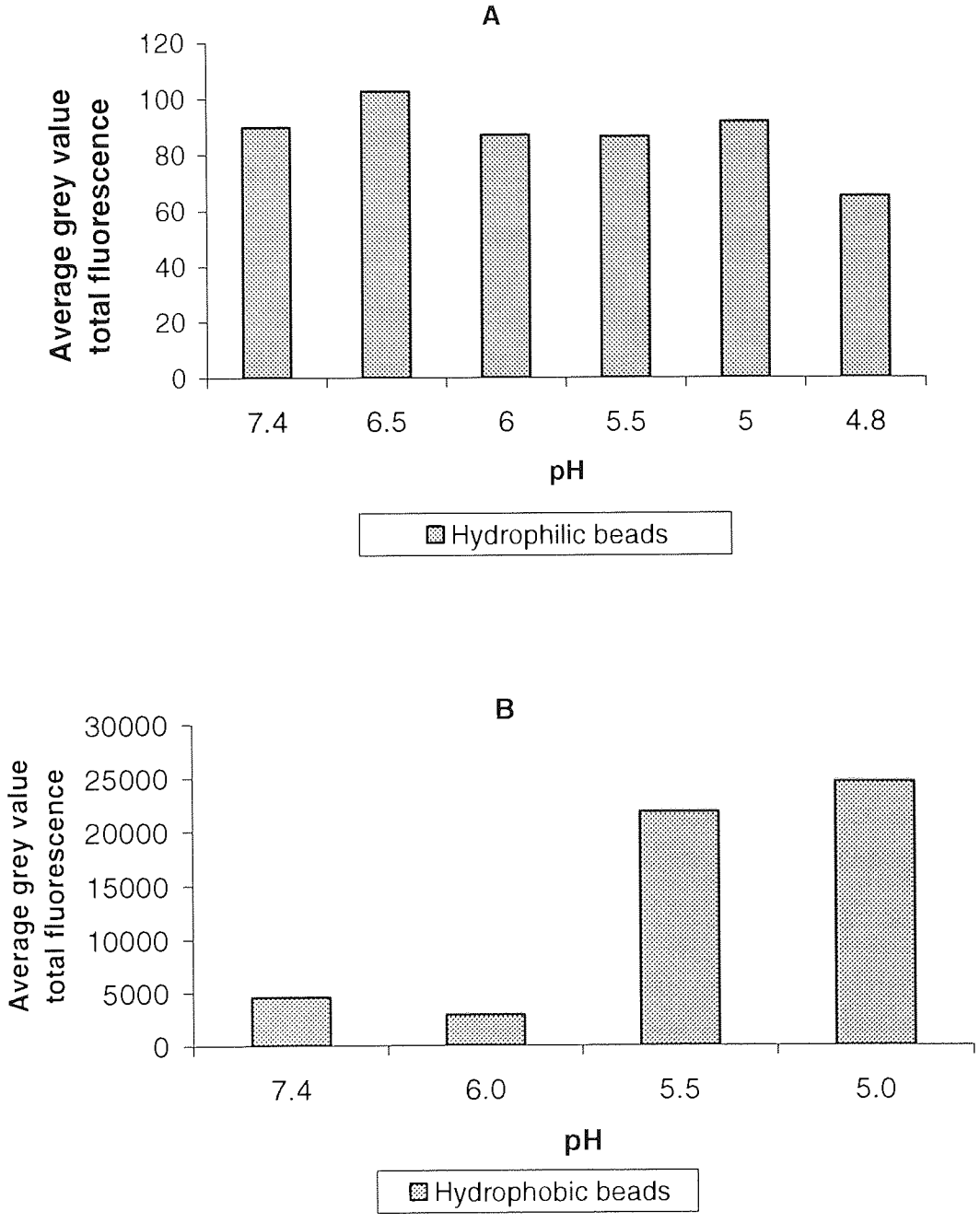


**Fig. 4-10 The average grey value total fluorescence obtained when PD20 (1 mg/ml) was mixed with either hydrophobic or hydrophilic SPA beads at various pH values. The average grey value total fluorescence was quantified through Methamorph™ image analysis software.**

fluorescence intensity (I) of PD20 following incubation with hydrophilic SPA beads is depicted in Fig. 4-10 (A). The fluorescence intensity (I) was found to be relatively similar at all pH values investigated (pH 4.8, 5.0, 5.5, 6.0, 6.5 and 7.4) when PD20 was mixed with hydrophilic SPA beads.

### 4.3 General Conclusions

The results shown for the gel filtration chromatography (GFC) of the PD20 molecule was consistent with the Cy3 bisamine fluorophore being conjugated into the backbone of the polymer, poly (L-lysine *iso*-phthalamide) but was not conclusive (see Section 4.2.1). As such, another method was sought to determine the manner in which the dye was attached to the polymer. Following PAGE analysis of the PD's (PD20, PD40, PD60 and PD80; see Section 4.2.2) confirmatory proof was provided that the Cy3 bisamine fluorophore was conjugated into the backbone of the polymer, poly (L-lysine *iso*-phthalamide) as clear separation of the positively charged Cy3 bisamine fluorophore from the negatively charged polymer was obtained.

Through the use of UV-Vis absorption, fluorescence, electrophoretic methods and confocal microscopy techniques, it was estasblished that the polymer, poly (L-lysine *iso*-phthalamide), displays a conformational change with respect to variations in pH. In the work presented here it has been demonstrated that PD20 changed conformation with respect to pH and pH dependent fluorescence was detected. When in its negatively charged state (pH 7.4), the conformation of the polymer is rigidised which thereby reduces fluorophore mobility and non-radiative energy loss. Association of the carboxyl groups along the polymer backbone on charge reduction led to a slight enhancement followed by a rapid decrease in the fluorescence of PD20 (see Fig. 4-4).

The data presented here described the physical characterisation of the PD's (PD20, PD40, PD60 and PD80). In addition, PD20 was shown to bind to other proteins. Human serum albumin (HSA) is a major circulatory protein with drug binding sites in the subdomain regions of 11A and 111A (Sulkowska, 2002). A large hydrophobic cavity is present in the 11A subdomain. The geometry of the pocket in 11A is different from that found in 111A. HSA has one tryptophan (Trp 214) present in the 11A subdomain, whereas BSA has two tryptophan moieties (Trp 135 and Trp 214), located in subdomains 1A and 11A respectively (Sulkowska, 2002). Albumin can serve as a transport carrier for drugs, and it is important to study the interactions of drugs with proteins. The effectiveness of these compounds as pharmaceutical agents depends on their binding ability.

Upon addition of serum (10%) to a solution of PD20 (1 mg/ml), an unexpected increase was observed in the fluorescence intensity of PD20. Bovine serum albumin (BSA) has a molecular weight of 67kD. At physiological pH (pH 7.4) it displays a high content of both positively and negatively charged amino acids (see Table 4-1; Peters, 1985). For example, the amino acids lysine, histidine, and arginine are all positively charged at physiological pH (pH 7.4) whereas aspartate and glutamate are both negatively charged. As such, one would expect to see greater absorption and fluorescence intensity (I) values of PD20 in the presence of serum (10%) since the unlabelled amphiphilic polymer is negatively charged at pH 7.4, in its extended conformation and would therefore bind quite readily with the positively charged amino acid contents of BSA. The binding of PD20 to positively charged amino acids would result in PD20 having a greater molecular weight thereby leading to greater rigidisation of the molecule and hence non-fluorescence energy loss. There may also have been

some electrostatic and hydrophobic interactions between dye and the protein which could lead to greater rigidisation of the conjugated polymer fluorophore.

A method which could be employed to mask the polymers adsorption to proteins which are present in blood serum would be to pegylate it. Pegylation is a procedure of growing interest for enhancing the therapeutic potential of peptides (Kodera *et al.*, 1998). When poly(ethylene glycol); PEG is covalently linked to a polypeptide, it has the potential to modify many of its features whilst maintaining the main biological functions. PEG conjugation masks the protein surface and increases the molecular size of the polypeptide, thus reducing its renal ultrafiltration, preventing the attack of antibodies or antigen presenting cells. It can also reduce the degradative properties encountered by proteolytic enzymes.

# CHAPTER 5

# THE SUBCELLULAR FATE OF POLYDYES

## 5.1 Introduction

The successful development of macromolecules as drug carriers requires knowledge of their fate within cells as discussed previously (see Chapter 1). In this Chapter, the internalisation and subcellular fate of PD20 was studied exploiting CHO cells cultured *in-vitro*. In addition, a study was completed to determine the subcellular fate of a lower molecular weight polydye (PD30) in both CHO and HepG2 cells cultured *in-vitro*. The work presented herein details the use of two commonly used techniques, fluorescence and laser scanning confocal microscopy (LSCM; see Chapter 1), to determine if internalisation of PD20 and PD30 occurred in CHO cells cultured *in-vitro* and to establish the subcellular fate of the polydye following internalisation.

The mechanism of endocytosis has been extensively discussed in Chapter 1 (see Section 1.2.5.2) and has been broadly defined as the internalisation of extracellular material due to invaginations of the extracellular membrane into the cytosol of the cell. This definition includes receptor-mediated and non-receptor-mediated (constitutive) endocytosis, and the phagocytosis of particles, whether they are macromolecular drugs packaged in delivery systems or bacterial vectors. Endocytic uptake includes the need to regulate the contribution of internalised material to the overall physiological state of the cell. It can often lead to the degradation of internalised material and the generation of either waste products or raw materials for anabolic processes (Provoda and Lee, 2000).

Several approaches exist for the cytosolic delivery of proteins and nucleic acids and were described in Chapter 1 (see Section 1.3.1). One method for the cytosolic delivery of proteins and nucleic acids is to partially or temporarily breach the

endosomal membrane to release the contained internalised therapeutic agents. This could be achieved by provoking membrane-perturbing activity preferentially in the low pH environment of endocytic compartments. Until recently efforts to promote the escape of internalised agents from the endosomal or lysosomal pathways have been mainly achieved using viruses or virus-derived endosomolytic peptides derived from the amino-terminal sequence of influenza virus hemagglutinin HA-2.

HA promotes fusion of the viral envelope with the endosomal membrane. It has been established that the acidic pH of the endosome lumen (pH 5.0-6.0) promotes a conformational change in the HA protein which leads to a fusion event. A variety of pH-sensitive synthetic peptides have been designed to demonstrate that a preferential breach of endosomal compartments can enhance the cytosolic delivery of macromolecules. These include the amphipathic peptides such as GALA and KALA (Provoda and Lee, 2000). It was envisaged that due to the pH-dependent properties of the polymer, poly (L-lysine *iso*-phthalamide), PD20 may behave in a similar manner to that of the HA virus once it became internalised into the endosomal compartment of the cell.

The experimental work presented in this chapter was designed to determine if internalisation of PD20 was possible in CHO cells cultured *in-vitro* and was aimed at demonstrating the association of PD20 with the extracellular membrane and its internalisation into CHO cells at physiological pH (pH 7.4). Subsequently, quantification of the fluorescence intensity of PD20 was assessed as it progressed from the extracellular membrane to various internal compartments within the cell such as the endosome. Quantification of the fluorescence intensity was achieved using Metamorph™ image analysis software (made available by Amersham Biosciences). Fluorescence intensity can be measured on a pixel to pixel basis. A pixel measures the

light intensity coming from a specific area of the image scene (for monochrome imaging) which is essentially the average photon intensity of that region. Each pixel measures the incident photons at that location which can be quantified for digital presentation. The photon counts are then eliminated and converted to a fixed scale, for example 8 or 1-256 bit where 1 corresponds to no photons (dark) and 256 corresponds to maximum brightness. By selecting an image of a single colour (red channel data) the average grey value total fluorescence within the image area could be determined where the term grey value was a measure of the intensity of the image in a particular pixel. The average grey value total can be described as the average fluorescence in the total number of pixels per image.

## 5.2 Results and Discussion

### 5.2.1 The association of PD20 with the extracellular membrane of CHO cells cultured *in-vitro*

Fluorescence microscopy images were obtained of CHO cells cultured *in-vitro* to determine if PD20 became associated with the extracellular membrane following incubation at pH values of 7.4 and 5.5 (see Chapter 2; Section 2.3.11). Fluorescence microscopy images indicated that at pH 7.4 (Fig. 5-1;A) a small amount of PD20 adsorbed onto the membrane of CHO cells following a thirty-minute incubation period at 37°C. By contrast, incubation under the same conditions at pH 5.5 led to extensive adsorption of the largely uncharged polymer (Fig. 5-1;B) onto the surface of the extracellular membrane of CHO cells. At physiological pH (pH 7.4) the polymer, poly (L-lysine *iso*-phthalamide) exists in an extended negatively charged conformational state with the hydrophobic groups exposed. It was established previously from potentiometric titration that poly (L-lysine *iso*-phthalamide) undergoes a hypercoiling

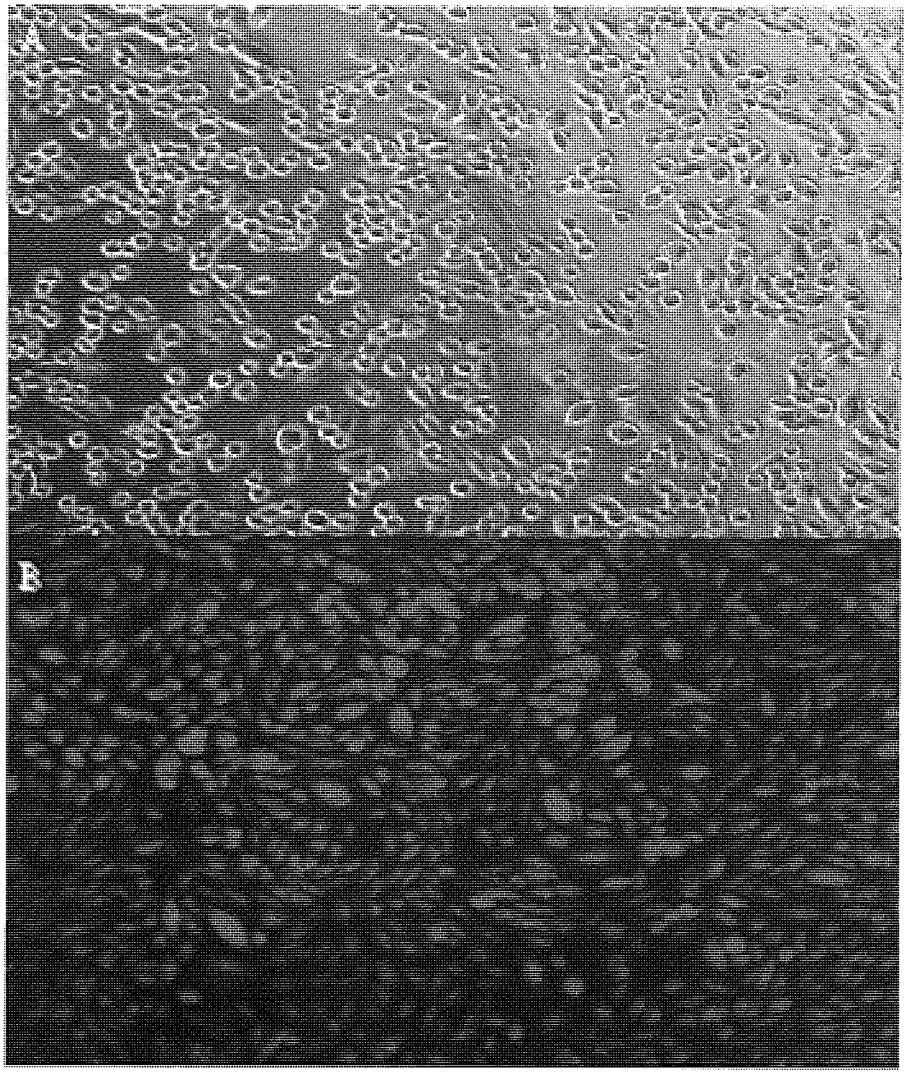


Fig. 5-1 The fluorescent photomicrogram images of CHO cells cultured *in-vitro* demonstrating PD20 (1 mg/ml) associating with the extracellular membrane (Image A; pH 7.4) and pH 5.5 (Image B). CHO cells in separate Wilco dishes were incubated with a 2 ml suspension of PD20 (1 mg/ml) at either pH 7.4 or pH 5.5 for 30 minutes at 37°C. Subseqently, PD20 treatments were removed, CHO cells were washed (x3) with D-PBS titrated to pH 7.4 and 5.5 and re-suspended in the appropriate buffers (pH 7.4 and pH 5.5). Fluorescence microscopy images (x20 magnification eyepiece) were used to highlight the adsorption of PD20 to the surface of the extracellular membrane. Internal organelles could not be visualised using this technique. Image A depicts a phase contrast image of CHO cells depicting the non-fluorescent CHOs at pH 7.4 and the fluorescence of the cells from Image B which have been overlaid on top of the phase contrast image to highlight the fluorescence of CHO cells at low pH (5.5). Scale bar (2 cm) represents a 75 $\mu$m width.

transition between pH 4 and 5 (Eccleston *et al.*, 1999). Such a transition is characterised by a change in polymer conformation into a tight coil stabilised by hydrophobic association. Thus associated or conjugated fluorophores would be brought into closer proximity effectively increasing the local concentration. This results in the polymer adhering more to the extracellular membrane of CHO cells at low pH (pH 5.5) than it appears to do at pH 7.4 as is demonstrated in Fig. 5-1.

### 5.2.2 The internalisation and subcellular fate of PD20 in CHO cells cultured *in-vitro*

A series of LSCM experiments were designed to investigate the short-term fate of PD20 (1 mg/ml) following a standard incubation period (10 minutes at 37°C) with CHO cells cultured *in-vitro* at pH 7.4 and 5.0. The method employed in these experiments was described previously (see Chapter 2; Section 2.3.12). The LSCM images obtained highlighted the association of PD20 to the surface of the extracellular membrane of CHO cells cultured *in-vitro*. LSCM images were also obtained to determine if internalisation of PD20 by CHO cells cultured *in-vitro* was possible at pH values of 7.4 and 5.0. Furthermore, images obtained using LSCM were analysed using Metamorph™ image analysis software to determine the average grey value total fluorescence from each image.

#### 5.2.2.1 The internalisation and subcellular fate of PD20 at pH 7.4

The LSCM images obtained (see Chapter 2; Section 2.3.12) to visualise the time-dependent internalisation of PD20 (1 mg/ml) by CHO cells cultured *in-vitro* (160,000/ml) at various time points (10 to 60 minutes) following an initial incubation period of 10 minutes at 37°C at pH 7.4 are depicted in Fig. 5-2 (images A-F). Closer

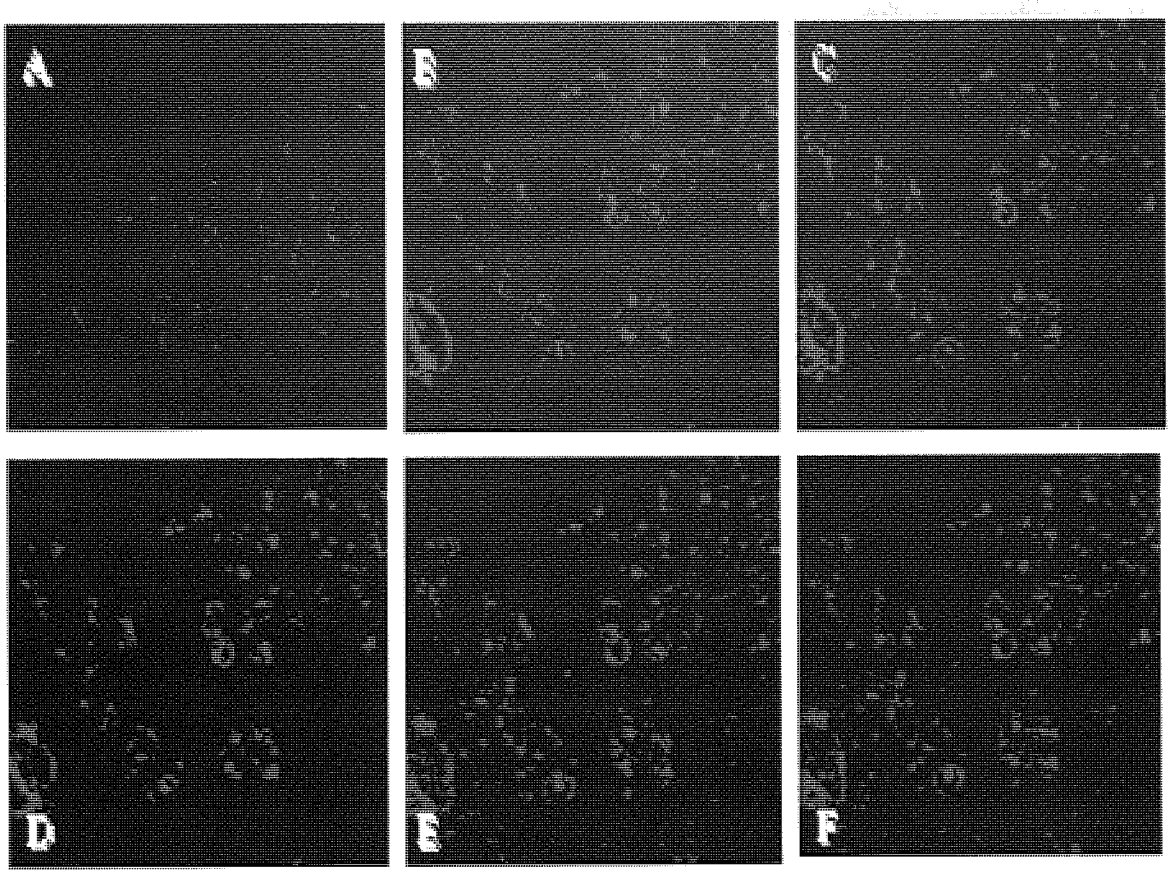


Fig. 5-2 The internalisation of PD20 (1 mg/ml) by CHO cells cultured *in-vitro* at pH 7.4. LSCM images (A-F) show the internalisation of PD20 at various time points (A:10, B:20, C:30, D:40, E:50 and F:60 minutes following an initial incubation period of 10 minutes at 37°C). The total population of CHO cells in the Willco dish were stained with PD20. In the entire image field endosmal regions were stained with PD20 by 20 minutes (image B) and nuclear localisation of PD20 was present in the majority (approximately 70%) of CHO cells (image B). Staining of the nucleus with PD20 appeared to be concurrent with endosomal staining. PD20 supernatant (2 ml) was removed following a 10 minute incubation period at 37°C, CHOs were washed (x3) with the appropriate serum free medium (pH 7.4) and re-suspended in fresh serum free medium (pH 7.4). Subsequently, LSCM images (red channel data; contrast 236, brightness 9999, pinhole 100, Zoom 1, Lens 63x with oil and a x10 eyepiece) were obtained at various time points (A:10, B:20, C:30, D:40, E:50 and F:60 minutes) to demonstrate internalisation of PD20 by CHO cells at pH 7.4. Scake bar (2 cm) represents a 50 μm width.

observation of these images revealed that PD20 progressed rapidly from the extracellular membrane of CHO cells (image A:10 mins) trafficking towards internal cellular organelles such as the endosome within 20 minutes (image B). Surprisingly some cells displayed nuclear staining 20 minutes post the initial incubation period (10 minutes) and images obtained thereafter (C, D, E, and F) indicated that PD20 tended to remain in endosomes and the nucleus of some cells.

The images shown (Fig. 5-2) demonstrated a marked increase in the labelling of intracellular structures as time progressed from 10 to 60 minutes. The punctate staining observed in the images (Fig. 5-2;B-F) represents endocytosis of PD20 (Jin *et al*, 2002). Upon closer observation of the images some obvious labelling of the nucleus was apparent in a subpopulation of CHO cells cultured *in-vitro* within the Wilco dish (Fig. 5-2;C). These findings indicate that PD20 was initially introduced to the extracellular membrane and later becomes incorporated into endosomal compartments. It is apparent that PD20 breached the endosomal compartment and escaped into the cytosol, allowing it to traffic to the nucleus.

The images obtained by LSCM demonstrating internalisation of PD20 at pH 7.4 (Fig. 5-2;A-F) were analysed for their average grey value total fluorescence using Metamorph™ image analysis software and the results are shown in Fig. 5-3. The results indicate that there was a marked increase in the average grey value total fluorescence of PD20 (1mg/ml) at pH 7.4 as it became endocytosed by CHO cells. This marked increase in fluorescence was most pronounced at around 50 to 60 minutes following internalisation of PD20 by CHO cells, suggesting that PD20 had breached the endosomal compartment and escaped into the cytosol and was trafficked towards the nuclear regions of some cells. The marked increase in the average grey value total fluorescence as time progressed (10 to 60 minutes) indicates that as PD20 is introduced

to the extracellular membrane (10 minutes post the initial incubation period) it becomes more distributed intracellularly leading to an increase in fluorescence. As PD20 trafficked towards further intracellular compartments such as the endosome and to some extent the nucleus of a subpopulation of CHO cells cultured *in-vitro* the fluorescence is greater due to a higher degree of distribution.

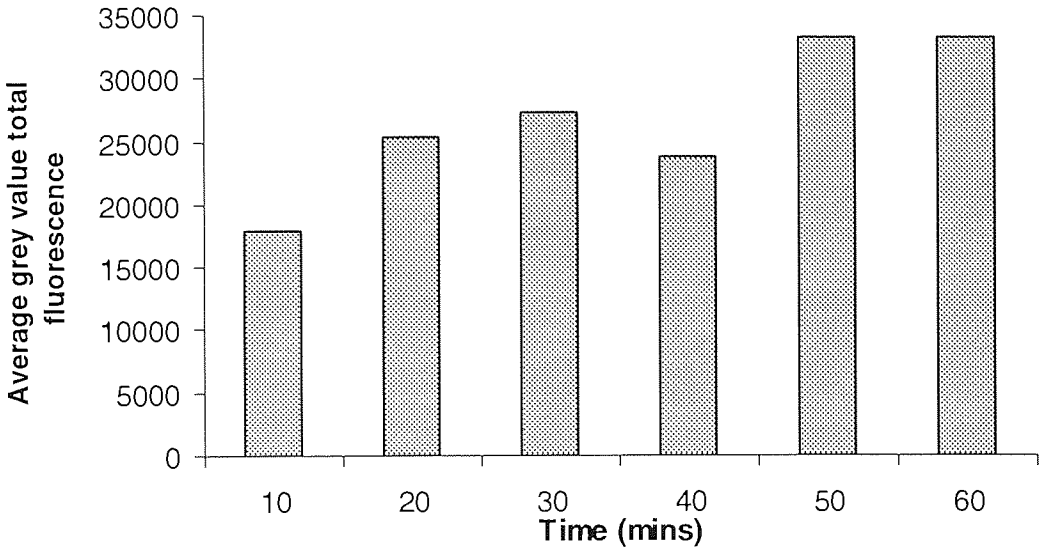


**Fig. 5-3 Quantification of the average grey value total fluorescence obtained when LSCM images depicting internalisation of PD20 by CHO cells at pH 7.4 (see Fig. 5-2;A-F) were analysed using Metamorph™ image analysis software. PD20 supernatant (2 ml) was removed from a Wilco dish containing CHOs following a 10 minute incubation period at 37°C (pH 7.4), CHOs were washed (x3) with the appropriate serum free medium (pH 7.4) and re-suspended in fresh serum free medium (pH 7.4). Subsequently, LSCM images (contrast 236, brightness 9999, pinhole 100, Zoom 1, Lens 63x with oil and a x10 eyepiece) were obtained at various time points (A:10, B:20, C:30, D:40, E:50 and F:60 minutes; see Fig. 5-2; A-F) to demonstrate internalisation of PD20 by CHO cells at pH 7.4. Subsequently, images obtained (see Fig. 5-2;A-F) were quantified for their average grey value total fluorescence using Metamorph™.**

Due to the presence of endosomal trafficking and to some extent nuclear localisation of PD20 in CHO cells cultured *in-vitro* it was envisaged that PD20 became

internalised via an endocytotic process which could be attributed to fluid-phase endocytosis at pH 7.4. Small solutes are readily taken up by cells due to passive diffusion or through the action of specific porters for certain substrates such as glucose and amino acids (Matthews *et al.,* 1996). Macromolecules however are unable to enter a cell via this route owing to their size. Natural macromolecules, such as, proteins, polysaccharides and polynucleotides are taken into the cell via endocytosis. Synthetic macromolecules also follow this route (Matthews *et al.,* 1996). Internalisation occurs via one of two clearly different mechanisms; pinocytosis or phagocytosis. Phagocytosis or 'cell-eating' takes place only in specialised cells such as macrophages and often results in the uptake of particles greater than 10-20 $\mu$m in diameter. With regard to the immune system, it is involved in the uptake and destruction of bacteria. This process is most important when using liposomes and microparticles as drug targeting approaches.

The presence of fluorescence in the nucleus of a subpopulation of CHO cells within the same Wilco dish indicates that endosomal release of PD20 into the cytosol occurred. However, this was not apparent in all cells and this effect could be attributed to the polydispersity of PD20. When PD20 becomes internalised into the endosomes the pH decreases to pH 5.0 resulting in hypercoiling of the polymer. This in turn causes the endosomal membrane to rupture releasing the contents and the lower molecular weight fractions may have been transported to nuclear regions in the cell via diffusion. Upon internalisation into an acidic compartment such as that of an endosome (pH 5.0-6.0) the polymer, poly (L-lysine *iso*-phthalamide) would begin to collapse in structure due to the change in pH. The naked polymer, poly (L-lysine *iso*-phthalamide) would be less negatively charged and more hydrophobic than at physiological pH (7.4) hence PD20 binds to the membrane of the endosome at pH 5.0-6.0. Fractions of higher molecular weight (17,000-60,000 D) may be too large to cross the nuclear membrane and this may

explain why only the nucleus of a subpopulation of CHO cells cultured *in-vitro* fluoresced.

### 5.2.2.2 The subcellular fate of PD20 at pH 5.0

A further study was conducted to generate LSCM images of PD20 and the association with CHO cells cultured *in-vitro* at pH 5.0 (see Chapter 2; Section 2.3.12). The images obtained are represented in Fig. 5-4 (images A-F) and depict the association of PD20 (1 mg/ml) with the extracellular membrane of CHO cells (160,000/ml) cultured *in-vitro* at various time points (10-60 minutes, A-F respectively) following an initial incubation period of 10 minutes at 37°C at pH 5.0. The images indicate that PD20 adsorbed very rapidly to the membrane of CHO cells cultured *in-vitro* following the initial incubation period of 10 minutes (see Fig. 5-4; image A). It was also established that PD20 appeared to adsorb solely to the membrane of CHO cells up to 60 minutes post incubation (see Fig. 5-4; 10-60 minutes; images A-F respectively).

The average grey value total fluorescence obtained from each of the images is shown in Fig. 5-5. The results indicated that the average grey value total fluorescence of PD20 (1 mg/ml) at pH 5.0 changed over time (refer to Fig. 5-5). Following a thirty-minute period after the initial incubation (37°C for 10 minutes) the average grey value total fluorescence of PD20 began to decline. It was expected that the change in polymer conformation at the onset of hypercoiling would be accompanied by a decrease in relative fluorescence intensity due to an increase in the local concentration of fluorophores, resulting in a decrease in the average grey value fluorescence values.

Due to the hydrophobicity of the polymer at pH 5.0 it was expected that internalisation of PD20 may have occurred due to an adsorptive pinocytotic event, which may have been non-specific due to changes in hydrophobicity and charge.

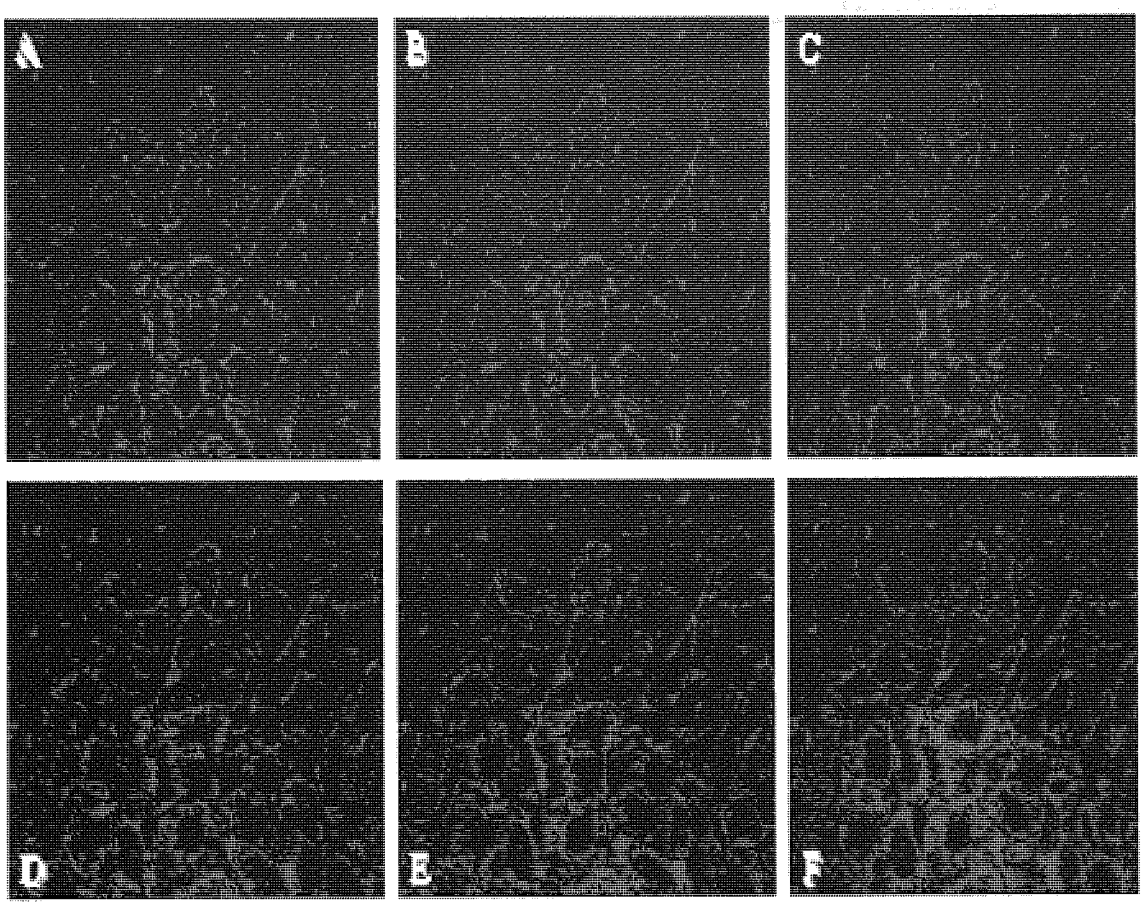


Fig. 5-4 The adsorption of PD20 (1 mg/ml) to the extracellular membrane of CHO cells cultured *in-vitro* at pH 5.0 following an initial incubation period of 10 minutes at 37°C. The images shown (A-F) demonstrate that PD20 accumulated on the external surface of CHO cells and that there was no apparent internalisation of PD20 throughout the imaging period at pH 5.0 (A-F). LSCM images (A–F) show adsorption of PD20 to the extracellular membrane of CHO cells cultured *in-vitro* at pH 5.0 at various time points (10:A, 20:B, 30:C, 40:D, 50:E and 60:F minutes following an initial incubation period of 10 minutes at 37°C; contrast 236, brightness 9999, pinhole 100, zoom 1, Lens 63x with oil and a x10 eyepiece). PD20 supernatant (2 ml) was removed following a 10 minute incubation period at 37°C (pH 5.0), CHOs were washed (x3) with the appropriate serum free medium titrated to pH 5.0 and re-suspended in fresh serum free medium (pH 5.0). Subsequently, LSCM images (contrast 236, brightness 9999, pinhole 100, Zoom 1, Lens 63x with oil and a x10 eyepiece) were obtained at various time points (A:10, B:20, C:30, D:40, E:50 and F:60 minutes) to demonstrate adsorption of PD20 to the surface of the extracellular membrane of CHO cells at pH 5.0. Scale bar (2 cm) represents a 50 μm width.

However, endocytosis of PD20 was not observed in CHO cells cultured *in-vitro*. Due to a change in the pH of the microenvironment surrounding the cells endocytosis may have been affected.

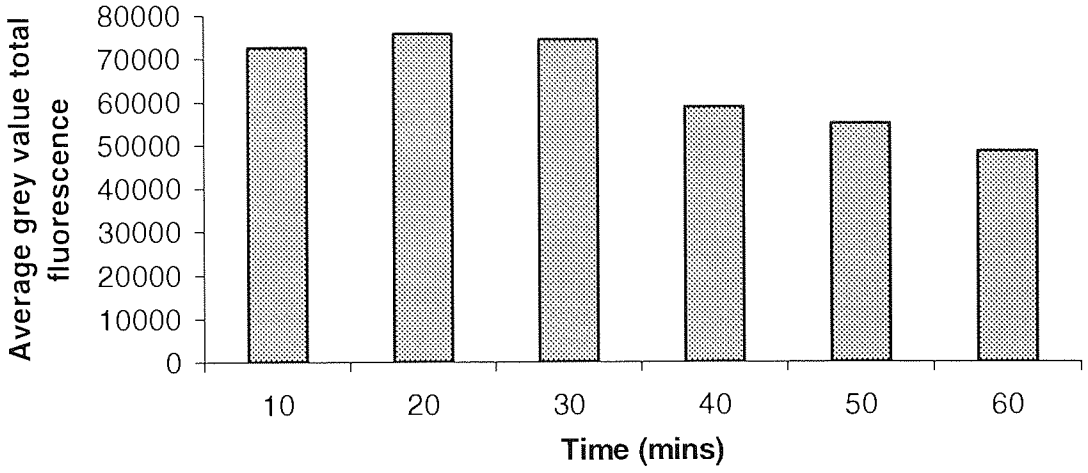


**Fig. 5-5 Quantification of the average grey value total fluorescence of PD20 when it was associated with the extracellular membrane of CHO cells at pH 5.0 (LSCM images A-F shown in Fig. 5-4) using Metamorph™ image analysis software. PD20 supernatant (2 ml) was removed from a Wilco dish containing CHOs following a 10 minute incubation period at 37°C (pH 5.0), CHOs were washed (x3) with the appropriate serum free medium (pH 5.0) and re-suspended in fresh serum free medium (pH 5.0). Subsequently, LSCM images (contrast 236, brightness 9999, pinhole 100, Zoom 1, Lens 63x with oil and a x10 eyepiece) were obtained at various time points (A:10, B:20, C:30, D:40, E:50 and F:60 minutes; see Fig. 5-4; A-F) to demonstrate adsorption of PD20 to the surface of the extracellular membrane of CHO cells at pH 5.0. Subsequently, images obtained (see Fig. 5-4;A-F) were quantified for their average grey value total fluorescence using Metamorph™. It is noteworthy that there was an apparent difference between the intensity of the fluorescence obtained in the images (LSCM images A-F shown in Fig. 5-4) and the bar graphs presented here. LSCM images shown in Fig. 5-4 imply that there was a large increase in fluorescence as time progressed (10-60 minutes) while the bar graphs presented here implies that the fluorescence decreased as time progressed.**

### 5.2.3 Internalisation and subcellular fate of free Cy3 bisamine fluorophore

A control experiment was completed to compare the internalisation of the free Cy3 bisamine fluorophore to that of PD20 by CHO cells cultured *in-vitro* at pH 7.4 (see Chapter 2; Section 2.3.12). By employing UV-Vis absorption spectroscopy the free Cy3 bisamine fluorophore (139 $\mu$g/ml) was prepared to an equivalent absorption value to that of PD20 (1 mg/ml). Images (A-E) depicting the time-dependent internalisation of the free Cy3 bisamine fluorophore is shown depicted in Fig. 5-6.

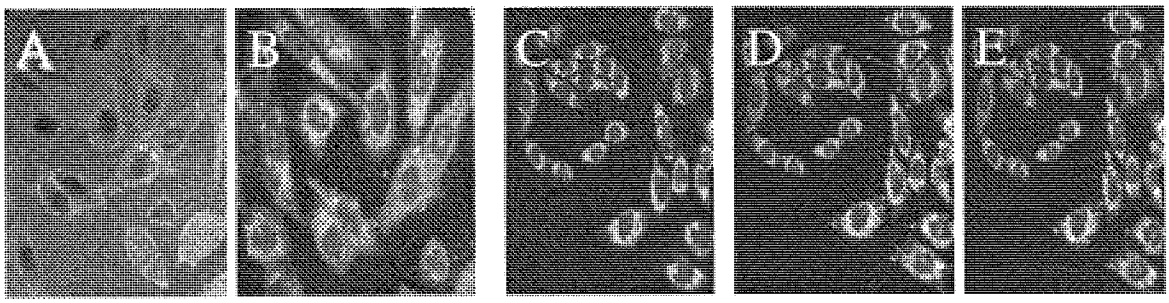


A and B
75 $\mu$m

C, D and E
100 $\mu$m

**Fig. 5-6 LSCM of CHO cells cultured *in-vitro* following incubation with free Cy3 bisamine fluorophore prepared to the same equimolar concentration (139 $\mu$g/ml) as PD20 (1 mg/ml). LSCM images (A-E) represents internalisation of the free Cy3 bisamine fluorophore at pH 7.4 (see Chapter 2; Section 2.3.12). Endosomal uptake and cytosolic localisation of the free Cy3 bisamine fluorophore by CHO cells is apparent in the images shown at various time points, following an initial 10 minute incubation period at 37°C, 15(A), 30(B), 45(C), 55(D), and 60(E) minutes. Scale bar (2 cm) represents 75 $\mu$m (A and B) and 100 $\mu$m (C, D and E) widths.**

The images shown indicate that the free Cy3 bisamine fluorophore became localised within the endosomal compartment of CHO cells after a ten minute incubation period at 37°C. The images shown in Fig. 5-6(A-E) also indicate some cytosolic delivery of the free Cy3 bisamine fluorophore. However, there was no indication of nuclear localization. The internalisation of the free Cy3 bisamine fluorophore was not unexpected due to the presence of charged quaternary nitrogen groups and its low molecular weight (443 D). Gated ion channels and and pumps regulate the import and export of small molecules and ions into and out of cells whereas large molecules and particles become internalised by endocytosis (Tung and Weissleder, 2002). Thus, the free Cy3 bisamine fluorophore can easily traverse the extracellular membrane of CHO cells cultured *in-vitro* and become trafficked towards endosomal regions. It also appears to breach the endosomal compartment and escape into the cytosol, which could be attributed to the diffusion of the small molecular weight molecules through the intact endosomal membrane.

### 5.2.4 The Co-localisation of PD20 with FITC-Alexa Fluor 488 at pH 7.4

It was previously determined that PD20 was internalised in CHO cells via an endocytic process (Fig. 5-2; A-F; see Section 5.2.2.1), possibly fluid phase endocytosis at physiological pH (pH 7.4). It was also concluded that PD20 had accumulated in lower acidic regions, such as that of endosomes (pH 5.0 - 6.0), and to some extent in the nucleus of some CHO cells. A co-localisation study was conducted to determine where PD20 became localised to following internalisation by HepG2 cells at physiological pH (pH 7.4; see Chapter 2; Section 2.3.13). The use of a specific endosomal marker, FITC-Alexa Fluor 488 was used in combination with PD20 to detect where PD20 trafficked to following internalisation at pH 7.4. HepG2 cells were selected for the co-localisation

study as they express transferrin receptors and the FITC-Alexa fluor conjugate becomes internalised via a transferrin receptor-mediated endocytic process. Transferrin is a monomeric serum glycoprotein (~80,000 D) that binds up to two $Fe^{3+}$ atoms for delivery to vertebrate cells through receptor-mediated endocytosis (Dautry-Varsat, 1986).

The LSCM images obtained when a mixture of both PD20 (1 mg/ml) and FITC-Alexa Fluor 488 (50 $\mu$g/ml) was incubated with HepG2 cells (160,000 cells/ml) at 37°C for 15 minutes are depicted in Fig. 5-7. To detect the presence of PD20 (see Fig. 5-7;A) excitation and emission wavelengths of 535 nm and 570 nm were used respectively and to detect FITC-Alexa Fluor 488 (see Fig. 5-7; B) excitation and emission wavelengths of 495 nm and 518 nm respectively were used. An overlay of Fig. 5-7(A) with Fig. 5-7(B) is depicted in Fig. 5-7(C). It was concluded that the fluorescence from PD20 and FITC-Alexa fluor 488 had coalesced and was observed discretely in endosomal regions of HepG2 cells (Fig. 5-7;C). LSCM analysis revealed colocalisation of PD20 with FITC-Alexa Fluor 488 in HepG2 cells, suggesting that PD20 enters early endosomes following internalisation at physiological pH (pH 7.4; see Fig. 5-7; A-C). It is noteworthy, that no fluorescence of PD20 was observed in the nucleus of HepG2 cells cultured *in-vitro*. Internalisation of PD20 at this pH (pH 7.4) was possibly due to fluid phase endocytosis, similar to results presented earlier relating to CHO cells cultured *in-vitro* (Fig. 5-2; images A-F).

The fluorescent dye, FITC contains an isothiocyanate group that can react with amine or alcohol groups. However there are no nucleophilic substitution sites present on the polymer which could have led to a possible reaction with the isothiocyanate group present on the FITC probe. Hence, the polymer poly (L-lysine *iso*-phthalamide) is non-reactive to any species present on the FITC-Alexa fluor colocalisation probe. Furthermore, in regions of the merged image that depicted colocalisation of both probes

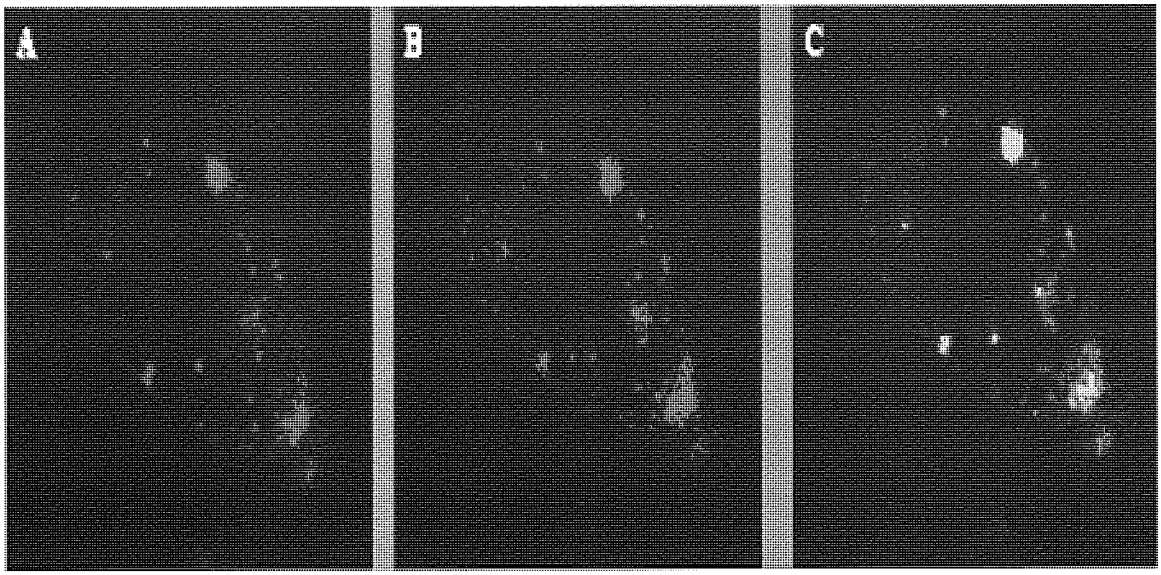


Fig. 5-7 LSCM images depicting colocalisation of PD20 (1 mg/ml) with an endosomal marker, FITC-Alexa fluor 488 (50 μg/ml). HepG2 cells cultured *in-vitro* were incubated with PD20 and Alexa Fluor 488 (A, B, C) for 15 minutes at 37°C and processed for fluorescence as described in cell assays (see Chapter 2; Section 2.3.13). PD20 (A; excitation and emission 535 nm and 570 nm respectively) and FITC-Alexa Fluor 488 (B; excitation and emission 495 nm and 518 nm respectively). Images from A and B were merged to obtain image C (PD20; red) and Alexa Fluor 488 (Green) co-localisation. Scale bar (2 cm) represents 8 μm width.

(Fig 5-7;C) yellow spots appear to be present. These yellow spots are attributed to fluorescence bleed-through between the green and red fluorescent channels. In a dual-labelled green or red sample, overlaying the images will make the pixels appear yellow or orange.

### 5.2.5 The internalisation and sucellular fate of PD30

Studies completed with PD20 indicated that it was internalised by CHO cells cultured *in-vitro* at pH 7.4 (see Fig. 5-2; images A-F) rapidly from the extracellular membrane towards internal organelles such as the endosome (pH 5.0 - 6.0; Fig. 5-2; image B; 20 minutes). Some of the images also highlighted that nuclear staining of some cells had occurred (Fig. 5-2; image C). This was attributed to PD20 having a high polydispersity index (data not shown) and containing small molecular weight components.

It was envisaged that tailoring a polydye to be of a lower molecular weight than PD20 could result in greater nuclear localisation in cells following endosomal release into the cytosol. A polydye denoted as PD30 herein was synthesised so that lysine:Cy3 bisamine fluorophore moieties were incorporated into the backbone of the polymer, poly (L-lysine *iso*-phthalamide) at a ratio of 30:1. It has since been characterised and was shown to have a number average molecular weight of 15,220 D (see Chapter 4; Table 4-1) with a polydispersity index of 1.20 D.

Two separate studies were completed to investigate the internalisation and internal trafficking of PD30 in both CHO and HepG2 cells cultured *in-vitro* (see Chapter 2; Section 2.3.14). In separate Wilco dishes, both CHO and HepG2 cells (160,000 cells/ml) were incubated with PD30 (1 mg/ml) for 10 minutes at 37°C. LSCM images were obtained 30 minutes post the initial incubation period (10 minutes at

37°C). Control experiments were also completed to determine if the free Cy3 fluorophores (Cy3 bisamine and Cy3 bissulphonic acid) were internalised by CHO and HepG2 cells cultured *in-vitro* (see Chapter 2; Section 2.3.14).

The association of the free Cy3 fluorophores (Cy3 bissulphonic acid and Cy3 bisamine monomers) with CHO cells cultured *in-vitro* is depicted in Fig. 5-8 (A and B). The image shown in Fig. 5-8(A) indicated that the free Cy3 bissulphonic acid fluorophore was membrane bound in CHO cells cultured *in-vitro* after 30 minutes post the initial incubation period (10 minutes at 37°C). Fig. 5-8(B) indicated that the free Cy3 bisamine fluorophore became internalised by CHO cells cultured *in-vitro* and similar to results presented earlier in Fig. 5-6, into the acidic regions of endosomes (pH 5.0-6.0).

The internalisation of PD30 by CHO cells cultured *in-vitro* is depicted in Fig. 5-8(C and D) and represents a single CHO cell whereby the cell appears to be undergoing mitotic cell division. PD30 had entered the cytosol of the cell and accumulated in the nuclei which are more brightly stained than the corresponding cytosol. Uptake of PD30 into endosomal regions was also apparent. Upon closer observation of Fig. 5-8;C, dark structures are apparent within the nuclei. These dark structures inside the nuclei are possibly nucleoli that excluded PD30. An image representing that of a single CHO cell is also shown in Fig. 5-8(D) and revealed staining of endosomal and possibly lysosomal regions with PD30. Similar to results shown in Fig. 5-8;C, the nucleus appears to be more brightly stained with PD30 than any other intracellular regions. The cytosol of this single CHO cell also appears to be stained with PD30. These images suggest that PD30 was possibly released from the endosomal compartment into the cytosol and either trafficked to the nucleus or to the lysosomes where degradation would occur.

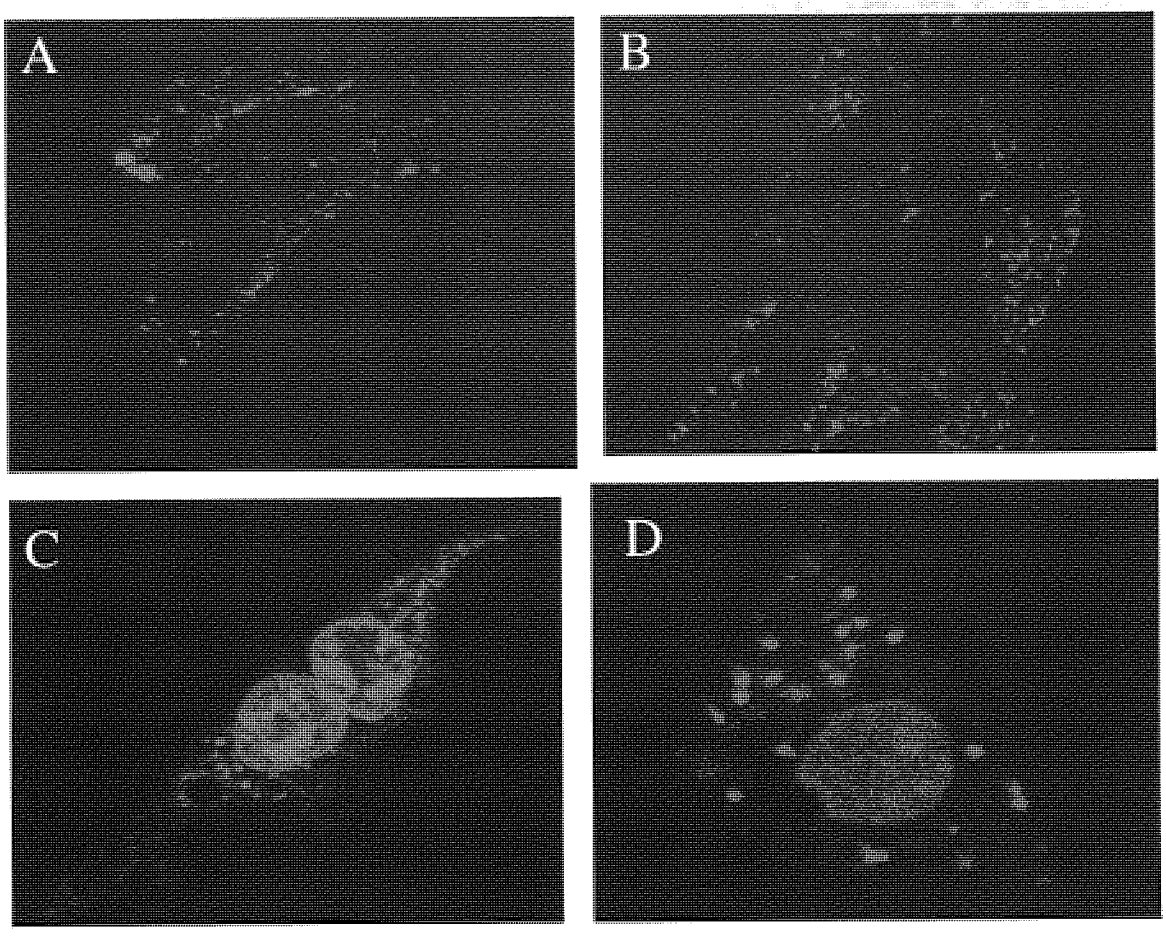


A, B and C
20$\mu$m

D
9 $\mu$m

Fig. 5-8 LSCM images demonstrating internalisation of PD30 (1mg/ml) by CHO cells cultured *in-vitro* at pH 7.4. CHO cells (160,000 cells/ml) cultured in Wilco dishes were incubated with samples of PD30 (2 ml;1 mg/ml) and free dyes (Cy3 bisamine and Cy3 bissulphonic acid fluorophores) for a period of 10 minutes at 37°C (pH 7.4; see Chapter 2; Section 2.3.14). Subseqently, PD and free dye samples were aspirated from the Wilco dishes, CHOs were washed (x3) with serum free medium (2 ml) and re-suspended in fresh serum free medium (2 ml). LSCM (images A and B) demonstrate the uptake of free Cy fluorophores (unknown concentration due to availability) by CHO cells cultured *in-vitro*. Image A demonstrates the association of a sample of the free Cy bissulphonic acid fluorophore (membrane bound) whereas image B shows that of a sample of the free Cy3 bisamine fluorophore (endosomal localisation). Uptake and nuclear localisation of PD30 (1 mg/ml) by a CHO cell (images C and D) was apparent 30 minutes post the initial incubation period (10 minutes at 37°C) at physiological pH (7.4). Image C represents nuclear localisation of PD30 by a single CHO cell undergoing mitotic division. No nuclear co-staining experiments were conducted to determine nuclear uptake of PD30. Scale bars (2 cm) represents 20 $\mu$m (A, B and C) and 9 $\mu$m (D) widths.

A further study was completed on a different cell line, HepG2 to determine whether or not the nuclear localisation of PD30 was cell specific. HepG2 cells are depicted in Fig. 5-9(A) and reveal that the control Cy3 bisamine fluorophore became internalised into endosomes but not in nuclear regions whilst Fig. 5-9(B) indicates that PD30 became internalised quite rapidly (30 minutes post the initial 10 minute incubation period). The cytosolic regions, lysosomes and the nucleus appear to be stained. Similar to those results found previously for CHO cells (Fig. 5-8; C) closer observation of Fig. 5-9(B) revealed the appearance of dark structures within the nucleolus, possibly areas of the nucleus that excluded PD30.

Gel filtration chromatograms (GFC) obtained from RAPRA technologies demonstrated that the number average molecular weight of PD40 and PD30 was 90,260 D and 15,220 D respectively (see Chapter 4; Table 4-1). It was expected that the number average molecular weight of PD20 was between that of PD30 and PD40. Nuclear localisation of PD20 was apparent in a subpopulation of CHO cells cultured *in-vitro* (Fig. 5-2;C). The lack of nuclear localisation in some cells could be attributed to PD20 being of a higher molecular weight than PD30. Molecules less than 17,000 D diffuse into the nucleus whereas molecules greater than 17,000 D but less than 60,000 D require active transport processes in order for them to be transported into the nucleus. In the initial LSCM studies there was some evidence that PD20 had been taken up into the nuclear compartment of some cells after 30 minutes (see Fig. 5-2). This could be due to PD20 being of a high molecular weight but with a high polydispersity index. As such molecular weights of less than 17,000 D were taken up into the nucleus following endosomal release into the cytoplasm, whereas molecules greater than 17,000 D might have been retained within the endosome. Using the modified version of PD20 (PD30) it was demonstrated that nuclear localisation took place in CHO and HepG2 cells

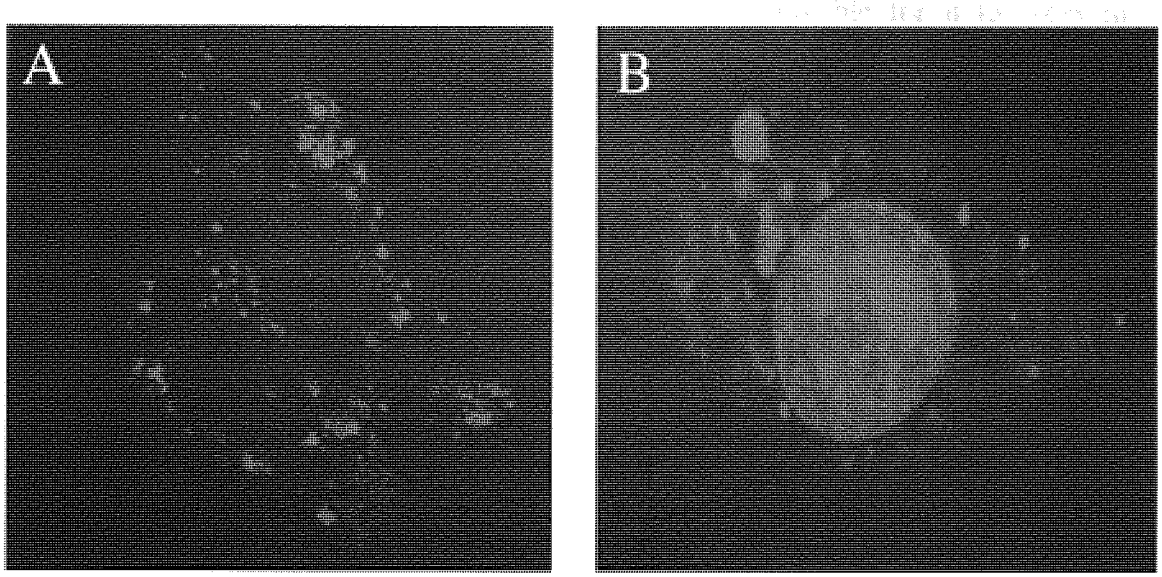


Fig. 5-9 LSCM images showing the internalisation and nuclear localisation of PD30 (1 mg/ml) by HepG2 cells (160,000 cells/ml) cultured *in-vitro* (image B) 30 minutes post the initial incubation period (10 minutes at 37°C) at physiological pH (pH 7.4). HepG2 cells cultured in Wilco dishes were incubated with samples of PD30 (2 ml;1 mg/ml) and free dye (Cy3 bisamine fluorophore) for a period of 10 minutes at 37°C (see Chapter 2; Section 2.3.14). Subseqently, PD and free dye samples were aspirated from the Wilco dishes, CHOs were washed (x3) with serum free medium (2 ml) and re-suspended in fresh serum free medium (2 ml). Image A represents the uptake of the free Cy3 bisamine fluorophore (endosomal localisation) by a single HepG2 cell. Image B shows a single HepG2 cell and reveals internalisation of PD30. Endosomal regions appear to be stained with PD30 in addition to lysosomal and cytosolic regions. The nucleus appears to be more brightly stained with PD30 than other organelles (image B) . Some areas within the nucleus appear to be more brightly stained than others indicating that PD30 is excluded from some regions in the nucleus. No nuclear co-staining experiments were conducted to determine nuclear uptake of PD30. Scale bars (2 cm) represent 20 μm (A) and 5 μm (B) widths.

cultured *in-vitro*. PD30 was found to have a number average molecular weight of 15,220 D (see Chapter 4; Table 4-1), whereby it was possible for it to cross the membrane of the nucleus owing to diffusion. As such, a polymeric-drug carrier capable of being trafficked to the nucleus due to the effective permeability of its membrane could be designed.

### 5.2.6 Time-dependent internalisation of PD30 by CHO cells cultured *in-vitro*

Previous experiments have indicated that nuclear trafficking of PD30 was possible in both CHO and HepG2 cells cultured *in-vitro* (see Section 5.2.5). Subsequently, LSCM experiments were designed to determine the short-term time dependent internalisation of PD30 (1 mg/ml) by CHO cells cultured *in-vitro* following a standard incubation period (10 minutes at 37°C) at pH 7.4. The method employed in these experiments was described previously (see Chapter 2; Section 2.3.15). The LSCM images obtained to visualise the time-dependent internalisation of PD30 (1 mg/ml) by CHO cells cultured *in-vitro* (160,000/ml) at various time points (10 to 60 minutes) following an initial incubation period of 10 minutes at 37°C at pH 7.4 are depicted in Fig. 5-10 (Images A-F). These images revealed that PD20 progressed quite rapidly from the extracellular membrane of CHO cells (Image A:10 mins) trafficking towards internal cellular organelles such as the endosome within 20 minutes (Image B). Surprisingly some cells displayed nuclear staining 20 minutes post the initial incubation period (10 minutes) and images obtained thereafter (A, B, C, D and E) indicated that PD30 tended to remain in endosomes and the nucleus of some cells.

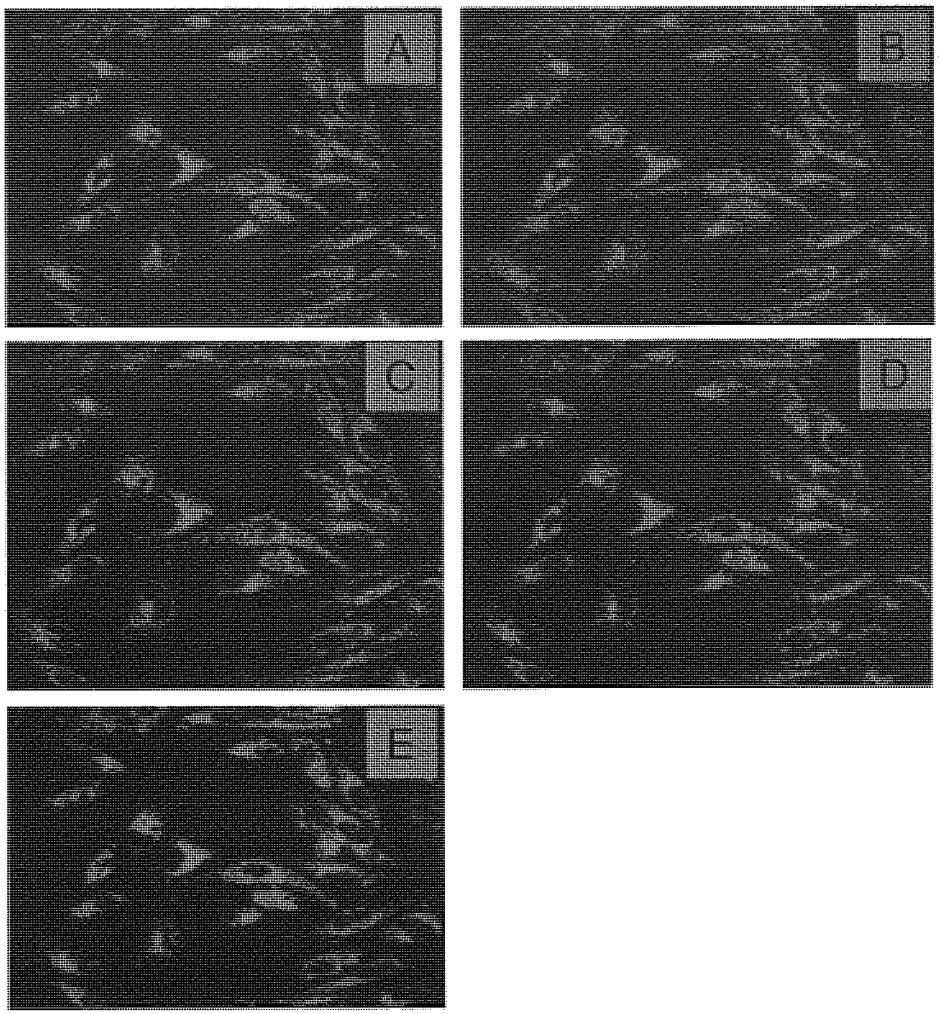


100 $\mu$m

Fig. 5-10 The time-dependent internalisation and trafficking of PD30 (1 mg/ml) by CHO cells cultured *in-vitro* at pH 7.4. LSCM images (A-E) show the internalisation of PD30 at various time points (20, 30, 40, 50, and 60 minutes; A-E respectively) by CHO cells cultured *in-vitro* following an initial incubation period (37°C) of 10 minutes at physiological pH (pH 7.4). PD30 supernatant (2 ml) was removed following a 10 minute incubation period at 37°C, CHOs were washed (x3) with the appropriate serum free medium (pH 7.4) and re-suspended in fresh serum free medium (pH 7.4). LSCM images (A-E) depict internalisation of PD30 by CHO cells cultured *in-vitro* and demonstrate that PD30 traversed the extracellular membrane quite rapidly towards endosomal regions. Nuclear localisation is evident in a subpopulation of CHO cells. However, this was not confirmed through the use of colocalisation studies. Scale bar (2 cm) represents 100 $\mu$m width.

Since nuclear trafficking of PD30 was possible in CHO cells cultured *in-vitro* following a short incubation period (10 minutes at 37°C, pH 7.4) it was thought that cells cultured *in-vitro* over a more extensive incubation period (24h at 37°C, pH 7.4; see Chapter 2; Section 2.3.15). LSCM images depicting the internalisation of PD30 (1 mg/ml) by CHO cells cultured *in-vitro* at pH 7.4 following a 24 hour incubation period at 37°C are shown in Fig. 5-11. Various images were obtained to determine the subcellular fate of PD30 (Fig. 5-11; A-C respectively). The images show that PD30 traversed the extracellular membrane of CHO cells cultured *in-vitro*, which could be attributed to fluid phase endocytosis. PD30 became internalised into endosomal and cytosolic regions. LSCM images represent the cytosolic and nuclear uptake of PD30 by a subpopulation of CHO cells.

### 5.2.7 Uptake of PD20 and LSCM of a cellular aggregate of an EBV-transformed B cell line

A small study was completed to determine if uptake of PD20 (1 mg/ml) by a cellular aggregate (5 mm) of an EBV-transformed B cell line was possible. The uptake of PD20 by a cellular aggregate of the EBV- transformed cell line is depicted in Fig. 5-12. The aggregates were formed in the rotary cell culture system (RCCS; Synthecon, Inc.) The principles of the RCCS was outlined previously (see Chapter 3; section 3.2.3).

A cell suspension of EBV-transformed B cells was inoculated into the RCCS and following 21 days of cultivation, the aggregates formed were incubated with 1mg/ml of PD20 for a period of 24 h. Subsequently, the aggregate was removed from the vessel, fixed in formalin (4%) at 4°C for 2 days and transferred to a vial containing PBS and stored thereafter at 4°C (see Chapter 2; Section 2.3.16.2). The aggregate was imaged using LSCM to determine if diffusion of PD20 was possible. The image shown

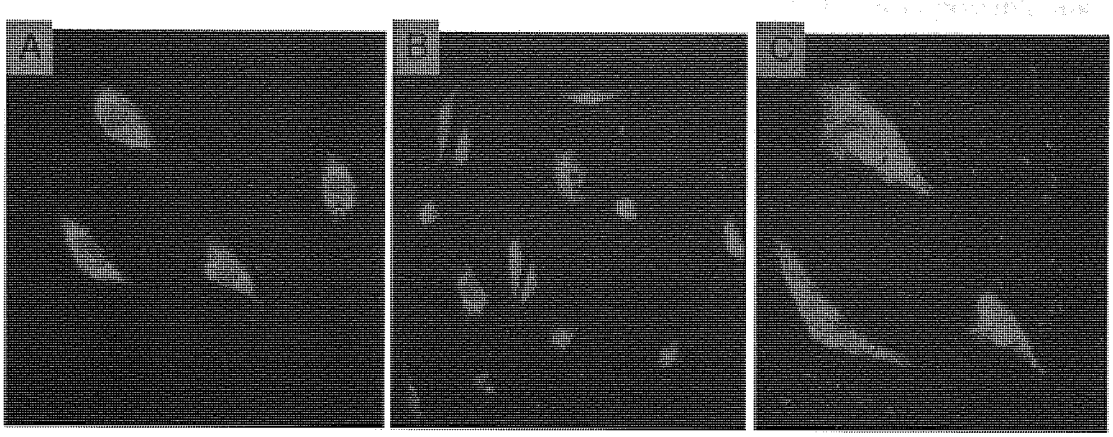


100 $\mu$m

Fig. 5-11 LSCM images depicting cytosolic and nuclear localisation of PD30 in a subpopulation of CHO cells cultured in-vitro following an incubation period of 24 hours at 37°C at pH 7.4. CHOs (160,000 cells/ml) were incubated with PD30 (2 ml;1 mg/ml) at pH 7.4 for a period of 24 h at 37°C. The following day PD30 was removed from the Wilco dish, CHOs were washed (x3) with D-PBS (pH 7.4) and re-suspended in fresh serum free medium (see Chapter 2; Section 2.3.15). No co-localisation studies were conducted to demonstrate nuclear uptake of PD30. Scale bar represents 100 $\mu$m width.

in Fig. 5-12 demonstrates that a cellular aggregate of the EBV-transformed cell line was produced through cultivation in the RCCS and that uptake of PD20 was possible and demonstrates an image highlighting the 3-dimensional structure of the aggregate. These results suggest that PD20 can diffuse into a cellular aggregate of the EBV-transformed cell line.

## 5.3 General Conclusions

Fluorescence microscopy was used as a tool to study the association of PD20 with the extracellular membrane of CHO cells cultured *in-vitro* at physiological pH of 7.4 and at the lower pH value of 5.5. There appeared to be greater association of PD20 with the extracellular membrane of CHO cells cultured *in-vitro* at the lower pH value (pH 5.0) owing to the hydrophobic nature of the polymer, poly (L-lysine *iso*-phthalamide) at this pH (pH 5.0).

The internalisation and subcellular fate of PD20 in CHO cells cultured *in-vitro* at physiological pH (pH 7.4) was monitored by LSCM. It was found that PD20 became internalised by CHO cells cultured *in-vitro* quite rapidly at pH 7.4. Internalisation of PD20 took place in CHO cells cultured *in-vitro* at pH 7.4 following a ten minute incubation period. Internalisation of PD20 at this pH (7.4) was attributed to an endocytotic mechanism whereby exposure of the hydrophobic groups on the polymer, poly (L-lysine *iso*-phthalamide) led to uptake by CHO cells. Following internalisation, PD20 was trafficked to acidic regions in the cell, the endosome (pH 5.0 - 6.0) and to some extent the cytoplasm and thereafter to the nucleus of some cells. Thus, there was some variability with respect to cells in the same sample-with a subpopulation of cells exhibiting quick cytoplasmic entry whereas in another subpopulation of cells PD20 tended to remain in the endosomes. Once PD20 entered the cytoplasm it accumulated in

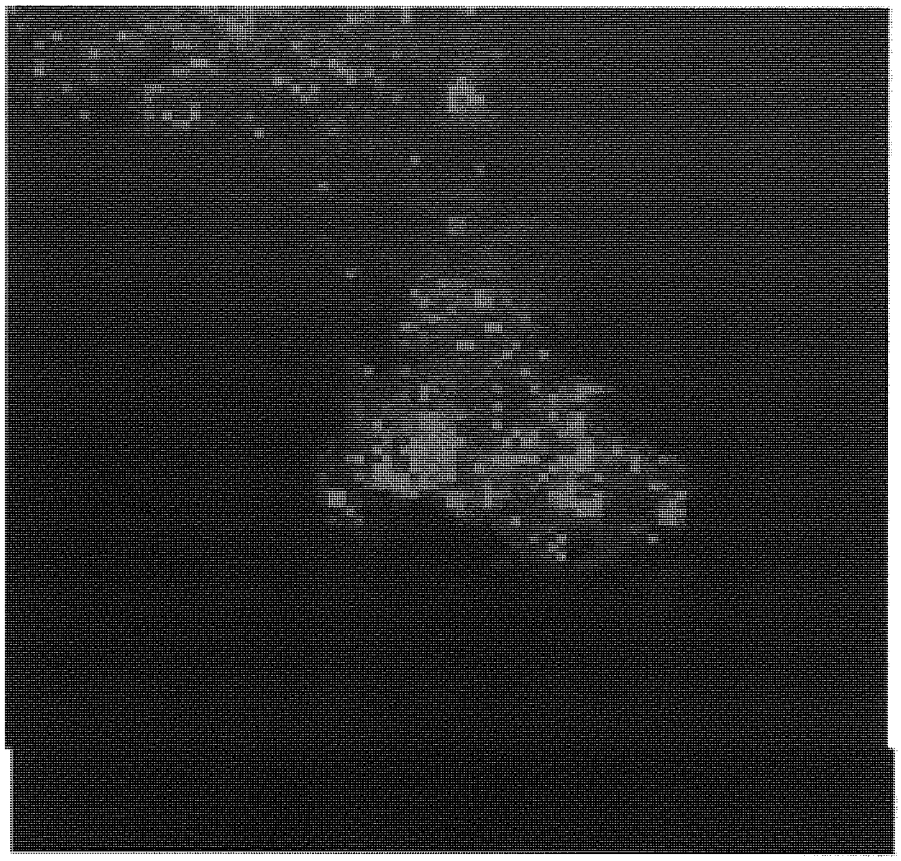

Fig. 5-12 The cellular uptake of PD20 by an aggregate of the EBV transformed cell line (see Chapter 2; Section 2.3.16.2). A cellular aggregate was formed in the RCCS (Synthecon, Inc.). Following 21 days of cellular growth an aggregate (5 mm) was produced and incubated with 1mg/ml of PD20 for a period of 24 h. Subsequently, the aggregate (5 mm) was removed from the vessel, fixed in formalin (4%) at 4°C for 2 days. The aggregate (5 mm) was then transferred to a vial containing fresh PBS solution and LSCM images were obtained using LSCM (Olympus FV300).

the nucleus of some cells. Studies which relate the physiological state of particular cells with the endosomal escape of PD20 may help in the mechanism of this phenomena.

LSCM images revealed the fate of PD20 when the pH of the surrounding medium of CHO cells cultured *in-vitro* was reduced to pH 5.0. Extensive adsorption of PD20 to the extracellular membrane of live CHO cells was found at pH 5.0. This phenomena can be explained in terms of the conformation of the polymer, poly (L-lysine *iso*-phthalamide) at low pH. At this pH, typically pH 5.0 the polymer is less negatively charged owing to the increased association of carboxyl groups along the polymer backbone leading to an increase in its hydrophobicity. The increase in hydrophobicity at low pH (5.0) increases the adsorption of PD20 to the extracellular membrane.

GFC chromatograms demonstrated that PD40 and PD30 had number average molecular weights of 89,360 D and 15,220 D respectively (see Chapter 4; Section 4.1:Table 4-1). Large macromolecules can easily traverse the extracellular membrane however this limits their transport to the nuclear region. PD30 was synthesised to be of a lower number average molecular weight (15,220 D) than that of PD40 (89,360 D) and its internalisation and subcellular fate was determined in both CHO and HepG2 cells cultured *in-vitro*. Nuclear localisation of PD30 was achieved in a subpopulation of both CHO and HepG2 cells cultured *in-vitro*. LSCM images depicting the time dependent internalisation of PD30 with CHO cells cultured *in-vitro* following an initial incubation period of 10 minutes at 37°C provided conclusive evidence that nuclear localisation of a lower molecular weight polydye (PD30) was possible. In addition, incubation of PD30 with CHO cells cultured *in-vitro* over a more extensive incubation period (24 hours at 37°C) provided evidence that both cytosolic and nuclear localisation of PD30 was feasible in a subpopulation of CHO cells cultured *in*-vitro. These results indicate that by

tailoring a macromolecule to be of a lower molecular weight, nuclear accumulation is possible which could lead to the synthesis of possible polymer-drug conjugates.

# CHAPTER 6

# CONCLUSIONS AND FURTHER WORK

## 6.1 Final Conclusions

The work presented in this thesis was concerned with investigating the pH-mediated cell membrane disruption characteristics of pH responsive pseudopeptides towards cell membranes and their subcellular fate following internalisation. It was motivated by observations from the literature that the pH responsive psudopeptides studied here may display similar membrane disruption characteristics to that of the hemagglutinin virus (HA). It was also thought possible that the pseudopeptides may be capable of changing conformation in the acidic environment of endosomes (pH 5.0-6.0) and that this may lead to fusion within the endosomal membrane due to the hydrophobicity of the polymer at low pH (pH 5.0). Furthermore, it was thought that fusion with the endosomal membrane would lead to a breach of the endosomal membrane and that the polymer of interest would be released into the cytosol resulting in nuclear trafficking thereafter.

The initial studies in this thesis were completed to determine the cell membrane disruptive properties of the pseudopeptides. *In-vitro* experiments were designed to investigate whether synthetic pseudopeptides behaved in a similar manner to the previously described hemagglutinin virus (HA). Initial experiments were completed using the MTT assay to investigate the toxicity of poly (L-lysine *iso*-phthalamide) and the copolymer, poly (L-lysine ethyl ester co L-lysine *iso*-phthalamide) towards a C26 (colorectal adenocarcinoma) cell line at physiological pH (7.4). The initial tests demonstrated that both polymers were well tolerated by C26 cells at physiological pH (7.4) at concentrations between 2-125 $\mu$g/ml. At concentrations above 125 $\mu$g/ml, both

polymers caused a decrease in cellular viability relative to control values. C26 cell viability was found to decrease by 24% in the presence of poly (L-lysine *iso*-phthalamide) and fell a further 65% in the presence of 500 μg/ml of the same polymer. Dosing with poly (L-lysine ethyl ester co-L-lysine *iso*-phthalamide) at concentration values between 250-500 μg/ml led to a decrease in C26 cellular viability relative to control values of 10.2% and 32% respectively. Thus, it was determined that poly (L-lysine *iso*-phthalamide) displayed greater cytotoxic effects than the copolymer poly (L-lysine ethyl ester co-L-Lysine *iso*-phthalamide).

Data presented here suggests that hypercoiling pseudopeptides can integrate with cell membranes and exhibit pH mediated cell membrane disruption, the extent of which can be varied by careful choice of polymer structure. Thus whilst poly (L-lysine dodecanamide), is mildly toxic at physiological pH (7.4), poly (L-lysine *iso*-phthalamide), and poly (L-lysine ethyl ester co L-lysine *iso*-phthalamide), show very little toxicity. At pH 5.5 a significant increase in toxicity for all polymers is seen and poly (L-lysine *iso*-phthalamide) appears to be approximately twice as toxic as poly (L-lysine ethyl ester co L-lysine *iso*-phthalamide) at the lower pH.

The development of synthetic, biocompatible polymers which are capable of pH dependent precipatative targeting towards tumour cells or acidic regions within tumours would offer the potential of diagnostic imaging tools of drug delivery devices. The most significant results pertaining to the study of these pH responsive polymers, poly (L-lysine dodecanamide), poly (L-Lysine ethyl ester co L-lysine *iso*-phthalamide), and poly (L-lysine *iso*-phthalamide), include data which displays their pH dependent interaction with cellular membranes, their ability to rupture membranes at low pH values, that is, similar to that of endosomes (pH 5.0 - 6.0), and to lyse cells upon hypercoiling. It was therefore envisaged that a more suitable approach was to use these polymers as potential

synthetic chaperones for the endosomal internalisation of conjugated molecules, since the polymers appear to behave in a similar manner to that of viral hemagglutinins and bear structural similarities with respect to the molecular arrangement of pendant carboxylic acid and hydrophobic moieties.

The cell toxicity studies provided conclusive evidence that cell membrane disruption by pseudopeptides was possible at pH 5.5. Subsequently, a Cy3 bisamine fluorophore derivative was conjugated into the backbone of the polymer, poly (L-lysine *iso*-phthalamide) at a dye:lysine ratio of 1:20, 1:40, 1:60 and 1:80. It was thought that fluorophore labelling of the polymer could be used to visualise the internalisation and subcellular fate of polydye through LSCM (see Chapter 5).

In Chapter 4 various techniques were employed to determine if the Cy3 fluorophore moieties were conjugated into the backbone of the polymer, poly (L-lysine *iso*-phthalamide). Gel filtration chromatography (GFC) of the PD20 molecule did not provide conclusive evidence that the Cy3 bisamine fluorophore was conjugated into the backbone of the polymer, poly (L-lysine *iso*-phthalamide; see Section 4.2.1). Subsequently, both native PAGE and HVPE experiments were completed to prove that the Cy3 bisamine moiteities were conjugated into the backbone of the polymer. Native PAGE analysis of the PD's (PD20, PD40, PD60 and PD80; see Sections 4.2.2 and 4.2.3) provided confirmatory proof that the Cy3 bisamine fluorophore was conjugated into the backbone of the polymer, poly (L-lysine *iso*-phthalamide). HVPE was also used to demonstrate the change in polymer conformation when the pH of the surrounding buffer was altered from pH 7.4 to pH 5.0. Results demonstrated that as the pH of the environment of the polydyes was reduced (pH 5.0) less electrophoretic mobilities of the polydyes was observed. This was attributed to a reduction in the net negative charge of the polymer at low pH (pH 5.0).

In Chapter 4 UV-Vis absorption, fluorescence, and confocal microscopy techniques, were used to establish that the polymer, poly (L-lysine *iso*-phthalamide) displayed a conformational change with respect to variations in pH. When in its negatively charged extended conformational state (pH 7.4), the polymer is rigidised in structure which reduces the fluorophore mobility and non-radiative energy loss. Association of the hydrophobic groups in charge reduction led to an enhancement in the fluorescence of PD20. Furthermore, PD20 was shown to bind to other proteins and an increased enhancement in fluorescence was observed for all polydyes (PD's 20, 40, 60 and 80) in the presence of serum.

In Chapter 5 experiments were designed to investigate the subcellular fate of PD20 following internalization by CHO cells cultured *in-vitro*. To determine the subcellular fate of PD20, LSCM of CHO cells was employed. Following short incubation times (15 minutes at 37°C) at pH 7.4, PD20 was found to enter cells and remain in small vesicles distributed throughout the cytoplasm which was representative of an endocytic process. The entry of PD20 into the cytoplasm was followed by accumulation into the nucleus of a subpopulation of CHO cells cultured *in-vitro* within the same Wilco dish. This was attributed to PD20 being of a high molecular weight but containing a range of lower molecular fractions that could breach the endosomal compartment following fusion at low pH (pH 5.0). Lower molecular weight fractions of PD20 could thereafter escape into the cytosol and traffic to the nucleus of some live CHO cells. However, it could be quenching effects in addition to different stages of the cell cycle which affected the distribution of the polymer following internalization of PD20 by CHO cells cultured *in-vitro*.

Following initial observations that PD20 became internalized by CHO cells cultured *in-vitro*, a smaller study was conducted to determine if a lower molecular

polydye (PD30) was capable of greater nuclear accumulation. This study was completed using CHO and HepG2 cells. Nuclear accumulation of PD30 was determined in a subpopulation of HepG2 cells and was more evident in cells which were undergoing mitotic division.

Finally, in Chapter 5 a study was completed to determine if diffusion of PD20 was possible in a cellular aggregate of the EBV-transformed cell line. Growth (21 days) of this aggregate was formed in the RCCS and was cultivated to be 5 mm in diameter. The RCCS was employed as it mimics the parent tissue. Diffusion of PD20 in a cellular aggregate of an EBV-transformed cell line was achieved following a 24 h incubation period at 37°C.

## 6.2 Future Work

It has been hypothesised that pH responsive pseudopeptides could be used as polymeric carriers of cytotoxic drugs to target regions such as that of the cytosol and nucleus. The Cy3 bisamine fluorophore conjugated poly (L-lysine *iso*-phthalamide) investigated in this study constitutes a surrogate hydrophobic moiety. Through peptidic structure we anticipate that the polymers of structure examined here will be biodegradable *in-vivo* and metabolised within cells. In so far as we have visibly observed the internalisation of polymer together with its conjugated fluorophore then there is strong reason to believe that such polymers could be used to transport cytotoxic drugs to the cytoplasm or nucleus of cells. It is thought that conjugation of the unlabelled polymer, poly (L-lysine *iso*-phthalamide) to a well known anti-cancer agent, doxorubicin (DOX) would yield a suitable polymer-drug conjugate for the selective killing of tumour cells.

More work is required to understand the variability of the polymer to escape into the cytoplasm and nucleus. Future experiments should analyse the cell cycle to determine if it has any effect on the distribution of the polymer. Microinjection experiments could be employed by microinjecting PD20 and PD30 into the cytoplasm of cells to ensure that the polymer accumulates in the nucleus. To better understand the results found in this study and to determine their universality, the subcellular fate of PD20 and PD30 in other cell lines should be investigated.

Polymers could be designed to target specific cell types. For example polymers could be labelled with galactosamine or folic acid derivatives to make them recognised by specific cell lines, hepatocytes and ovarian carcinoma cell lines respectively. This would ensure that the polymers would be internalised by a receptor-mediated endocytosis mechanism.

Future work could encompass the design and synthesis of pH specific, biodegradable, fluorescent probes for tumour imaging and would exploit the ability of certain hydrophobically modified polyelectrolytes to change conformation at specific pH values. We have established the synthesis of such materials including polymers containing Cy3 bisamine fluorophores and have determined their conformational, and pH dependent fluorescence. Tuning of hydrophobicity allows precise control of conformation within a particular pH environment. When charged, the rigid, rod-like conformation of the polymer diminishes fluorophore mobility and non-radiative energy loss enhancing fluorescence output. A ≈15x enhancement of conjugated Cy3 bisamine fluorophore has been observed as opposed to free Cy3 bisamine fluorophore (Data not shown). Association of the hydrophobic groups on charge reduction decreases fluorophore separation and quenching that leads to a reduced signal in single Cy3

bisamine containing polymers. This facilitates determination of polymer conformation allowing rapid screening of candidate polymers.

Tumour vasculature often displays enhanced permeability to macromolecules promoting access to the interstitium where retention, due to ineffective lymph drainage, can result in tumour to blood ratios of macromolecule of up to a 1000. Mahmood *et-al* (1999) demonstrated the feasibility of targeting macromolecular fluorophore supports to, and subsequent extra-corporeal infra-red imaging of tumour. Cy 5.5 was conjugated to PEGylated polylysine resulting in self-quenching. Following passive accumulation within a mouse xenograft the conjugate was internalised into intra-cellular lysosomal compartments where enzymatic degradation of the peptidic backbone liberated unquenched free Cy moieties, detectable by a CCD camera imaging system. This approach is limited by the fluorescence output and background detection sensitivity of conventional fluorophores. In fluorescence resonant energy transfer (FRET) energy absorbed by one fluorophore is transferred to a second fluorophore whose excitation spectrum overlaps the emission spectrum of the first probe. Light is then re-emitted from the second fluorophore at a longer wavelength. The process only takes place over short distances and so by including FRET pairs of dyes within a responsive polymer the FRET process can be switched on and off. It is expected that the enhancement of fluorescence displayed by the single fluorophore polymers will apply to multiple fluor-containing polymers. The hetero-polymeric probes proposed would permit *in-situ* activation to reduce background levels and increase sensitivity, potentially allowing deeper imaging of smaller nodes.

Amphipathic polymers synthesized using established methods would be modified by the incorporation of FRET Cy-dye moieties along the polymer backbone. The distance between the dye pairs will be adjusted so that FRET is minimized in the

extended conformation, leading to low fluorescence output. When hypercoiled, at the (often) low pH within the tumour interstitium, or following internalisation, within the endosomal compartment the FRET pairs would be brought into close proximity leading to a fluorescence signal in a process analogous to the reduction in fluorescence output on hypercoiling observed with the homo-fluor polymers. Excitation and detection of NIR signal will be achieved using LSCM.

The synthetic challenges include synthesis of a suitable polymeric precursor with the required pH response and inclusion of the FRET dye pairs within the polymer at suitable degrees of loading. Demonstration of the FRET effect upon hypercoiling of the initial polymers would be used to feed back information in an iterative approach to selection of candidate fluorescent polymers for *in-vitro*-testing. In a final synthetic stage the effect of partial PEGylation of the fluorescent polymer (to avoid serum protein binding *in-vivo*) on the responsive nature of the probes will be investigated prior to *in-vitro* testing. Loss or reduction in pH response on PEGylation of the probe polymers might be circumvented by use of pH or enzymatically sensitive linking groups that would be cleaved upon internalisation of the modified probe.

Demonstration of effect and determination of detection limits would be conducted by imaging studies on polymer injected into biological tissues (e.g. meat samples of various thickness) to simulate non-invasive *in-vivo* imaging. Also, tumour spheroids will be grown *in-vitro* using a rotating cell culture sysyem (RCCS) established in our laboratory. The technique allows large spheroids (diameters > 5 mm) to be grown, exposed to polymer samples and removed for histological examination or imaging. Direct administration of the polymer into the tumour spheroid and observation by LSCM could be investigated. The use of FRET fluorophores would allow independent monitoring of localization (monitored at the lower emission wavelength)

and subsequent activation of the probe (monitored at the higher emission wavelength, that is, only once FRET occurs on hypercoiling). The effect of molecular weight and PEGylation of the fluorescent polymers on plasma half-life and tumour imaging would need to be assessed by *in-vivo* experiments.

It is expected that the synthesis, characterisation and *in-vitro* studies of the fluorescent polymers will lead to two publications.

# REFERENCES


Abe K and Matsuki N (2000) Technical note: Measurement of cellular 3-(4,5-dimethylthiazol-2-yl)-2,5-diphenyltetrazolium bromide (MTT) reduction activity and lactate dehydrogenase release using MTT, *Neuroscience Research,* **38,** 325-329

Alberts R, Bray D, Lewis J, Raff M, Roberts K and Watson J.D (1994) Molecular biology of the cell, 3rd Edition, Garland Publishing, New York

Altan N, Chen Y, Schindler M and Simon S.M (1999) Tamoxifen inhibits acidification in cells independent of the estrogen receptor, *Proceedings of the National Academy of Sciences, USA,* **96**, 4432-4437

Amersham Biosciences, Gel filtration: principles and methods, 8th Edition, Catalogue Number 18-1022-18, Uppsala, Sweden

Aspedon A and Groisman E.A (1996) The antibacterial action of protamine: Evidence for disruption of cytoplasmic membrane energization in *Salmonella typhimurium, Microbiology-UK*, **142**(12), 3389-3397

Benachir T and Lafleur M (1995) Study of vesicle leakage induced by melittin, *Biochimica et Biophysica Acta (BBA) – Biomembranes,* **1235** (2), 452-460

Besterman J.M, Airhart J.A, Woodworth R.C and Low R.B (1981) Exocytosis of pinocytosed fluid in cultured cells: kinetic evidence for rapid turnover and compartmentation, *Journal of Cell Biology,* **91,** 716-727

Blakey D.C (1992) Drug targeting with monoclonal antibodies: A review, *Acta Oncology*, **31**, 91-97

Borden K.A, Eum K.M, Langley K.H and Tirrell D.A (1987) Interactions of synthetic polymers with cell membranes and model membrance systems: On the mechanism of polyelectrolyte-induced structural reorganisation in thin molecular films, *Macromolecules*, **20**(2), 454-456

Brocchini S, James K, Tangpasuthadol V and Kohn J (1997) A combinatorial approach for polymer design, *Journal of the American Chemical Soc*iety, **119**(19), 4553-4554

Brocchini S and Duncan R (1999) Polymer drug conjugates: drug release from pendent linkers. In Encyclopedia of Controlled Release, E. Mathiowitz (Ed) Wiley, New York, 786-816

Bullough P.A, Hughson F.M, Skehel J.J and Wiley D.C (1994) Structure of influenza haemagglutinin at the pH of membrane fusion, *Nature,* **371**(6492), 37-43

Carrasco L (1994) Entry of animal viruses and macromolecules into cells, *FEBS Letters*, **350**(2-3), 151-154

Christie R.J and Grainger D.W (2002) Design strategies to improve macromolecular delivery constructs, *Advanced Drug Delivery Reviews,* **1**, 1-17

Coley H.M, Lewandowicz G, Sargent J.M and Verill M.W (1997) Chemosensitivity testing of fresh and continuous tumour cell cultures using lactate dehydrogenase, *Anticancer Research,* **17**, 231-236

Dacosta M.H.B and Chaimovich H (1997) Structure-activity relationships in the fusion of small unilamellar phosphotidylcholine vesicles induced by a model peptide, *Biochimie*, **79**(8), 509-516

Dautry-Varsat A (1986) Receptor-mediated endocytosis: The intracellular journey of transferrin and its receptor, *Biochimie,* **68**, 375-381, Patent number 9901.

Decker T and Lohmann-Matthes M.L (1988) A quick and simple method for the quantitation of lactacte dehydrogenase release in measurements of cellular cytotoxicity and tumour necrosis factor (TNF) activity, *Journal of Immunological Methods,* **115**(11), 61-69

Duguid J.G, Li C, Shi M, Logan M.J, Alila H, Rolland A, Tomlinson E, Sparrow J.T and Smith L.C (1998) A Physiochemical approach for predicting the effectiveness of peptide-based gene delivery systems for use in plasmid-based gene therapy, *Biophysical Journal*, **74**(6), 2802-2814

Duncan R (1992) Drug polymer conjugates – potential for improved chemotherapy, *Anti-Cancer Drugs*, **3**(3), 175-210

Duncan R (1999) Polymer conjugates for tumour targeting and intracytoplasmic delivery, The EPR effect as a common gateway? *Pharmaceutical Science and Technology Today*, **2**, 441-449

Duncan R (2000) Polymer therapeutics into the 21st century: In Drug Delivery in the 21st Century, K. Park and R. Mrsny (Eds), ACS Books 350-363

Duncan R, Kopecek J, Rejmanova P and Lloyd J.B (1983) Targeting of *N*-(2-hydroxypropyl)methacrylamide copolymers to liver by incorporation of galactose residues, *Biochimica et Biophysica Acta*, **75**(3), 518-521

Duncan R, Ferruti P, Sgouras D, Tuboku-Metzger A, Ranucci E and Bignotti F (1994) A polymer-triton X-100 conjugate capable of pH-dependent red blood cell lysis: a model system illustrating the possiblity of drug delivery within acidic intracellular compartments, *Journal of Drug Targeting*, **2**(4), 341-347

Duncan R, Dimitrijevic S and Evagorou E.G (1996) The role of polymer conjugates in the diagnosis and treatment of cancer, *STP Pharma Sciences*, **6**(4), 237-263

Eccleston M.E, Slater N.K.H and Tighe B.J (1999) Synthetic routes to responsive polymers; co-polycondensation of tri-functional amino acids with diacylchlorides, *Reactive and Functional Polymers*, **42**(2), 147-161

Eccleston M.E, Kuiper M, Gilchrist F.M and Slater N.K.H (2000) pH-responsive pseudo-peptides for cell membrane disruption, *Journal of Controlled Release,* **69**(2), 297-307

Ehrlich P (1906) Studies in Immunity, Plenum Press, New York

El Ouahabi A, Thriy M, Pector V, Fuks R, Ruysschaert J.M and Vandenbraden M (1997) The role of endosome destabilising activity in the gene transfer process mediated by cationic lipids, *FEBS Letters*, **414**, 187-192

Esposito B.P and Najjar R (2002) Interactions of antitumoural platinum-group metallodrugs with albumin, *Coordination Chemistry Reviews,* **232**, 137-149

Eum K.M, Langley K.H and Tirrell D.A (1989) Quasi-elastic and electrophoretic light scattering studies of the reorganisation of dioleoylphosphatidylcholine vesicle membranes by poly(2-ethylacrylic acid), *Macromolecules*, **22**(6), 2755-2760

Falnes P.Ø and Sandvig K (2000) Penetration of protein toxins into cells, *Current Opinion in Cell Biology,* **12**, 407-413

Ferruti P, Richardson S and Duncan R (1998) Poly(amidoamine)s as tailor-made soluble polymer carriers: In Targeting of Drugs; Stealth Therapeutic Systems G. Gregoriadis and B. McCormack (Eds.), Plenum Press, New York, 207-224

Ferruti P, Manzoni S, Richardson S.C.W, Duncan R, Pattrick N.G, Mendichi R and Casolaroû M (2000) Amphoteric linear poly(amido-amine)s as endosomolytic polymers: Correlation between physico-chemical and biological properties, *Macromolecules*, **33**(2), 7793-7800

Folkman J and Shing Y (1992) Angiogenesis, *Journal of Biological Chemistry*, **267**(16), 10931-10934

Foster S and Lloyd J.B (1988) Solute transport across the mammalian lysosome membrane, *Biochimica Biophysica Acta*, **947**, 465-491

Gianasi E, Wasil M, Evagorou E.G, Keddle A, Wilson G and Duncan R (1999) HPMA copolymer platinates as novel antitumour agents: *In-vitro* properties, pharmacokinetics and antitumour activity *in vivo*, *European Journal of Cancer*, **35**(6), 994-1002

Gottschalk S, Sparrow J.T, Hauer J, Mims M.P, Leland F.E, Woo S.L and Smith L.C (1996) A novel DNA-peptide complex for efficient gene transfer and expression in mammalian cells, *Journal of Gene Therapy*, **7**, 1947-1954

Haensler J and Szoka F.C (1993) Polyamidoamine cascade polymers mediate efficient transfection of cells in culture, *Bioconjugate Chemistry*, **4**(5), 372-379

Hahn K.H and Kim H (1991) Fusion and fragmentation of phospholipid-vesicles by apohaemoglobin at low pH, *Journal of Biochemistry*, **110**(4), 635-640

Hames B.D and Rickwood D (1990) Gel electrophoresis of proteins, 2nd edition, IRC Press, Oxford

Hoes C.J.T, Ankone M, Grootoonk J, Feijen J, Vanderstruick E, Vandoornmalen A, Pham D, DeMan A, VanEttekoven A, Schlachter I, Boon P.J, Kaspersen F and Bos E.S (1996) Synthesis and biological evaluation of immunoconjugates of adriamycin and a human IgM linked by poly[N-5-(2-hydroxyethyl)-L-glutamine], *Journal of Controlled Release*, **38**(2-3), 245-266

Jain R.K (1989) Delivery of novel therapeutic agents in tumours – physiological barriers and strategies, *Journal of the National Cancer Institute,* **81**, 570-576

Jensen K.D, Kopeckova P, Bridge J.H.B and Kopecek J (2001) The cytoplasmic escape and nuclear accumulation of endocytosed and microinjected HPMA copolymers and a basic kinetic study in HepG2 cells, *AAPS PharmSci*, **3**(4), 1-14

Jin M, Park J, Lee S, Park B, Shin J, Song K.J, Ahn T-I, Hwang S.Y, Ahn B-Y and Ahn K (2002) Hantaan virus enters cells by clathrin-dependent receptor-mediated endocytosis, *Journal of Virology,* **294**, 60-69

Kirchhausen T (2000) Clathrin, *Annual Review of Biochemistry*, **69**, 699-727

Kodera Y, Matsushima A, Hiroto M, Nishimura H, Ishii A, Ueno T and Inada Y (1998) Pegylation of proteins and bioactive substances for medical and technical applications, *Progress in Polymer Science*, **23**, 1233-1271

Kopecek J, Kopeckova P, Minko T and Lu Z (2000) HPMA copolymer-anticancer drug candidates: Design, activity, and mechanism of action, *European Journal of Pharmacy Biopharmacy,* **50**, 61-81

Korzeniewski C and Callewaert D.M (1983) An enzyme release assay for natural cytotoxicity, *Journal of Immunological Methods,* **64**, 313-320

Krieglstein J, Meiler W and Staab J (1972) Hydrophobic and ionic interactions of phenothiazine derivatives with bovine serum albumin, *Biochemical Pharmacology*, **21**(7), 985-994

Kost J and Langer R (1992) Responsive polymer systems for controlled delivery of therapeutics, *Trends in Biotechnology*, **10**(4), 127-131

Kost J and Langer R (2001) Responsive polymeric delivery systems, *Advanced Drug Delivery Reviews*, **46**(1-3), 125-148

Lackey C.A, Murthy N, Press O.W, Tirrell D.A, Hoffman A.S and Stayton P.S (1999) pH-dependent haemolytic activity of smart polymer-protein bioconjugates, *Bioconjugate Chemistry,* **10**, 401-405

Laemmli U.K (1970) Cleavage of structural proteins during assembly of the head of bacteriophage T4, *Nature*, **227**, 680-685

Langer R (1998) Drug delivery and targeting, *Nature*, **392**, 5-10

Lear J.D and DeGrado W.F (1987) Membrane binding and conformational properties of peptides representing the $NH_2$ terminus of influenza HA-2, *The Journal of Biological Chemistry*, **262**, 6500-6505

Luo D and Saltzman W.M (2000) Synthetic DNA delivery systems, *Nature Biotechnology*, **18**(1), 33-37

Maeda H (2001a) SMANCS and polymer-conjugated macromolecular drugs: Advantages in cancer chemotherapy, *Advanced Drug Delivery Reviews*, **46**(1-3), 169-185

Maeda H (2001b) The enhanced permeability and retention (EPR) effect in tumour vasculature: The key role of tumour-selective macromolecular drug targeting, *Advances in Enzyme Regulation*, **41**, 189-207

Maeda H, Takeshita R and Kanamaru A (1979) A lipophilic derivative of neocarzinostatin, *International Journal of Peptide and Protein Research*, **14**, 81-87

Maeda H, Sawa T and Konno T (2001) Mechanism of tumour-targeted delivery of macromolecular drugs, including the EPR effect in solid tumour and clinical overview of the prototype polymeric drug SMANCS, *Journal of Controlled Release*, **74**(1-3), 47-61

Mahato R.I, Monera O.D, Smith L.C and Rolland A (1999) Peptide-based gene delivery, *Current Opinion in Molecular Therapy*, **1**, 226-243

Mahmood U, Tung C.H, Bogdanov A and Weissleder R (1999) Near infrared optical imaging of protease activity for tumour detection, *Radiology*, **213**(3), 886-870

Marsh M (2001) Endocytosis, edited by Mark Marsh, Frontiers in Molecular Biology series, Oxford University Press, Oxford

Marsh M, Griffiths G, Dean G.E, Mellman I and Helenius A (1986) Three-dimensional structure of endosomes in BHK-21 cells, *Proceedings of the National Academy of Science, USA*, **83**, 2899-2903

Matthews S.E, Pouton C.W and Threadgill M.D (1996) Macromolecular systems for chemotherapy and magnetic resonance imaging, *Advanced Drug Delivery Reviews*, **18**(2), 219-267

McSheehy P.M.J, Stubbs M and Griffiths J.R (2000) Role of pH in tumour-trapping of the anticancer drug 5-fluorouracil, *Advances in Enzyme Regulation*, **40**, 63-80

Mellman I (1996) Endocytosis and molecular sorting, *Annual Review of Cell Developmental Biology*, **12**, 575-625

Mellman I and Warren G (2000) The road taken: Past and future foundations of membrane traffic, *Cell*, **100**(1), 99-112

Midoux P, Kichler A, Boutin V, Maurizot J.C and Monsigny M (1998) Membrane permeabilisation and efficient gene transfer by a peptide containing several histidines, *Journal of Bioconjugate Chemistry,* **9**, 260-267

Mitteregger R, Vogt G, Rossmanith E and Falkenhagen D (1999) Rotary cell culture system (RCCS): A new method for cultivating hepatocytes on microcarriers, *The International Journal of Artificial Organs*, **22**(12), 816-822

Moore G.E and Woods L.K (1976) Culture Media for Human Cells- RPMI 1603, RPMI 1634, RPMI 1640 and GEM 1717, *Tissue Culture Manual*, **3**, 503-508

Moran J.H and Schnellmann R.G (1996) A rapid β-NADH-linked fluorescence assay for lactate dehydrogenase in cellular death, *Journal of Pharmacological and Toxicological Methods,* **36**(1), 41-44

Mossman T (1983) Rapid colorimetric assay for cellular growth and survival: Application to proliferation and cytoxicity assays, *Journal of Immunology*, **65**, 55-63

Mukherjee S, Ghosh R.N and Maxfield F.R (1997) Endocytosis, *Physiological Review,* **77**(3), 759-803

Murthy N, Robichaud J, Stayton P.S, Press O.W, Hoffman A.S and Tirrell D.A (1998) Design of polymers to increase the efficiency of endosomal release of drugs, *Proceedings of the International Symposium Controlled Release Bioactive Material*, **25**, 224-225

Murthy N, Robichaud J.R, Tirrell D.A, Stayton P.S and Hoffman A.S (1999) The design and synthesis of polymers for eukaryotic membrane disruption, *Journal of Controlled Release*, **61**(1-2), 137-143

Ogris M, Carlisle R.C, Bettinger T and Seymour L.W (2001) Melittin enables efficient vesicular escape and enhanced nuclear access of non-viral gene delivery vectors, *Journal of Biological Chemistry*, **276**(50), 47550-47555

Ogris M and Wagner E (2002) Targeting tumours with non-viral gene delivery systems, *Drug Discovery Today*, **7**(8), 479-485

Orekhova N.M, Akchurin R.S, Belyaev A.A, Smirnov M.D, Ragimov S.E and Orekhov A.N (1990) Local prevention of thrombosis in animal arteries by means of magnetic targeting of aspirin-loaded red cells, *Thrombosis Research*, **57**(4), 611-616

Ostolaza H, Bakas L and Goñi F.M (1997) Balance of electrostatic and hydrophobic interactions in the lysis of model membranes by *E.coli* alpha-haemolysin, *Journal of Membrane Biology*, **158**(2), 137-145

Parente R.A, Nir S and Szoka F.C (1988) pH-dependent fusion of phosphatidylcholine small vesicles: Induction by a synthetic amphipathic peptide, *Journal of Biological Chemistry*, **263**(10), 4724-4730

Parente R.A, Nadeasdi L, Subabrao N.K and Szoka F.C (1990) Association of a pH-sensitive peptide with membrane vesicles: Role of amino-acid sequence, *Journal of Biochemistry,* **29**, 8713-8719

Pawley J.B (ed) (1995) Handbook of Biological Confocal Microscopy, 2nd Edition, Plenum Press, New York

Peters T (1985) Serum albumin: In advances in protein chemistry, Academic Press

Plank C, Oberhauser B, Mechtler K, Koch C and Wagner E (1994) The influence of endosome-disruptive peptides on gene-transfer using synthetic virus-like gene-transfer systems, *Journal of Biological Chemistry,* **269**(17), 12918-12924

Plank C, Zauner W and Wagner E (1998) Application of membrane-active peptides for drug and gene delivery across cellular membranes, *Advanced Drug Delivery Reviews,* **34**(1), 21-35

Presley J.F, Mayor S, Dunn K.W, Johnson L.S, McGraw T.E and Maxfield F.R (1993) The End2 mutation in CHO cells slows the exit of transferrin receptors from the recycling compartment but bulk membrane recycling is unaffected, *Journal of Cell Biology,* **122,** 1231-1241

Provoda J.C and Lee K.D (2000) Bacterial pore-forming hemolysins and their use in the cytosolic delivery of macromolecules, *Advanced Drug Delivery Reviews,* **41**(2), 209-221

Putnam D and Kopecek J (1995) Polymer conjugates with anticancer activity, *Advanced Polymer Science*, **122**, 55-123

Raso V, Brown M, McGrath J, Liu S and Stafford W.F (1997) Antibodies capable of releasing diptheria toxin in response to the low pH found in endosomes, *Journal of Biological Chemistry*, **272**(44), 27618-27622

Richardson S.C.W, Ferruti P and Duncan R (1999) Poly(amidoamine)s as potential endosomolytic polymers: Evaluation *in vitro* and body distribution in normal and tumour-bearing animals, *Journal of Drug Targeting*, **6**(6), 391-404

Ringsdorf H (1975) Structure and properties of pharmacologically active polymers, *Journal of Polymer Science Polymer Symposium*, **51**, 135-153

Roos J and Kelly R.B (1997) Is dynamin really a 'pinchase', *Trends in Cell Biology*, **7**(7), 257-259

Rothman J.E and Schmid S.L (1986) Enzymatic recycling of clathrin from coated vesicles, *Cell*, **46**(1), 5-9

Ryser HJ-P and Shen W.C (1978) Conjugation of methotrexate to poly(L-lysine) increases drug transport and overcomes drug resistance in cultured cells, *Proceedings of the National Academy of Science*, **75**, 3867-3870

Scheller A, Oehlke J, Wiesner B, Dathe M, Krause E, Beyermann M, Melzig M and Bienert M (1999) Structural requirements for cellular uptake of alpha-helical amphipathic peptides, *Journal of Peptide Science,* **5**(4), 185-194

Shiah J.G, Konak C, Spikes J.D and Kopecek J (1998) Influence of pH on aggregation and photoproperties of *N*-(2-hydroxypropyl)methacrylamide copolymer–mesochlorin $e_6$ conjugates, *Drug Delivery*, **5**, 119-126

Shinoda T, Takagi A, Maeda A, Kagatani S, Konno Y and Hashida M (1998) *In vivo* fate of folate-BSA in non-tumour- and tumour bearing mice, *Journal of Pharmaceutical Sciences,* **87**(12), 1521-1526

Simkis K (1998) Cell membranes: Barriers, regulators and transducers? *Comparative Biochemistry and Physiology Part A*, **120**, 17-22

Skinner S.A, Tutton P.J and O'Brien P.E (1990) Microvascular architecture of experimental colon tumours in the rat, *Cancer Research*, **50**, 2411-2417

Smith I (1968) HVPE in chromatographic and electrophoretic techniques, Zone Electrophoresis, 4th Edition, Williams Heinemann Medical Books Ltd, London

Stayton P.S, Hoffman A.S, Murthy N, Lackey C, Cheung C, Tan P, Klumb L.A, Chilkoti A, Wilbur F.S and Press O.W (2000) Molecular engineering of proteins and polymers for targeting and intracellular delivery of therapeutics, *Journal of Controlled Release*, **65**(1-2), 203-220

Steyger P.S, Baban D.F, Brereton M, Ulbrich K and Seymour L.W (1996) Intratumoural distribution as a determinant of tumour responsiveness to therapy using polymer-based macromolecular prodrugs, *Journal of Controlled Release*, **39**, 35-46

Subbarao N.K, Parente R.A, Szoka F.C.J, Nadasdi L and Pongracz K (1987) pH-dependent bilayer destabilisation by an amphipathic peptide, *Biochemistry*, **26**(11), 2964-2972

Sulkowska A (2002) Interaction of drugs with bovine and human serum albumin, *Journal of Molecular Structure*, **614**(1-3), 227-232

Thomas J.L and Tirrell D.A (1992) Polyelectrolyte-sensitized phospholipid vesicles, *Accounts of Chemical Research*, **25**(8), 336-342

Thomas J.L, Barton S.W and Tirrell D.A (1994) Membrane solubilisation by a hydrophobic polyelectrolyte: Surface activity and membrane binding, *Biophysical Journal*, **67**(3), 1101-1106

Thomas J.L, You H and Tirrell D.A (1995) Tuning the response of a pH-sensitive membrane switch, *Journal of the American Chemical Society*, **117**(10), 2949-2950

Tirrell D.A, Takigawa D.A and Seki K (1985) pH sensitisation of phospholipid vesicles via complexation with synthetic poly(carboxylic acids), *Annals of the N.Y. Academy of Science*, **44**, 237-248

Torchilin V.P (2000) Drug targeting, *European Journal of Pharmaceutical Science*, **11**(2), S81-S91

Torchilin V.P (2002) PEG-based micelles as carriers of contrast agents for different imaging modalities, *Advanced Drug Delivery Reviews*, **54**(2), 235-252

Torchilin V.P, Papisov M.I, Orekhova N.M, Belyaev A.A, Petrov A.D and Ragimov S.E (1988) Magnetically driven thrombolytic preparation containing immobilised streptokinase-targeted transport and action, *Haemostasis*, **18**, 113-116

Torchilin V.P, Zhou F, Huang L (1993) pH-sensitive liposomes, *Journal of Liposome Research*, **3**, 201-255

Tung C-H and Weissleder R (2002) Arginine containing peptides as delivery vectors, *Advanced Drug Delivery Reviews*, **1**, 1-14

Uherek C, Fominaya J and Wels W (1998) A modular DNA carrier protein based on the structure of diphtheria toxin mediates target cell-specific gene delivery, *Journal of Biological Chemistry*, **273**(15), 8835-8841

Umata T and Mekada E (1998) Diptheria toxin translocation across endosome membranes: A novel cell permeabilisation assay reveals new diphtheria toxin fragments in endocytic vesicles, *Journal of Biological Chemistry*, **273**(14), 8351-8359

Umata T, Sharma K.D and Mekada E (2000) Diptheria toxin and the diphtheria-toxin receptor: In handbook of Experimental Pharmacology (Aktories K and Just I :Eds), **145,** 45-46 Springer-Verlag Berlin, Heidelberg, Germany

Uherek C and Wels W (2000) DNA-carrier proteins for targeted gene delivery, *Advanced Drug Delivery Reviews*, **44**, 153-166

Van Deurs B, Holm P.K, Kayser L, Sandvig K and Hansen S.H (1993) Multivesicular bodies in HepG2 cells are maturing endosomes, *European Journal of Cell Biology*, **61**, 208-224

Vasey P, Twelves C, Kaye S, Wilson P, Morrison R, Duncan R, Thomson A, Hilditch T, Murray T, Burtles S, Frasier D, Frigerio E and Cassidy J (1999) Phase I clinical and pharmacokinetic study of PKI (HPMA copolymer doxorubicin): First member of a new class of chemotherapeutic agents, drug-polymer conjugates, *Clinical Cancer Research*, **5**(1), 83-94

Veronese F.M and Morpugo M (1999) Bioconjugation in pharmaceutical chemistry, *Fármaco*, **54**, 497-516

Wagner E (1998) Effects of membrane-active agents in gene delivery, *Journal of Controlled Release,* **53**, 155-158

Wagner E, Plank C, Zatloukal K, Cotten M and Birnstiel M.L (1992) Influenza-virus hemagglutinin HA-2 *N*-terminal fusogenic peptides augment gene-transfer by transferrin-polylysine-DNA complexes: toward a synthetic virus-like gene-transfer vehicle, *Proceedings of the National Academy of Sciences*, **89**(17), 7934-7938

Wagner E, Curiel D and Cotten M (1994) Delivery of drugs, proteins and genes into cells using transferin as a ligand for receptor-mediated endocytosis, *Advanced Drug Delivery Reviews*, **14**(1), 113-16

Wiley D.C and Skehel J.J (1987) The structure and function of the hemagglutinin membrane glycoprotein of influenza virus, *Annual Review of Biochemistry*, **56**, 365-394

Williams A.S, Camilleri J.P, Goodfellow R.M and Williams B.D (1996) A single intra-articular injection of liposomally conjugated methotrexate suppresses joint inflammation in rat antigen-induced arthritis, *British Journal of Rheumatology*, **35**, 719-724

Wilson I.A, Skehel J.J and Wiley D.C (1981) Structure of the hemagglutinin membrane glycoprotein of influenza virus at 3-A resolution, *Nature*, **289**, 366-373

Zauner W, Kichler A, Schmidt W, Mechtler K and Wagner E (1997) Glycerol and polylysine synergise in their ability to rupture vesicular membranes: A mechanism for increased transferring-polylysine mediated gene transfer, *Experimental Cell Research*, **232**, 137-145

# Appendices

## Appendix ICell Culture Media components

| A. Components of RPMI-1640 medium | g/L |
|---|---|
| **INORGANIC SALTS** | |
| $Ca(NO_3)_2 \cdot 4H_2O$ | 0.1 |
| $MgSO_4$ (Anhyd) | 0.04884 |
| KCl | 0.4 |
| $NaHCO_3$ | 2.0 |
| NaCl | 6.0 |
| $Na_2HPO_4$ (Anhyd) | 0.8 |
| **AMINO ACIDS** | |
| L-Arginine | 0.2 |
| L-Asparagine (anhydrous) | 0.05 |
| L-Aspartic Acid | 0.02 |
| L-Cystine•2HCl | 0.0652 |
| L-Glutamic Acid | 0.02 |
| Glycine | 0.01 |
| L-Histidine | 0.015 |
| Hydroxy-L-Proline | 0.02 |
| L-Isoleucine | 0.05 |
| L-Leucine | 0.05 |
| L-Lysine•HCl | 0.04 |
| L-Methionine | 0.015 |
| L-Phenylalanine | 0.015 |
| L-Proline | 0.02 |
| L-Serine | 0.03 |
| L-Threonine | 0.02 |
| L-Tryptophan | 0.005 |
| L-Tyrosine•2Na•$2H_2O$ | 0.02883 |
| L-Valine | 0.02 |
| **Vitamins** | |
| D-Biotin | 0.0002 |
| Choline Chloride | 0.003 |
| Folic Acid | 0.001 |
| myo-Inositol | 0.035 |
| Niacinamide | 0.001 |
| p-Amino Benzoic Acid | 0.001 |
| D-Pantothenic Acid•0.5Ca | 0.00025 |
| Pyridoxine•HCl | 0.001 |
| Riboflavin | 0.0002 |
| Thiamine•HCl | 0.001 |
| Vitamin B-12 | 0.000005 |
| **OTHER** | |
| D-Glucose | 2.0 |
| Glutathione (reduced) | 0.001 |
| Phenol Red•Na | 0.0053 |

## B. Components of Nutrient Mixture F-12 Medium

| | g/L |
|---|---|
| **INORGANIC SALTS** | |
| $CaCl_2 \cdot 2H_2O$ | 0.0441 |
| $CuSO_4 \cdot 5H_2O$ | 0.0000025 |
| $FeSO_4 \cdot 7H_2O$ | 0.000834 |
| $MgCl \cdot 6H_2O$ | 0.123 |
| KCl | 0.224 |
| $NaHCO_3$ | 1.176 |
| NaCl | 7.599 |
| $Na_2HPO_4$ | 0.14204 |
| $ZnSO_4 \cdot 7H_2O$ | 0.000863 |
| **AMINO ACIDS** | |
| L-Alanine | 0.009 |
| L-Arginine•HCl | 0.211 |
| L-Asparagine•$H_2O$ | 0.01501 |
| L-Aspartic Acid | 0.0133 |
| L-Cysteine•HCl•$H_2O$ | 0.035 |
| L-Glutamic Acid | 0.0147 |
| Glycine | 0.00751 |
| L-Histidine•3HCl•$H_2O$ | 0.02096 |
| L-Isoleucine | 0.00394 |
| L-Leucine | 0.0131 |
| L-Lysine•HCl | 0.0365 |
| L-Methionine | 0.00448 |
| L-Phenylalanine | 0.00496 |
| L-Proline | 0.0345 |
| L-Serine | 0.0105 |
| L-Threonine | 0.0119 |
| L-Tryptophan | 0.00204 |
| L-Tyrosine 2Na•2$H_2O$ | 0.00778 |
| L-Valine | 0.0117 |
| **VITAMINS** | |
| D-Biotin | 0.0000073 |
| Choline Chloride | 0.01396 |
| Folic Acid | 0.00132 |
| Myo-Inositol | 0.018 |
| Niacinamide | 0.000037 |
| D-Pantothenic Acid•0.5Ca | 0.00048 |
| Pyridoxine•HCl | 0.000062 |
| Riboflavin | 0.000038 |
| Thiamine•HCl | 0.00034 |
| Vitamine B-12 | 0.00136 |
| **OTHER** | |
| D-Glucose | 1.802 |
| Hypoxanthine | 0.00408 |
| Linoleic Acid | 0.000084 |
| Phenol Red (sodium) | 0.0013 |
| Putrescine•HCl | 0.000161 |
| Pyruvic Acid (sodium) | 0.11 |
| Thioctic Acid | 0.00021 |
| Thymidine | 0.00073 |

## C. Components of DMEM Medium

| | g/L |
|---|---|
| **INORGANIC SALTS** | |
| $CaCl_2 \cdot 2H_2O$ | 0.264 |
| $Fe(NO_3) \cdot 9H_2O$ | 0.00010 |
| KCl | 0.400 |
| $MgSO_4 \cdot 7H_2O$ | 0.200 |
| NaCl | 6.4 |
| $NaHCO_3$ | 3.7 |
| $NaH_2PO_4 \cdot 2H_2O$ | 0.141 |
| **AMINO ACIDS** | |
| L-Arginine•HCl | 0.084 |
| L-Cysteine | 0.048 |
| Glycine | 0.03 |
| L-Histidine HCl•$H_2O$ | 0.042 |
| L-Isoleucine | 0.105 |
| L-Leucine | 0.105 |
| L-Lysine HCl | 0.146 |
| L-Methionine | 0.030 |
| L-Phenylalanine | 0.066 |
| L-Serine | 0.042 |
| L-Threonine | 0.095 |
| L-Tryptophan | 0.016 |
| L-Tyrosine | 0.072 |
| L-Valine | 0.094 |
| **VITAMINS** | |
| D-Ca pantothenate | 0.004 |
| Choline Chloride | 0.004 |
| Folic Acid | 0.004 |
| I-Inositol | 0.0072 |
| Nicotinamide | 0.004 |
| Pyridoxine•HCl | 0.004 |
| Riboflavin | 0.00040 |
| Thiamine•HCl | 0.004 |
| **OTHER** | |
| D-Glucose | 4.50 |
| Phenol Red | 0.015 |
| Sodium Pyruvate | 0.110 |

## Appendix II The excitation and emission spectra for PD20 at various pH values

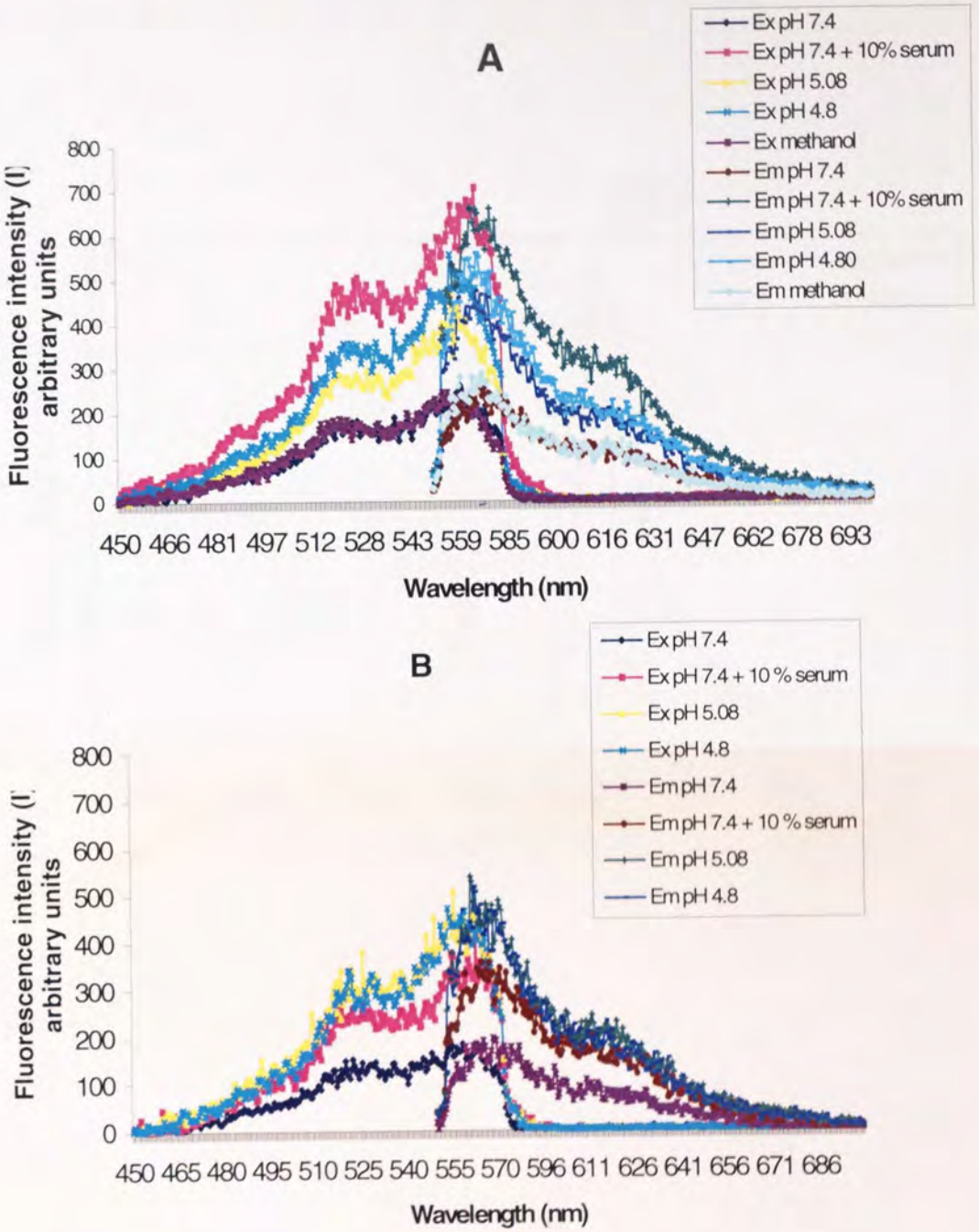


**Appendix II The excitation and emission spectra for PD20 when samples of PD20 were measured for their fluorescence output. Graph A represents the fluorescence output of PD20 ($1.9\times10^{-2}$ $gL^{-1}$) in either serum containing or serum free medium at various pH values (pH 7.4, 5.08 and pH 4.8) or in methanol. All samples apart from those prepared in methanol were further analysed (Graph B) by preparing all samples to the same absorption units (0.09 +/-0.001).**

**Appendix 111 The excitation and emission spectra for the free Cy3 bisamine fluorophore (Supplied by Amersham Biosciences, Cardiff, UK)**